

 **Tomas Bata University in Zlín**  
Faculty of Technology

*Doctoral Thesis*

**Preparation and modifications of biodegradable  
polyesters for medical applications**

Příprava a modifikace biodegradabilních polyesterů  
pro medicínální aplikace

Pavel Kucharczyk

September 2013

Zlín, Czech Republic

**Doctoral study programme: P 2808 Chemistry and Materials  
Technology**

2808V006 Technology of Macromolecular  
Compounds

**Supervisor: doc. Ing. Vladimír Sedlařík, Ph.D.**

**Consultant: doc. Ing. Marián Lehocký, Ph.D.**

# CONTENTS

CONTENTS .....	3
ABSTRACT .....	4
ABSTRAKT .....	5
LIST OF PAPERS .....	6
THEORETICAL BACKGROUND .....	7
1. Introduction to materials for medicine .....	7
2. Biodegradable polyesters .....	11
2.1. Polylactic acid (PLA) .....	12
2.2. Polyglycolic acid (PGA).....	13
2.3. Poly( $\epsilon$ -caprolactone) (PCL).....	14
2.4. Polydioxanone (PDO) .....	15
2.5. Poly(lactic-co-glycolic acid) (PLGA) .....	15
3. Chemical synthesis of biodegradable polyesters.....	16
4. Conducting polycondensation of polyesters .....	18
5. Modifications to biodegradable polyesters.....	21
5.1. Bulk modifications .....	21
5.2. Surface modifications .....	26
6. Biodegradation of synthetic polyesters under physiological conditions.....	28
7. Applications of synthetic biodegradable polyesters in medicine .....	31
AIMS OF THE DOCTORAL STUDY.....	34
SUMMARY OF THE PAPERS .....	35
CONCLUSIONS.....	39
CONTRIBUTIONS TO SCIENCE AND PRACTICE .....	41
ACKNOWLEDGEMENTS .....	43
LIST OF SYMBOLS AND ACRONYMS.....	44
LIST OF FIGURES AND TABLES.....	45
REFERENCES.....	47

## **ABSTRACT**

The work presented here summarizes the very latest advances in the synthesis, modification and degradation of biodegradable polyesters. This body of recognized knowledge was applied to specific polymer systems based on lactic acid – polylactides. Within the experimental part of this work, most attention is paid to polylactide synthesis optimization, involving non-metallic and non-toxic catalyst. Furthermore, chemical modification, through introducing specific groups into the polylactide structure, in addition to chain length prolongation of polymers, by using special postpolycondensation techniques, were undertaken and thoroughly studied in order to meet the relevant requirements for complex polymer applications in medicine. Degradation studies of the polylactides developed under various conditions that simulate the human body provide a comprehensive view on the topic under study.

**Keywords:** biodegradable polymers, synthetic polyesters, synthesis, modification, biodegradation, postpolycondensation, medical application

## **ABSTRAKT**

Tato doktorská práce poskytuje shrnutí dosavadního stavu poznání v oblasti syntézy, modifikace a degradace biologicky rozložitelných polyesterů. Tento přehled doposud známých poznatků byl aplikován na konkrétní polymerní systémy na bázi polymerů kyseliny mléčné, polylaktidu. Hlavní pozornost v rámci experimentální práce věnována optimalizaci syntézy polylaktidu za použití netoxických nekovových katalyzátorů. Vzhledem k aplikačnímu zaměření této směrem k medicínám využitím a k požadavkům na fyzikálně chemické vlastnosti polymerních matric je významná pozornost věnována chemické modifikaci připravených polylaktidů ve smyslu zavádění polárních skupin do struktury polymeru a nebo zvyšování délek řetězců pomocí speciálních postpolykondenzačních technik. Pro ucelený přehled je experimentální část doplněna o komplexní studii zaměřující se na charakterizaci hydrolytického rozkladu připraveného polylaktidu za specifických podmínek simulující různá prostředí lidského organismu.

Klíčová slova: biodegradovatelné polymery, syntetické polyestery, syntéza, modifikace, postpolykondenzace, biodegradace, aplikace v medicíně

# LIST OF PAPERS

## Paper I

SEDLARIK, V., KUCHARCZYK, P., KASPARKOVA, V., DRBOHLAV, J., SALAKOVA, A., SAHA, P. Optimization of the Reaction Conditions and Characterization of L-Lactic Acid Direct Polycondensation Products Catalyzed by a Non-Metal-Based Compound, *J. Appl. Polym. Sci.* 2010, vol. 116, no. 3, p. 1597-1602

## Paper II

KUCHARCZYK, P., POLJANSEK, I., SEDLARIK, V., KASPARKOVA, V., SALAKOVA, A., DRBOHLAV, J., CVELBAR, U., SAHA, P. Functionalization of Polylactic Acid Through Direct Melt Polycondensation in the Presence of Tricarboxylic Acid. *J. Appl. Polym. Sci.* 2011, vol. 122, p. 1275–1285.

## Paper III

KUCHARCZYK, P., POLJANSEK, I., SEDLARIK, V. The effect of various catalytic systems on solid-state polymerization of poly-(L-lactic acid). *J. Macromol. Sci. A.* 2012, vol. 49, no. 10, p. 795-805.

## Paper IV

KUCHARCZYK, P., HNATKOVA, E., DVORAK, Z., SEDLARIK, V. Novel aspects of the degradation process of PLA based bulky samples under conditions of high partial pressure of water vapour. *Polym. Degrad. Stabil.* 2012, vol. 98, no. 1, p. 150-157.

# THEORETICAL BACKGROUND

## 1. Introduction to materials for medicine

During recent decades great progress has been made in the medical and pharmaceutical field around the world. It is also known that such development has been attributed to discovering and utilizing a new sort of material – biomaterial(s). [1]

There are several definitions of biomaterial published in the literature:

According to BLACK (1982): “A *biomaterial is any pharmacologically inert material, viable or non-viable, natural product or man-made, that is a part of or is capable of interacting in a beneficial way with a living organism*” [2, 3].

Later, WILLIAMS (1987) stated, that: “A *biomaterial is any non-living material used in medical devices intended to interact with biological systems*” [3, 4].

One of the first definitions of biomaterial was determined by the Clemson Advisory Board for Biomaterials and adopted at the sixth Annual International Biomaterials Symposium, 1974 [3, 5].

“A *biomaterial is a systemically, pharmacologically inert substance designed for implantation within or for incorporation with a living system*”,

From a material point of view biomaterials can be divided into 5 groups [6, 7].

Of these, polymeric materials are of special interest due to their unique properties [8, 9, 10].

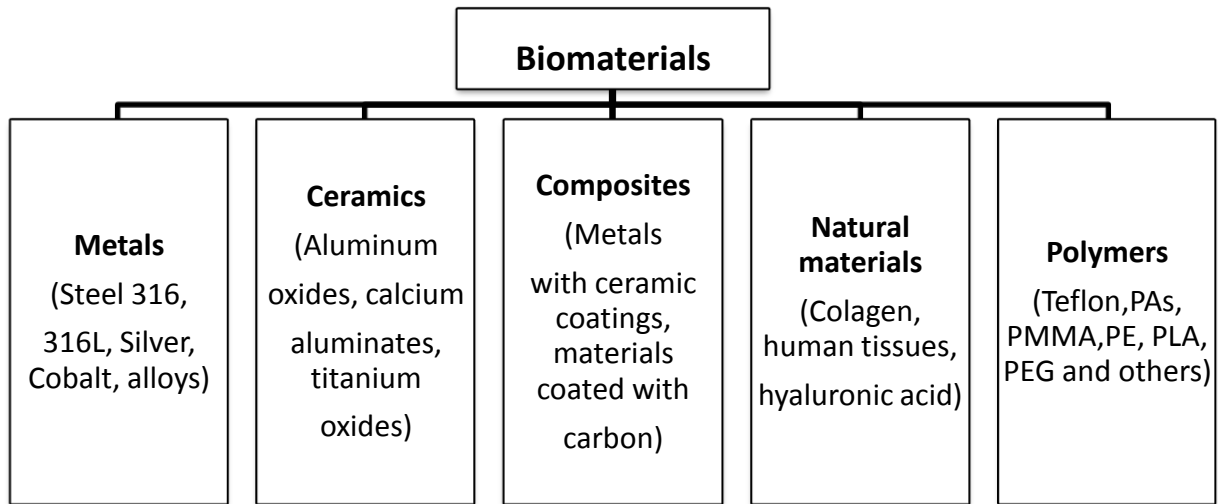


*Figure 1 - Basic types of biomaterials*

## **Synthetic polymers for medicine**

On the basis of the definition of biomaterial, it is clear that this should fulfil some specific requirements/features [11, 12].

- 1) The material should not cause a sustained inflammatory or undesirable toxic response after implantation into a living organism.
- 2) The shelf life of a material should be satisfactory.
- 3) The material should possess appropriate permeability and processability for the intended application.

*If a material is designed so as to be degradable, then:*

- 4) The mechanical properties of a material should be appropriate for the designated purpose and their variation during degradation should be compatible and predictable with the healing or recovery process.
- 5) The time of degradation should match the duration of the healing or regeneration process.

- 6) The degradation products and intermediates should be harmless and able to become metabolized or filtered out from the body. In other words, the material should be bioresorbable (defined in section 2).

Similar to other non-polymeric materials, biocompatibility is strictly affected by various factors (material properties), e.g. material chemistry, molecular weight, solubility, the shape and structure of the implant, hydrophilicity/hydrophobicity, lubricity, surface energy, water absorption, degradation and the erosion mechanism [9].

Although there are dozens of synthetic polymers fulfilling points 1-4, there is a relatively narrow range of synthetic materials exhibiting the desired degradation ability described in points 5 and 6. These materials are called *biodegradable*.

## **Synthetic biodegradable polymers for medicine**

The exhaustive definition of biodegradable polymers was stated by VERT et al. (1992). *“Biodegradability relates to solid polymeric materials and devices which break down due to macromolecular degradation with dispersion in vivo but with no proof of elimination from the body. Biodegradable polymeric systems or devices can be attacked by biological elements so that the integrity of the system, and in some cases (albeit not necessarily) of the macromolecules themselves, is affected and results in fragments or other degradation by-products. Such fragments can move away from their site of action but not necessarily from the body”* [13].

Based on the above-stated definition it is clear that biodegradable polymers must have a specific chemical structure which can lead to chain scission under conditions of a living organism, and which also permits sufficient mechanical and physical behaviour during its application [14].

Biodegradable polymers attract significant attention in a broad variety of research and industrial efforts because materials possessing control decomposition and absorption in the body are desirable for many short or even long-term applications [15].

## Division of synthetic biodegradable polymers for medicine according to chemical structure

Table 1 - Division of synthetic biodegradable polymers based on chemical structure

Group and Possible Structure	Group and Possible Structure
Polyesters $\left[ \text{R}-\overset{\text{O}}{\parallel}{\text{C}}-\text{O} \right]_n$	Ref. [12, 17] Polyester amides $\left[ \left[ \text{O}-\text{R}^1-\overset{\text{O}}{\parallel}{\text{C}} \right]_{m_1} \left[ \text{N}-\text{R}^2-\overset{\text{O}}{\parallel}{\text{C}} \right]_{n_2} \right]_n$
Ref. [9, 18] Poly(ortho esters) $\left[ \text{O}-\text{C}(\text{O}-\text{R})-\text{C} \right]_n$	Ref. [9, 20, 21] Polyurethanes $\left[ \overset{\text{O}}{\parallel}{\text{C}}-\text{N}-\text{X}-\text{N}-\overset{\text{O}}{\parallel}{\text{C}}-\text{O}-\text{Y}-\text{O} \right]_n$
Ref. [9, 19] Poly(ortho esters) $\left[ \text{O}-\text{C}(\text{O}-\text{R})-\text{C} \right]_n$	X - di-isocyanate Y - polyol
Poly(anhydrides) $\left[ \overset{\text{O}}{\parallel}{\text{C}}-\text{R}-\text{O}-(\text{CH}_2)-\overset{\text{O}}{\parallel}{\text{C}}-\text{O} \right]_n$	Ref. [22] Polyester urethanes $\left[ \text{R}-\overset{\text{O}}{\parallel}{\text{C}}-\text{O}-\left[ \text{R}-\overset{\text{O}}{\parallel}{\text{C}}-\text{O}-\overset{\text{O}}{\parallel}{\text{C}} \right]_{m_1}-\text{N} \right]_n$
Ref. [23, 24] Polyphosphazenes* $\left[ \text{N}=\text{P}(\text{R}^1)(\text{R}^2) \right]_n$	Ref. [23, 24] Polyalkylcyanoacrylates $\left[ \text{CH}_2-\overset{\text{CN}}{\underset{\text{C}=\text{O}}{\text{C}}}-\text{OR} \right]_n$
Ref. [9, 25] Poly(vinyl alcohol) $\left[ \text{C}(\text{H})(\text{OH})-\text{C}(\text{H}) \right]_n$	Ref. [9, 27]

\*R<sup>1</sup>, R<sup>2</sup> - for example: imidazoles, aminoesters, alcohols – OC<sub>2</sub>H<sub>5</sub>, OCH<sub>3</sub>

Table 1 summarizes the division of common synthetic biodegradable polymers according to the chemical structure of the main chain [16].

There are many more polymers considered as biodegradable and suitable for medical application; however, these materials may lack a synthetic quality (starch, cellulose, microbial polyesters, etc.) and as a consequence are not included in this work.

It should be also noted that the biodegradation mechanism of the polymers described above varies significantly. While polyesters, poly(amide-enamine)s, polyanhydrides, polyphosphazenes, poly(ortho esters), and poly(alkyl cyanoacrylates) can be break down thorough hydrolysis of the main chain, polyurethanes, polyureas and polyvinyl alcohol are degraded by microorganisms or enzymes [9, 16]. Of these, polyester-amides and polyester urethanes consist of an easily hydrolysable ester bond and hydrolytically very stable amide and urethane bond, respectively. This leads to either only partial biodegradation or requirements of conditions concerning both specific enzymes (e.g. papain, subtilisin for polyurethanes) and water [9, 18].

Some monomers used as raw materials for polymer synthesis tend to be incompatible or often toxic to living organisms. Prime examples are diisocyanates (4, 4'-methylenediphenyl diisocyanate) or diamines, as used in polyurethane and polyamide manufacturing, respectively. To overcome such limitations other biocompatible diisocyanates such as lysine diisocyanate (LDI), and 1,4-diisocyanatobutane (BDI) have been developed [9, 30, 31].

## **2. Biodegradable polyesters**

Of synthetic biodegradable polymers, it is polyesters that especially play a dominant role. This is due to their relatively easy availability and good physico-chemical properties, but specifically their bioresorbability, which is defined as follows by VERT et al. (1992): *“The ability of materials and devices to show bulk degradation and further desorption in vivo; e.g. polymers, which are*

*eliminated through natural pathways either because of simple filtration of degradation by-products or after their metabolization” [13].*

## **2.1. Polylactic acid (PLA)**

Also known as polylactide, this belongs to the family of aliphatic polyesters (Figure 2) commonly made from  $\alpha$ -hydroxy acids. PLA is a high strength and high modulus thermoplastic. Due to its properties it is used in a number of applications - from biomedical to conventional thermoplastics [32].

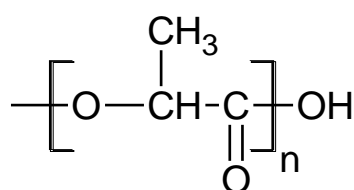


*Figure 2 - Chemical structure of PLA*

PLA is thermoplastic polyester which can be prepared in either crystalline or amorphous form. This is caused by the stereo regularity of the monomer (lactic acid or cyclic dimer lactide), hence PLA can exist in 3 forms - PLLA, PDLA and PDLLA. All of these three forms could possess different properties depending on their isomer composition. While PLLA is crystalline, PDLLA is a completely amorphous polymer. Due to its crystallinity, poly(L-lactide) possesses better mechanical properties than poly(DL-lactide). Pure PLLA can crystallize, but if more than 15% D form is present in the polymer chain, it is only possible to obtain amorphous material [33, 34].

Under normal conditions PLA is a brittle and hard polymer with a glass transition temperature of between 55°C-65°C and a melting point at around 160°C-170°C. Its comparison with other plastic is shown in Figure 5. Chemical, physical, mechanical and other properties are functions of temperature, molecular weight, chemical composition (copolymer presence), additives and processing methods, etc [32].

PLA is soluble in chloroform, acetone, dichloromethane and benzene but insoluble in cyclohexane, methanol and ethanol. It demonstrates reasonable resistance to fats and oils. Its solubility parameter is as follows:  $\delta_p$  at 25°C = 19-20.5 J<sup>0.5</sup>.cm<sup>-1.5</sup>. The most important mechanical properties are summarized in Table 2 [35].

*Table 2 - Typical mechanical properties of PLA*

<b>Property</b>	<b>Unit</b>	<b>Value</b>
Tensile strength	[MPa]	68
Elongation at break	[%]	4
E-Modulus	[MPa]	3000
Flexural strength	[MPa]	98
Izod impact	[J.m <sup>-1</sup> ]	29
Density	[kg.m <sup>-3</sup> ]	1.26

As a monomer, lactic acid or preferably lactide (3,6-Dimethyl-1,4-dioxane-2,5-dione) is used. Reaction can be performed in the molten state as well as in solution under an elevated temperature (120°C - 200°C). The synthesis of most polyesters for medical application is very similar and will be further discussed in a separate section.

## **2.2. Polyglycolic acid (PGA)**

PGA is the simplest linear aliphatic polyester. It is a highly crystalline polymer (45% - 55%) with a high melting point ( $T_m \sim 225^\circ\text{C}$ ) and a relatively high glass transition temperature ( $T_g \sim 40^\circ\text{C}$ ). Its high crystallinity makes this material insoluble in most organic solvents, excluding some highly fluorinated organic solvents, e.g. hexafluoroisopropanol.

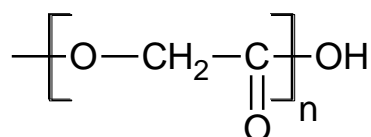


*Figure 3 - Chemical structure of PGA*

Its density is higher than in the case of PLA 1.5-1.7 g.cm<sup>-3</sup>. Although PGA exhibits great strength (>65 MPa), E-modulus (up to 7000 MPa) and elongation 15% - 20%, its stiffness makes it unsuitable for most applications in implant or suture specializations. Furthermore, its relatively high degradation rate is undesirable and can cause localized damage to living cells (localized lowering of pH). However, after copolymerization of PGA with another polyester (especially PLA, PCL), such materials exhibit excellent properties for medical applications [36, 37].

### 2.3. Poly( $\epsilon$ -caprolactone) (PCL)

PCL is also a semi-crystalline polymer with  $T_m \sim 60^\circ\text{C}$  and  $T_g \sim -60^\circ\text{C}$  (the lowest in the family of common hydrolysable synthetic polyesters) [37].

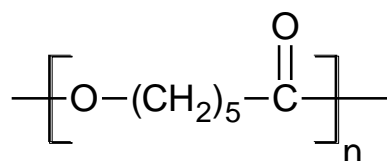


Figure 4 - Chemical structure of PCL

PCL is soluble in chloroform, dichloromethane, carbon tetrachloride, benzene, toluene, cyclohexanone and 2-nitropropane at room temperature. It has low solubility in acetone, 2-butanone, ethyl acetate, dimethylformamide and acetonitrile and is insoluble in alcohol, petroleum ether and diethyl ether. The tensile strength of bulk PCL ranges from 10.5 to 16 MPa, E-modulus  $\sim 350$  MPa, which is much lower compared to PLA or PGA. On the contrary, elongation of 300% - 500% is more than 10 fold higher. Although PCL was one of the earliest synthetic biodegradable polyesters synthesised in the early 1930s, its popularity in the research field was suppressed especially due to its long degradation time (2 - 3 years). However, with furthering development in the field of biomaterial applications, especially in tissue engineering in the last 20 years, PCL is once again in the limelight [37, 38, 39].

## 2.4. Polydioxanone (PDO)

In contrast with other polymers discussed in this section, PDO is not a pure polyester but poly(ether-ester) (an ether bond in the main chain, Figure 5). As in previous cases, PDO is a semi-crystalline polymer (up to 55%) demonstrating  $T_m \sim 60^\circ\text{C}$  and  $T_g \sim 0^\circ\text{C}$ .

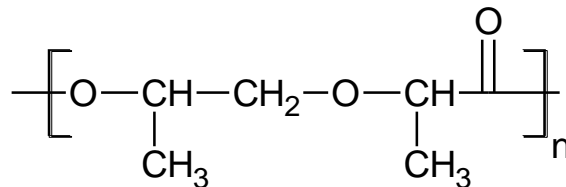


Figure 5 - Chemical structure of PDO

PDO exhibited a tensile strength  $\sim 48$  MPa and E-modulus of about 1500 MPa, which is lower than for PLA and PGA but considerably higher than for PCL. However, elongation in the range 500% - 600% is comparable to PCL and far exceeds PLA and PGA. PDO is soluble in most common organic solvents ( $\text{CHCl}_2$ ,  $\text{CHCl}_3$ ) and is often used as a suture in surgical applications [38, 40, 41, 42].

## 2.5. Poly(lactic-co-glycolic acid) (PLGA)

The high rigidity of PLA and its low degradation times can be significantly improved by copolymerization with other polyesters. In particular, the copolymers of PLA (including PDLA) and PGA (Figure 6) have very good properties and are widely used in many applications from implants and sutures to drug encapsulation. While both pure homopolymers tend to be crystalline, their copolymers are highly amorphous (in composition in the region of 25% - 70% of the glycolide unit). This is caused by chain irregularity due to the presence of a second component [37].

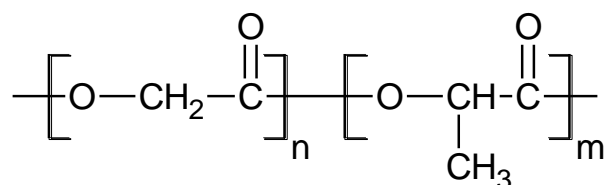


Figure 6 - Chemical structure of PLGA

The glass transition temperature of copolymers lies between 50°C - 55°C and their degradation time is strictly dependent on composition and usually varies in the region of several months. It is interesting that, for example, a copolymer containing 50% glycolide and 50% DL-lactide degrades faster than either homopolymers. The mechanical properties of PLGA are close to those of PDLA: tensile strength ~ 35 MPa, Modulus ~ 1700 MPa, elongation ~ 5% [35, 37, 38, 43].

### 3. Chemical synthesis of biodegradable polyesters

The chemical synthesis of the above-mentioned polyesters can be performed either through simple polycondensation of the bifunctional monomer (hydroxyacid, Figure 7) or by so-called ring opening polymerization (ROP) of cyclic monomers (Figure 8) [35]. Both methods involve elevated temperature and the presence of a catalyst (acid, organometallic compound, etc.). Typical conditions for synthesis of a biodegradable polyester are shown in Table 3.

Table 3 - Typical ROP and polycondensation conditions

	<b>ROP</b>	<b>Polycondensation</b>
<b>Temperature</b>	120°C - 170°C	160°C - 220°C
<b>Catalyst</b>	Organometallic compounds, ligands	acids
<b>Monomer purity</b>	extremely high	can contain water
<b>Reaction time</b>	~ 12 hours	~ 24 hours
<b>Environment</b>	Low pressure or inert atm.	Low pressure
<b>Performing</b>	melt	melt, solution, solid state

## Polycondensation

From a practical viewpoint, the polycondensation of appropriate hydroxy acids is simple because of their low cost and easy availability [44, 45]. For example, lactic acid can be prepared from renewable resources by fermenting naturally occurring sugars [46]. The only exception is for synthesis of PDO, which is limited merely to ROP; (p-dioxanone is synthesized by oxidative dehydrogenation of diethylene glycol over CuO) [47].

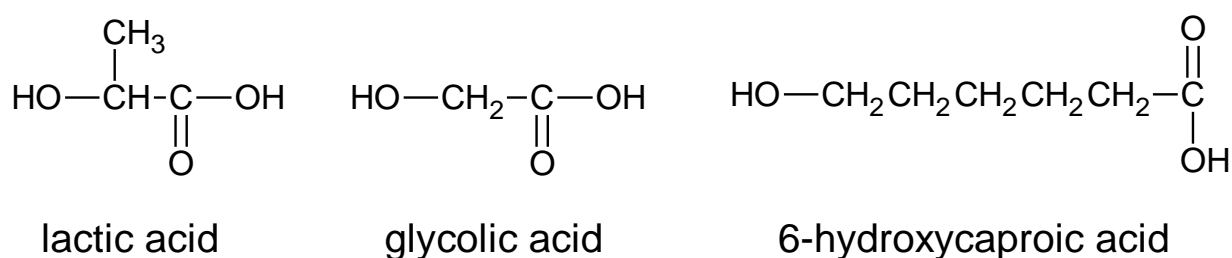


Figure 7 - Linear hydroxy acids as monomers for polycondensation

## Ring opening polymerization

However, ROP requires lower reaction times and the molecular weight reached can be significantly higher than in the previous case (several hundreds of thousands vs. tens of thousands). Moreover, no low molecular by-product is formed [43, 45, 46].

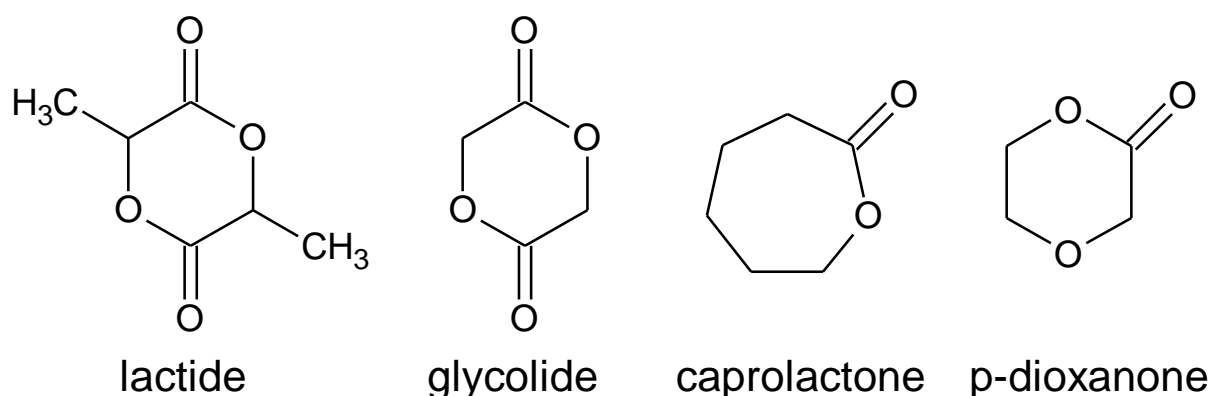


Figure 8 - Cyclic monomers for ROP

Nevertheless, preparing and purifying cyclic monomers is a very expensive and time-consuming operation [32].

### **Other methods**

In addition to chemical synthesis, some of these polymers, e.g. lactic acid, can be prepared by a biotechnological pathway - enzymatic synthesis, which is, however, beyond the scope of this thesis [48].

## **4. Conducting polycondensation of polyesters**

Synthetic polycondensation of simple hydroxy acids can be practically performed in 3 different ways (states).

### **Polycondensation in the molten state**

In direct melt polycondensation, hydroxy acid is transferred into polyester by condensation reactions between hydroxyl (OH) and carboxyl (COOH) groups, without using any solvents or external coupling agents. Due to the structure of the monomer - one hydroxyl and one carboxyl group in the molecule - a 1:1 equilibrium of reaction groups is always maintained. However, it is difficult to synthesize high molecular weight polymer in a satisfactory time due to the high viscosity of the polymer melt. Therefore, this method is not widely used [32, 49, 50].

### **Solution polycondensation (SP)**

SP is a method which can afford polyesters with a high molecular weight ( $M_w \sim 1 \cdot 10^5 \text{ g} \cdot \text{mol}^{-1}$ ). Nevertheless, a relatively long reaction time and high temperature is required and the simultaneous use of solvents results in complexity of the process's control, resulting in high cost of the product. Furthermore, it is hard to remove the solvent completely from the end product [51]. As regards the solvent, there exists the option to use p-xylene, o-

chlorotoluene and diphenyl ether. The  $M_w$  reached varied from  $2.6 \times 10^4$  to  $4.0 \times 10^4 \text{ kg.mol}^{-1}$  (in the case of lactic acid polycondensation) [52].

## Solid State Polycondensation (SSP)

SSP (or an ester interchange reaction) appears to be an effective route for PLA and PGA polyester synthesis, when compared with ROP and simple polycondensation.

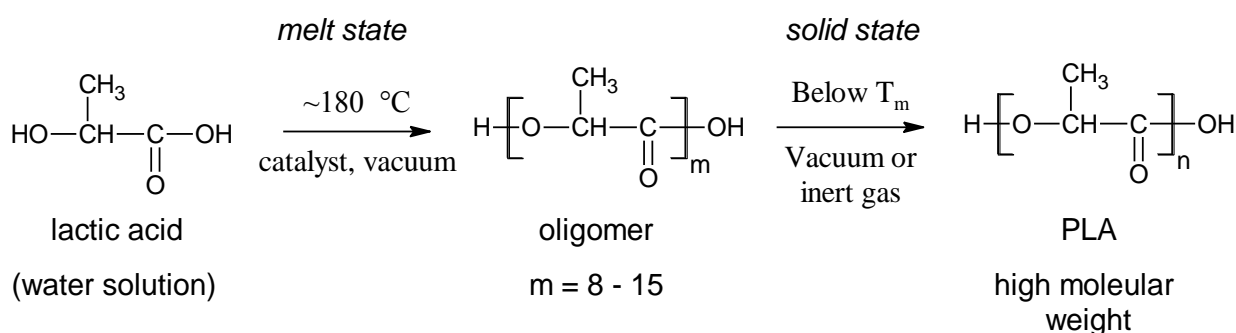


Figure 9 - Solid state polycondensation process

This is based on catalyzed reactions between hydroxyl and carboxyl end groups inside the amorphous region of a low molecular weight prepolymer (Figure 10), which leads to a rise in molecular weight. The process is as appears in Figure 9, where PLA was taken as an example [53].

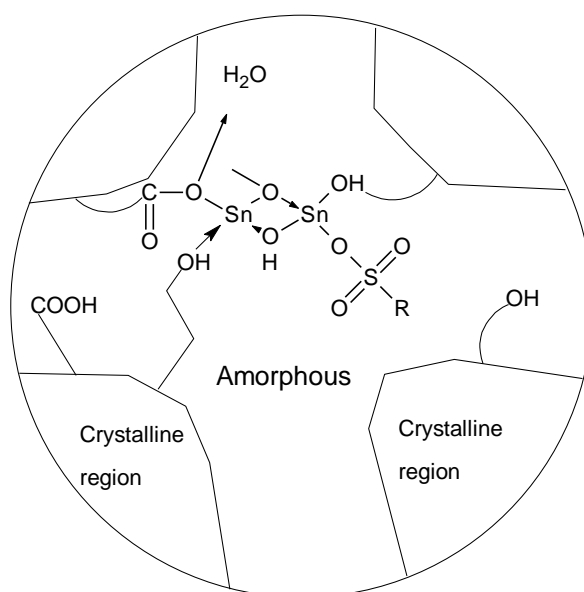


Figure 10 - Mechanism of SSP of PLA catalyzed by binary catalyst system [49]

A semi crystalline solid prepolymer of relative low molecular weight in powder, pellet, chip or fibre form is prepared. Then it is heated to a temperature below  $T_m$  (5 - 15°C) but above  $T_g$  (to improve the mobility and subsequent reaction of the end groups) in the presence of a suitable catalyst [53, 54]. Molecular weight can reach  $5 \cdot 10^5 \text{ g} \cdot \text{mol}^{-1}$  but reaction time is relatively long (~ 30 h). The advantages of SSP include low operating temperatures, which control any side reactions, as well as thermal, hydrolytic and oxidative degradations, in addition to reduced discoloration and degradation of the product. SSP polymers often have improved properties, because monomer cyclization and other side reactions are limited. There is practically no environmental pollution, as no solvent is required [50, 55].

Prior to SSP it is favourable to promote crystallization of prepolymer of low molecular weight, and facilitate concentration of the catalyst and remaining monomer into amorphous regions. In the case of the SSP of PLA, it was observed that bimodal distribution is often achieved. This was explained by heterogeneous elongation of the polymer chain, which simultaneously crystallizes during SSP [49].

### **Selection of catalyst**

As all synthetic biodegradable polyesters are primarily used in biological applications or in contact with food (packaging), the catalyst used for synthesis should be carefully chosen. Tin compounds are one of the most effective catalysts for producing biodegradable polyesters. However, some of them, especially the organic-based type, exhibited toxicity that increased in conjunction with concentration; it is also problematic to remove them from the polymer after synthesis [49, 56, 57].

## **5. Modifications to biodegradable polyesters**

In some cases the properties of the materials described above are unsuitable for certain applications, hence chemical or physical modification to them is desirable. For example, the high degree of crystallinity of PGA makes it insoluble in most solvents. Furthermore, the low hydrophilicity of PLA and PCL causes poor adhesion of cells to their surfaces. This is especially important in tissue engineering applications [58, 59].

Therefore, the reason to modify these polymers is, in particular, to fine-tune their mechanical properties, degradation behaviour, crystallinity and processability or surface properties. These improved properties can be obtained through two main approaches - bulk and surface modification [58, 59].

### **5.1. Bulk modifications**

There are three main types of bulk modification utilized for biodegradable polyesters: blending, copolymerization and chemical functionalization [59].

#### **- Blending**

This is one of the most common bulk modification techniques in the polymer industry. It is based on adding a low molecular weight component to the polymer system or mixing two or more polymers. In the case of biodegradable and biocompatible polyesters, plasticizers (e.g. tributyl citrate added to PLA) and various stabilizers are supplemented. The polymer blends/polymers of these materials have also been intensively studied, especially in order to manipulate hydrophilicity and degradation behaviour. Various compounds from the family of natural (starch, proteins) and synthetic (PEG, PVA) polymers have been used, in addition to which mutual blends of biodegradable polymers such as PLA/PCL have proven highly promising. The blends can be prepared by straightforward mixing of the

components in molten state (in an extruder) or in a suitable solvent [60, 61, 62, 63].

Finally, biodegradable polyesters have turned out to be a suitable matrix for particular fillers, of organic or even inorganic type. Such composites exhibit improved mechanical and thermal properties. As fillers, investigation has been conducted on clay, carbon nanotube, calcium carbonate, natural fibres and many other forms [64, 65, 66].

### - Copolymerization

The term copolymerization means polymerization of two or more monomers, in which the copolymer is formed. The copolymers usually possess significantly different properties than each homopolymer. In relation to biodegradable polyesters, various types of copolymer with a broad range of properties have been synthesized. In this chapter, attention will be paid to some of the most interesting materials.

#### A) Poly(Lactide-co-Glycolide) (PLGA)

PLGA (Figure 11) can be synthesized through a polycondensation reaction, or via ROP of cyclic diesters. Of these, ROP is the preferred method of synthesis due to shorter reaction times and higher monomer conversion rates [67].

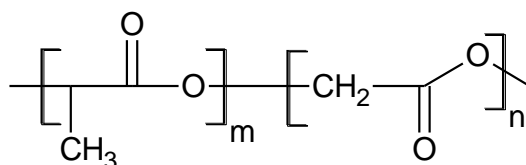


Figure 11 - Structure of PLGA copolymer

PLGAs usually exhibit lower crystallinity and melting temperatures. The degradation characteristics of the PLGA could be adjusted by controlling the ratio of LA to GA in the feeding dose. The degradation rate of PLGA is faster than that of PLA, and can be enhanced by increasing GA content. Typical degradation times are between 30-80 days, with the composition of GA between

15-50%. PLGA composed of the ratio 50:50 is entirely amorphous. [68] The PLGA copolymer is used as a suture material in the form of various bioabsorbable stents (Vicryl) and meshes, as well as matrixes for drug delivery applications [67].

### B) Poly(Lactide-co-Ethyleneglycol)

Probably the most extensively studied copolymer of synthetic biodegradable polyester PLA, this is a block copolymer of PLA (A) and PEG (B) of the structure A-B-A or A-B. These types of copolymers have exhibited phase separation due to incompatibility between both components; hence mechanical properties are usually poor. The scheme of catalysed synthesis from methylated PEG and lactide by ROP is depicted in Figure 12.

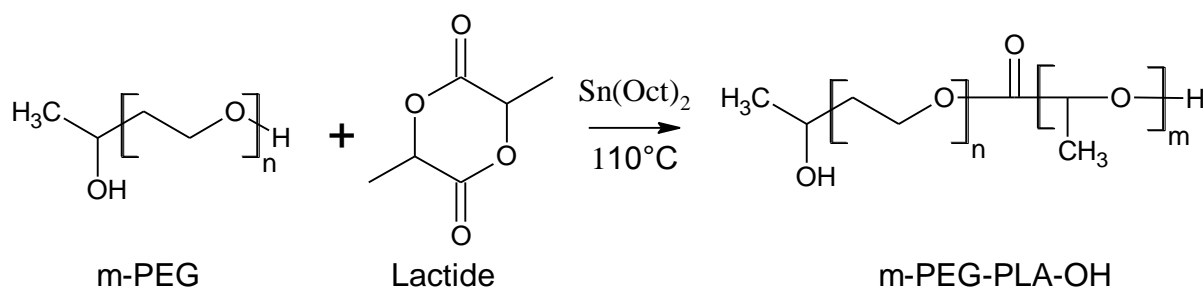


Figure 12 - ROP synthesis of PLA/PEG copolymer type A-B

Due to the presence of the PEG block in the polymer chain, hydrophilicity can be greatly enhanced, in addition to which molecular weight can be modified depending on the PEG used. The degradation products of the PEG-PLA block copolymer can enter the tricarboxylic acid cycle or be eliminated by the kidney. Thus, in low concentration the copolymer is non-toxic and not accumulative *in vivo*. These materials are widely used in drug delivery applications due to their unique properties. The amphiphilic nature of these copolymers enables the formation of micelles in water through a self-assembly process, with the hydrophobic PLA acting as the core (reservoirs) for hydrophilic PEG and the drug, as the shell projecting into the aqueous environment. The use of PEG in

the copolymers is also to reduce particle uptake by the mononuclear phagocytic system, sometimes also referred to as the “stealth or hindering function”, compared with particles without PEG attachment. This function enables the particle to circulate longer *in vivo* [69, 70].

Based on composition and preparation methods, various forms of PLA-PEG structures, such as nanomicelles, polymersomes, nanospheres and nanocapsules, can be prepared.

### **C) Graft copolymers**

The highly promising materials with this structure are copolymers of biodegradable polyesters with natural polymers, e.g. starch, dextran and chitosan. These natural polymers are enzymatically degradable as well as biocompatible. Chitosan-grafted-PLA hydrogels can be prepared by attaching PLA to the chitosan main chain and these materials can be used as hydrogels [71, 72].

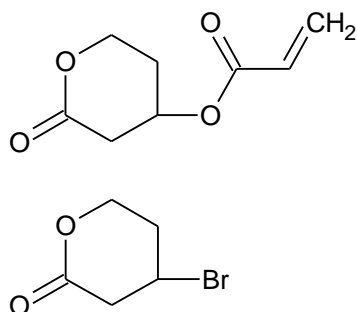
#### **- Chemical functionalization**

A disadvantage of all the synthetic biodegradable polyesters mentioned above is the absence of any reactive group along the main chain. The term chemical functionalization denotes the introduction of new chemical groups into the polymer chain, or change in the nature of those that are already present (terminal groups). This can be achieved via three approaches:

#### **A) Polymerization of substituted monomers**

This utilizes ROP reactions of substituted cyclic monomers (e.g. lactides, caprolactone). Different functional groups, especially hydrophilic, halogenated, and unsaturated groups, are attached to aliphatic polyester chains. Although these functional aliphatic polyesters are potentially biodegradable and biocompatible, their properties have to be assessed. Applying them in various spheres has yet to be explored [73, 74]. The structure of some substituted cyclic monomers and corresponding polymers are shown in Figure 13.

### Functionalized monomer



### Resulting polymer

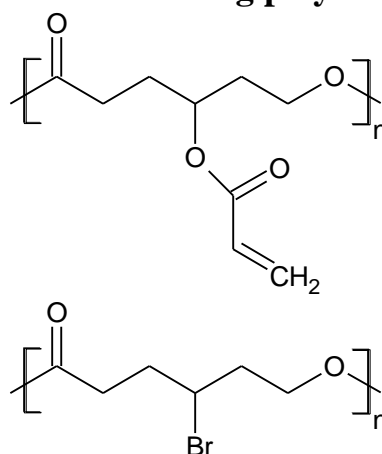


Figure 13 - The structures of functionalized PCL monomers with a corresponding polymer structure

The disadvantages of this approach primarily include substantial requirements for monomer purity, frequently complicated synthesis and the necessity to deprotect the functional group [74, 75, 76].

### B) Postpolymerization reactions

Here, the reactions are performed either on the end groups or along the polymer chain. Although there are no reactive side groups in the simple homopolymers of synthetic biodegradable polyesters, it is possible to graft unsaturated polyanhydrides that are able to undergo further reaction (e.g. with amines). The reaction below (Figure 14) is catalyzed by peroxides [77].

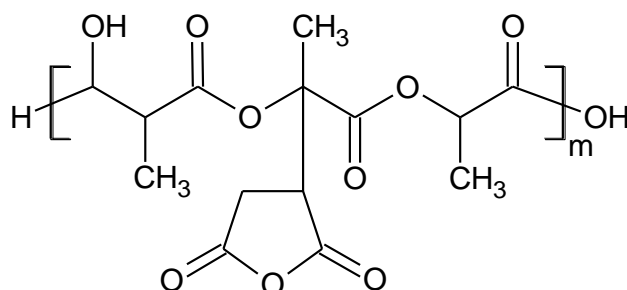


Figure 14 - Structure of maleic anhydride grafted on a PLA chain

The chemical modification of end groups is another means of getting new functional groups in the polymer structure. The reactions are usually relatively simple to perform even under moderate conditions [78]. As an example, hydroxyl end groups can be converted to chloride, amine or carboxylic. However, due to relatively low concentrations of the end groups, these types of modifications usually only exhibit a minor effect on polymer bulk properties [73].

### **C) Polymerization in the presence of a modifying agent**

This represents a rather specific type of modification. It is based on the polycondensation reaction of corresponding di-acids in the presence of a small amount of another, usually bi-functional, compound (PEG, dicarboxylic acid). Such modified polymers exhibit increased hydrophilicity and are often further used for reaction with chain linkers to provide a high molecular weight polymer. The disadvantage of such products is their low molecular weight because the modifying agents terminate the growing polymer chain. If a tri-compound and more functional compound are used as a modifier, then highly branched structures can be achieved.

## **5.2. Surface modifications**

Special surface chemical functionalities, hydrophilicity, roughness, topography, surface energy and charge govern the biocompatibility, cell affinity and necessity for control. A variety of synthetic polymers, natural polymers and biomacromolecules have been used to tailor these properties through a variety of techniques. Surface-modification methods can be classified as temporary (non-covalent attachment) and permanent (covalent attachment) [59].

### **- Coating**

This is one of the simplest and cheapest techniques for surface modification. It is based on deposition or absorption of the modifying

agent to the surface of polymer. It is commonly used in the case of proteins, e.g. fibronectin or collagen, as well as various block copolymers [58, 59].

- **Entrapment**

A method requiring a miscible mixture of a solvent and non-solvent, the surface-modifying molecules of which are soluble in the mixture and the non-solvent. Exposing the polymer surface to the solvent/non-solvent mixture leads to gelation of the polymer at the surface, allowing the modifier to diffuse inside. The swelling is reversed upon exposure to a non-solvent [58, 59].

- **Plasma treatment**

Plasma can be described as a mixture of positive ions and electrons produced by ionization. It is possible to create various functional groups on the polymer surface via this technique. The form of such functional groups is driven by the type of plasma used ( $\text{NH}_3$ ,  $\text{N}_2$ ,  $\text{O}_2$ ). Plasma treatment has been successfully used to improve wettability and cell affinity. However, the main disadvantage of this technique is that the effectiveness of the surface modification is partially reduced due to surface rearrangement [58, 59].

- **Chemical modification**

This is a method based on the reaction of reactive groups on the polymer surface with a modifying agent (e.g. proteins, other polymers or copolymers).

In the case of biodegradable polyesters, it is possible to partially hydrolyse the ester bonds on the surface by treating with NaOH solution. The carboxylic groups created increase hydrophylicity and allow further functionalization by chemical reaction. It is also possible to obtain reactive end groups on the surface through conducting polymerization of functionalized monomers, as described in the previous chapter. An

example of chemical surface modification is shown in Figure 15. The reactivity of COOH groups is firstly boosted by reacting with  $\text{PCl}_2$ ,  $\text{SOCl}_2$  or carbodiimides, followed by a chemical reaction with amine ( $-\text{NH}_2$ ) or hydroxyl ( $-\text{OH}$ ) functionalities [58, 59, 74].

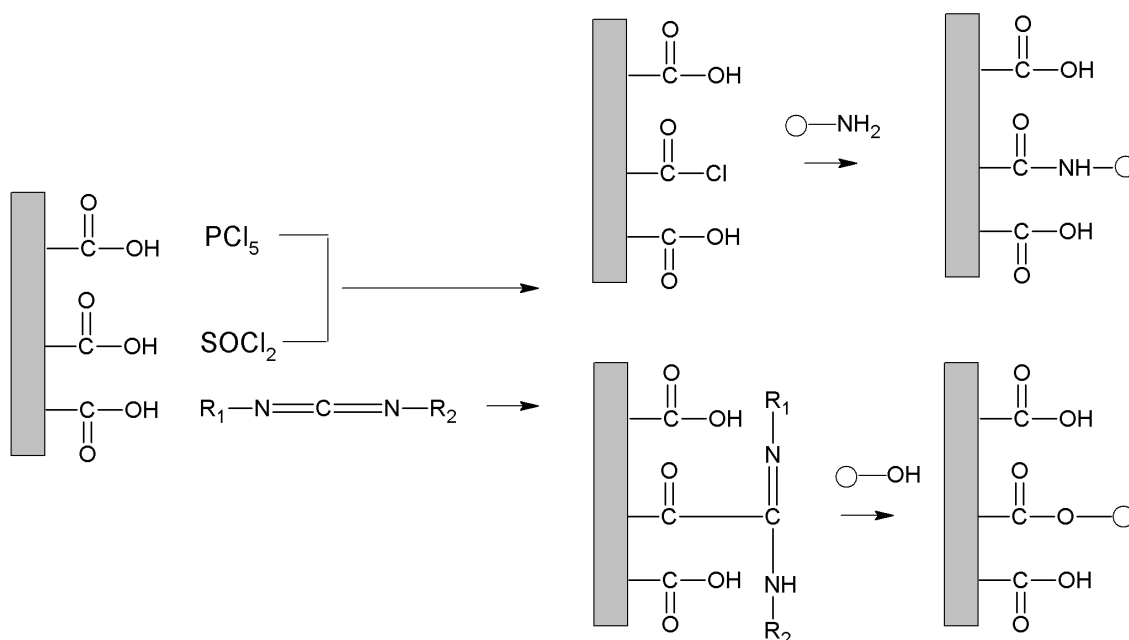


Figure 15 - Chemical surface modification through carboxylic groups [58]

#### - **Micro- and nano-patterning**

A method significantly different from all those mentioned above, it is based on creating a specific physical pattern, e.g. ridges, grooves or pillars on the polymer surface, usually via lithography, where the typical depth is about  $2\ \mu\text{m}$ . Besides a physical pattern, it is also possible to create a chemical one through the means of microcontact printing [58, 59].

## 6. **Biodegradation of synthetic polyesters under physiological conditions**

Biodegrading synthetic polyesters require two steps. Firstly, the ester which is bound is attacked and hydrolyzed either by molecules of water or enzymatically. Then, low molecular weight intermediates (corresponding

hydroxy acids and oligomers) can be converted to the end products H<sub>2</sub>O and CO<sub>2</sub> through a citric acid cycle or are excreted via the kidneys. The degradation rate depends on many factors such as temperature, humidity, crystallinity, additives, the presence of a catalyst, the size and shape of a product and molecular weight [79]. For synthetic polyesters there are two different mechanisms of degradation, which are depicted in Figure 16a-c [38, 80].

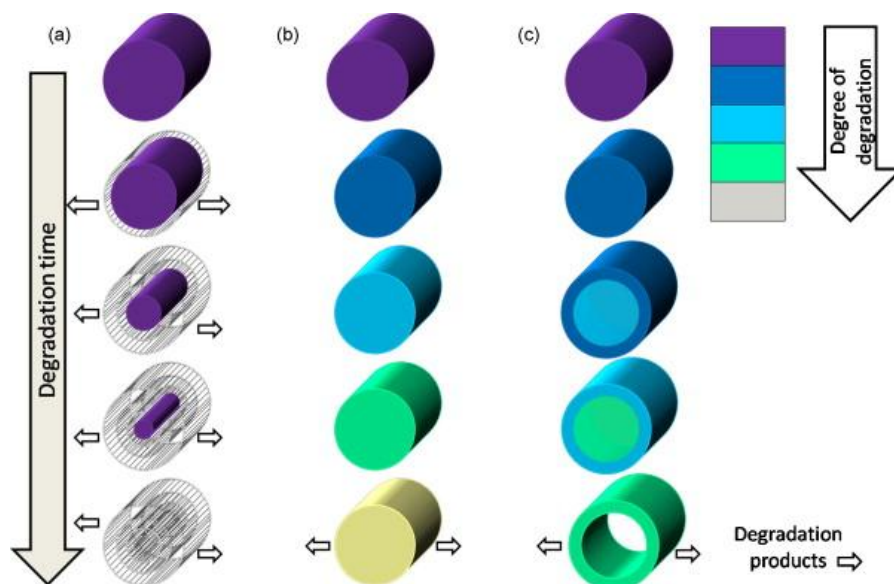


*Figure 16 - Degradation modes for degradable polymers: surface erosion (a); bulk degradation (b); bulk degradation with autocatalysis (c). Reproduced with permission from (2010) Elsevier [38]*

## Bulk degradation

PLA, PGA, PCL and PDO: for these polymers it is typical that chain scission is homogenous along the whole cross section of a sample. This is caused by penetration of water into an approximate hydrophilic matrix, which triggers the hydrolysis of ester bonds (Figure 16b). In some special cases (high volume sample-like implants) degradation could be faster inside than on the surface due to the difficulty of low molecular weight compounds (acidic) to diffuse out, which leads to autocatalysis and faster hydrolysis inside rather than outside of the specimen (Figure 16c). As a consequence there is either no loss or minor mass loss till a certain time has passed. After this period, significant loss

of mass started as the degradation products are diffused out and the integrity of the specimen is highly disrupted [80, 81].

### **Surface erosion**

Described as degradation, this occurs at the surface and progresses from it into the bulk (Figure 16a). This is typical for polyanhydrides and poly(ortho-esters). Mass loss during degradation is linear because degradation products are simultaneously removed to the surrounding environment; however, the molecular weight of the remaining sample stays constant because water cannot penetrate the specimen. A surface erosion mechanism is especially desirable in the application of drug delivery [81].

### **Degradation rates of common synthetic polyesters**

Comparisons of the degradation times of synthetic biodegradable polyesters discussed in this work are summarized in Table 4. The differences in degradation rates are mainly related to the ability of water to diffuse to the polymers and sterical hindering of the bound ester by the presence of the pendant group (methyl-in polylactides). The former is principally affected by the degree of crystallinity and hydrophobicity. It is known that amorphous regions are degraded much faster than crystalline ones. Copolymers are generally degraded faster than homopolymers due to restricted crystallization, as mentioned in section 5.6 [82].

*Table 4 - Degradation times of different polyesters under physiological conditions [83]*

<b>Polymer</b>	<b>Degradation time (months)</b>
PLLA	18 - 24
PDLA	12 - 16
PGA	2 - 4
PDO	6 - 12
PCL	> 24
PLGA (50:50)	2
PDLGA (85:12)	5
PDLCL* (90:10)	2

\* copolymer of DL-lactide and caprolactone

## 7. Applications of synthetic biodegradable polyesters in medicine

The general applications of synthetic polyesters can be divided into two groups - medical and ecological. The latter is mainly limited to PLA and includes the packaging and fibre-producing sectors. However, this does not directly pertain to the main task of this work. Therefore, importance is paid to medical applications [12].

### Implants and surgery

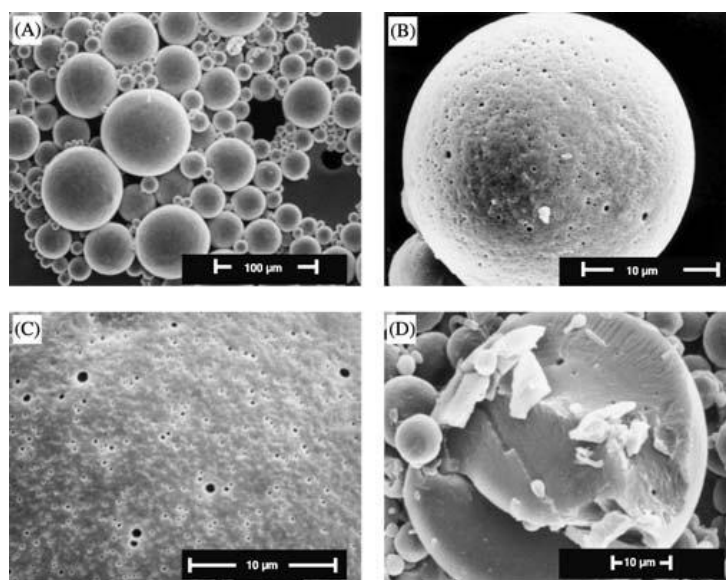
The first medical utilization of synthetic biodegradable polyesters was in sutures (Dexon®, Vicryl®), followed by fixation devices (Biofix). They are currently used in orthopaedic and oral surgeries in the form of plates, pins, screws, and wires. In contrast with metal devices, they do not need removal by further surgery after re-joining fractured bones, which is highly beneficial to patients. Degradation is driven mainly by the composition of the polymer (copolymerization). For sutures, the copolymers PLA, PGA, PCL and PDO tend to be used rather than pure homopolymers, while large implants are mainly based on PLA and PGA due to their good mechanical properties [37, 84]. Some examples of applications are shown in Figure 17. These products are produced by traditional processing methods for polymers, e.g. injection moulding [85, 86].



Figure 17 - Bioresorbable suture made from PDO (left); implants for fracture fixation (right)[86]

## Drug delivery systems (DDS)

The release of drugs, absorbed or encapsulated by polymers, involves their slow and controllable diffusion from/through polymeric materials. The objectives of DDS include the sustained release of drugs for a desired duration at an optimal dose and targeting drugs to diseased sites without affecting healthy sites. To this end, nanospheres (micelles), microspheres, or other shaped polymeric devices are utilized [12]. The shape of the most widely used drug carriers is a microsphere, which incorporates drugs and releases them through physical diffusion, followed by resorption of the microsphere material. Such microspheres can simply be prepared via a solvent-evaporation method [51, 87, 88, 89]. An example of a drug-loaded microparticle is depicted in Figure 18.



*Figure 18 - SEM micrographs of leuprorelin-loaded, poly(lactic-co-glycolic acid) (PLGA) based microparticles (Lupron Depot®) used for treating prostate cancer: A - overview on an ensemble of microparticles, B - surface of a single (smaller) microparticle, C - surface of a single (larger) microparticle, D - partial cross-section of a single microparticle. Reproduced with permission from (2006) Springer [90]*

## Scaffolds

Scaffolds are required for tissue construction if the lost part of the tissue is so large that it cannot be cured by conventional drug administration. Generally, scaffolds used in tissue engineering are porous and three-dimensional to encourage infiltration of a large number of cells into the scaffolds (Figure 19).

Currently, polymers used for scaffolding include PLGA, PCL and natural biopolymers [12]. For scaffold formation techniques the electrospinning process or solvent casting/salt leaching method are widely used [38, 91].

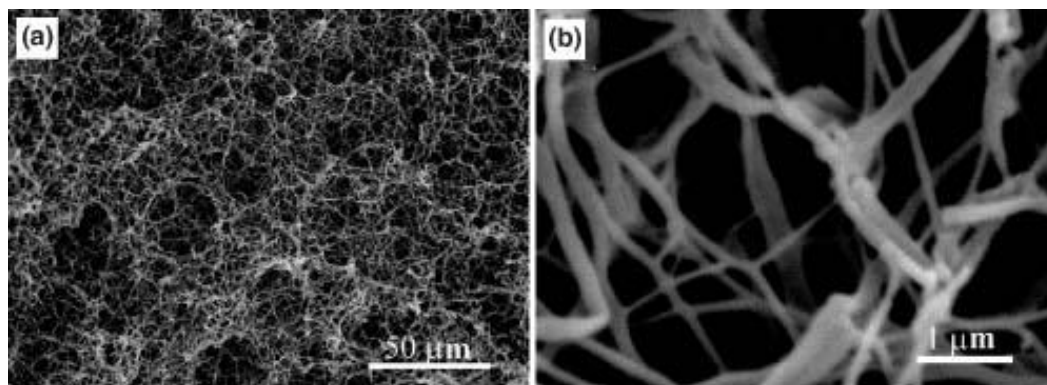


*Figure 19 - SEM micrographs of a poly(l-lactic acid) (PLLA) under different magnification (a, b.) Open access journal (2011) International Journal of Polymer Science [92]*

## **Hydrogels**

Hydrogels are three-dimensional networks formed from hydrophilic homopolymers, copolymers, or macromers (pre-formed macromolecular chains) crosslinked to form insoluble polymer matrices [93]. Biodegradable hydrogels can be used as haemostatic agents, wound covers, adhesion prevention layers, adhesives and drug carriers. As the synthetic polyesters discussed are bi-functional and relatively hydrophobic, their application in the hydrogel area is only possible in conjunction with the presence of cross-linkable components (PVA, Gelatine, PEG). An exhaustive review of these materials can be found under References [93, 94].

## **AIMS OF THE DOCTORAL STUDY**

Biodegradable polyesters appear to be materials with great potential in medical applications, such as drug delivery systems or tissue engineering. Polylactide is one of these promising types. Despite many works existing on synthesis, modification and/or degradation of PLA, many questions remain unanswered. Firstly, there is the question of the potential toxicity of the residual catalysts. Secondly, there is a need for polymer functionalization with respect to the relevant compatibility of the polymer with living organisms. Describing and understanding the degradation process under specific conditions is also important. The following goals have been defined on the basis of review of the literature and latest advances in the given field:

- Developing and optimizing the polylactide synthesis method through polycondensation of the lactic acid monomer using a non-metallic catalyst. The output should provide relevant information about reaction conditions providing a polymer with optimal molecular weight.
- Developing a novel synthesis procedure, leading to the introduction of polar functional groups into the structure of the polylactide. Detailed characterization of the product is a crucial part of this task.
- Investigating possible methods for increasing polylactide molecular weight by using novel postpolycondensation techniques.
- Describing the degradation process of the developed material under various conditions simulating the human body.

Besides these aims, the application aspect of research outcomes shall be considered. Cooperation with private companies as well as other academic institutions is naturally expected.

## SUMMARY OF THE PAPERS

In the following chapter, short summaries, major results and findings published in Papers I to IV, as attached, are presented. This chapter is divided into two thematic parts according to the main aims of the doctoral study; (i)*synthesis and modification of lactic acid based polymers and (ii)degradation behaviour under a specific abiotic condition.*

In **Paper I - “Optimization of reaction conditions and the characterization of L-Lactic acid direct polycondensation products catalysed by a non-metal-based compound”**, an investigation was conducted on preparing PLA catalysed by a non-metallic-based compound, methanesulfonic acid (MSA). The paper focused on researching optimal MSA concentration, reaction temperature and time.

The reaction was performed in a glass flask under the reduced pressure of 15 kPa and the following parameters were setup: Temperatures – 130, 145, 160, 175 and 190°C, MSA concentration – 0 - 1.6 wt%, reaction time - 6, 12, 18 and 24 hours. The products of polycondensation were characterized by gel permeation chromatography (GPC), viscometric measurements, Fourier transform infrared spectroscopy (FTIR) and differential scanning calorimetry (DSC). Prior to analyses, all the products were dissolved, precipitated into a water/methanol mixture, washed with distilled water a number of times and finally dried under reduced pressure for several days (30°C).

The results show that the optimal concentration of MSA was 0.5 wt%. The optimal MSA concentration was taken from the highest value of  $[\eta]$  after 24 hours (0.16 dl.g<sup>-1</sup>) and reaction conditions: 160°C, pressure 15 kPa. This concentration was maintained in all other experiments conducted at various temperatures and reaction times.

As the optimal reaction condition, the temperature 175°C and time of 18 hours were found to be most favourable. The values of  $M_w$  reached 17,200  $\text{g}\cdot\text{mol}^{-1}$ , with a polydispersity of below 2. Thermal analysis of the prepared PLAs showed the possible occurrence of two crystalline phases. The melting temperature and  $T_g$  shifted toward higher values with a rising  $M_w$ . The sample with the highest  $M_w$  showed melting peaks at 132°C and 147°C,  $T_g$  at 57°C and crystallinity ( $X_c$ ) of 40%.

The low molecular weight PLA obtained can be used in drug delivery applications or further copolymerization or modification through end groups.

**Paper II - “Functionalization of polylactic acid through direct melt polycondensation in the presence of tricarboxylic acid”** - described the modification of PLA by citric acid (CA). The goal of this work was to bring COOH groups into the polymer structure and investigate the resulting material properties.

In addition, detailed study of the co-polycondensation process, its limitations and an investigation into reaction products properties are other matters this article deals with.

The influence of CA on molecular weight, thermal and physicochemical properties and chemical structure of the products was investigated, using viscometric measurements, GPC, H-NMR spectroscopy, DSC, acidity number determination, and FTIR and UV spectroscopy.

Generally, adding CA to the reaction mixture led to significant reduction in the molecular weight of the polycondensation products. It was believed that CA terminated the growth of the polycondensates chain. However, at a low concentration of CA (up to 1 wt%), the involvement of citryl units in the polymer chain as well as subsequent branching is possible. The termination processes are predominant at higher CA contents. The thermal behaviour

showed that the materials possessed a semi-crystalline structure, but melting temperature generally dropped alongside increasing CA concentration.

The functionalized PLA material obtained can be potentially used in applications where improved interactions with living systems are required. In addition, the introduction of carboxyl provides an option for further functionalization of the material through immobilizing or entrapping bioactive species

**Paper III - “The effect of various catalytic systems on solid-state polymerization of poly(L-lactic acid)”** - was dedicated to evaluating the effect of various catalyst systems on solid-state polymerization (SSP) of PLA. This synthesis approach was found to be highly promising due to its simplicity, minimal energy requirements and high quality of the so prepared polymer. In this work, the following catalysts were used: tin dichloride, tin dioxide, tin octoate, citric acid, sulphuric acid, toluenesulfonic acid and methanesulfonic acid at the concentrations 0, 0.5, 1 and 2 wt%. The properties of the material prepared were studied in terms of molecular weight, structure and thermal properties.

Solid-state polycondensation was carried out under the pressure of 100 Pa and temperature of 130°C. In terms of molecular weight, the best results were achieved with methanesulfonic acid, sulphuric acid and tin octoate, with  $M_w$  ranging between 57,000 – 92,000 g.mol<sup>-1</sup>. Of these, sulphuric acid caused serious discoloration, probably connected with side reactions, although thermal stability was better than other two catalysts mentioned above. On the contrary, tin octoate was found to be the most effective catalyst from the viewpoint of  $M_w$ , however, its thermal stability was very poor, which can prove limiting in practical usage. Finally, 1 wt% MSA could be considered an optimal catalytic system for PLA post-polycondensation reaction, due to provision of a

reasonable balance between  $M_w$  enhancement as well as thermal stability of the products.

**Paper IV – “Novel aspects of the degradation process of PLA based bulky samples under conditions of high partial pressure of water vapour”** - described differences between the degradation of poly(L-lactic acid) bulky samples in a high humidity environment versus a buffered liquid medium. It is known that in some specific areas of the human body, like the respiratory tract or middle ear area, a high humidity environment is typical hence information on PLA degradation is essential.

In this work, the PLA specimens had the shape of a tube with the dimensions 10 x 4 mm in length and inner diameter, respectively. The PLA was synthesised in the laboratory, its  $M_w$  equalling 34,000 g.mol<sup>-1</sup>. Analytical techniques of optical and electron microscopy, GPC and SC were used to evaluate the material's morphology, molecular weight, crystallinity and thermal properties.

Degradation was studied separately in the core and surface of the test specimens under both testing conditions (100% relative humidity and liquid buffered medium, pH=7.4). It was found that degradation in the liquid medium led to multiphase core-cortex morphology formation, while the environment with high humidity provided homogeneous-like bulk degradation. Mass loss was more dominant in a liquid buffered medium due to the ability of the degradation product to dissolve and diffuse out from the specimen.

The measuring of thermal properties showed a noticeable decrease in the  $T_g$  and  $T_m$  of samples exposed to 100% relative humidity in contrast with the liquid buffered medium, probably due to the presence of degradation products which could not leave the matrix.

The results obtained can be applied, for example, in modelling and predicting PLA degradation in a high humidity environment.

## CONCLUSIONS

On the basis of the theoretical part of this work, it is clear that synthetic biodegradable polyesters are one of the most important biomaterials. Of these, particularly poly(lactic acid) and its copolymers play the most significant roles. They can be synthesized by polycondensation or ring opening polymerization to possess different variations and performance. Amongst these, simple polycondensation and solid-state polycondensation were the main focus of the practical part of this thesis.

Although this group of polymers exhibit very good performance in terms of mechanical and degradation behaviour, for certain applications it is sometimes necessary to modify them. Most adjustments are based on bulk (copolymerization, functionalization) or surface (plasma treatment) modifications.

The degradation of these kinds of materials under various conditions is widely known and described. Generally, the degradation of all synthetic biodegradable polyesters passes through hydrolysis of the ester bonds, which can even be random in complete matter, (homogenous – PLA, PGA), or can leach from its surface (heterogeneous – PCL). Once hydrolysis has reached a certain limit, when low molecular weight fragments are presented, these can be converted to waste or filtered out from a living system.

Such materials can be found in various medicinal applications, e.g. implants, scaffolds and drug delivery systems.

The practical part of this thesis can be concluded in two parts. The first is dedicated to the synthesis and modifications of a PLA based polymer, while the second describes degradation behaviour under a non-specific degradation environment. On the basis of experiments, the following general conclusions can be stated:

- Methanesulfonic acid can be used as a catalyst for the synthesis of PLA in such cases when non-toxic compounds are required.
- Citric acid can be used for carboxyl end group modification of PLA by a simple polycondensation reaction.
- Solid state polycondensation of low molecular weight PLA is an effective way of preparing high molecular weight, and particularly methanesulfonic acid and stannous octoate are very effective catalysts to achieve this.
- The degradation (hydrolysis) of a bulky PLA sample in an environment of high humidity is significantly different from that observed in a liquid buffered medium.

## **CONTRIBUTIONS TO SCIENCE AND PRACTICE**

The work presented provides the following contributions to science and technology.

- A PLA polymer containing a non-toxic and environmentally friendly catalyst has been successfully prepared by simple polycondensation reaction of lactic acid. The optimal reaction condition and its basic properties have been determined. The product can be potentially used in medicinal applications, like drug delivery.
- A polymer of lactic acid, containing citric acid was successfully synthesized and the structure and properties of this carboxyl-functionalized PLA were deeply described. It is believed that the material could find potential use in fabrication where enhanced hydrophilicity is necessary, or in further polymerization reactions, e.g. chain linking.
- New information on the catalysis and conditions of solid-state polycondensation of low molecular weight PLA was brought. This method is especially suitable due to low energy requirements and high polymer quality.
- Degradation of a PLA bulky sample in an environment of high humidity was described in detail and compared with that performed in a traditional liquid buffered medium. This information has never been published before and might be useful for predicting and modelling PLA implant degradation.

The research activities proceed within this work were parts of following projects implementations:

- CZ.1.05/2.1.00/03.0111 - Centre of Polymer Systems (MSM/RDIOP, 2011-2014)
- 2B08071 - New methods of using of whey, as byproduct from dairy production for production of biologically degradable polymers (MSM/2B Health and quality of life, 2008-2011)

- ME09072 - Study of polylactide based material for packaging applications (MSM/ME-KONTAKT, 2009 -2012)
- MEB061102 - Functionalized polymers of lactic acid for biocomposite preparation (MSM/ME-KONTAKT, 2011-2012)

Some of the results achieved within this work were protected by utility models. Transfer of the results is implemented through follow-up project in cooperation with private companies.

## **ACKNOWLEDGEMENTS**

Firstly, I would like to express the deepest gratitude to my supervisor, doc. Ing. Vladimír Sedlařík, Ph.D., for his professional leadership. My thanks go to him for creating an excellent research environment, his openness to discussion and willingness to impart knowledge and experience. Moreover, he has supported the author's participation at conferences and a foreign study programme.

I would also like to thank to my consultant, doc. Ing. Marian Lehocky, Ph.D., for rewarding discussions on the topics of the physico-chemical properties of polymers.

Special thanks goes to the author's colleague, Ing. Petr Stloukal, for help with brainstorming many ideas and his effective cooperation.

I also cannot fail to mention and thank all the co-authors of contributions, especially Dr Ida Poljansek from the University of Ljubljana and Dr Jan Drbohlav, Milcom a.s., Prague.

Last but not least, the author would like to thank friends and family for their understanding, patience and encouragement during the entire study period.

## LIST OF SYMBOLS AND ACRONYMS

GPC		gel permeation chromatography
DSC		differential scanning calorimetry
FTIR		Fourier transform infrared spectroscopy
H-NMR		proton nuclear magnetic resonance
TGA		thermogravimetry
PA		polyamide
PMMA		poly(methyl methacrylate)
PE		polyethylene
PLA		poly(lactic acid), polylactide
PLLA		poly(L-lactic acid), poly(L-lactide)
PEG		poly(ethylene glycol)
PDLA		poly(D-lactic acid), poly(D-lactide)
PDLLA		poly(DL-lactic acid), poly(DL-lactide)
PCL		poly( $\epsilon$ -caprolactone), poly(caprolactone)
PGA		poly(glycolic acid), polyglycolide
PDO		polydioxanone
PLGA		poly(lactic-co-glycolic acid)
ROP		ring opening polymerization
SP		solution polycondensation
MSA		methanesulfonic acid
PLA-PEG		poly(lactic acid-co-ethylene glycol)
$\delta_p$	$J^{0.5} \cdot cm^{-1.5}$	solubility parameter
$M_w$	$g \cdot mol^{-1}$	weight average molecular weight
SSP		solid state polymerization
$T_m$	$^{\circ}C$	melting temperature
$T_g$	$^{\circ}C$	glass transition temperature
DDS		drug delivery systems
PDLGA		poly(DL-lactic acid-co-glycolic acid), poly(DL-lactide-co-glycolide)
PDLCL		poly(DL-lactic acid-co-caprolactone), poly(DL-lactide-co-caprolactone)
PVA		poly(vinyl alcohol)

## LIST OF FIGURES AND TABLES

Figure 1 - Basic types of biomaterials .....	8
Figure 2 - Chemical structure of PLA .....	12
Figure 3 - Chemical structure of PGA .....	13
Figure 4 - Chemical structure of PCL.....	14
Figure 5 - Chemical structure of PDO .....	15
Figure 6 - Chemical structure of PLGA.....	16
Figure 7 - Linear hydroxy acids as monomers for polycondensation .....	17
Figure 8 - Cyclic monomers for ROP .....	17
Figure 9 - Solid state polycondensation process.....	19
Figure 10 - Mechanism of SSP of PLA catalyzed by binary catalyst system	19
Figure 11 - Structure of PLGA copolymer .....	22
Figure 12 - ROP synthesis of PLA/PEG copolymer type A-B.....	23
Figure 13 - The structures of functionalized PCL monomers with corresponding polymer structure .....	25
Figure 14 - Structure of maleic anhydride grafted on PLA chain .....	25
Figure 15 - Chemical surface modification through carboxylic groups .....	28
Figure 16 - Degradation modes for degradable polymers: surface erosion (a); bulk degradation (b); bulk degradation with autocatalysis (c). .....	29
Figure 17 - Bioresorbable suture made from PDO (left); implants for .....	31
Figure 18 - SEM micrographs of leuprorelin-loaded, poly(lactic-co-glycolic acid) (PLGA) based microparticles (Lupron Depot®) used for treating prostate cancer: A - overview on an ensemble of microparticles, B - surface of a single (smaller) microparticle, C - surface of a single (larger) microparticle, D - partial cross-section of a single microparticle.....	32
Figure 19 - SEM micrographs of a poly(l-lactic acid) (PLLA) under different magnification (a, b.).....	33

Table 1 - Division of synthetic biodegradable polymers based on chemical structure .....	10
Table 2 - Typical mechanical properties of PLA.....	13
Table 3 - Typical ROP and polycondensation conditions .....	16
Table 4 - Degradation times of different polyesters under physiological conditions .....	30

## REFERENCES

- [1] LANGER, R., TIRREL, D.A. Designing materials for biology and medicine. *Nature* 2004, vol. 428, p. 487-492.
- [2] BLACK, J. The education of the biomaterialist: Report of a survey 1980–81. *J. Biomed. Mater. Res.* 1982, vol. 16, no. 2, p. 159-167.
- [3] SHARMA, C., P. Biomaterials and Artificial Organs: Few Challenging Areas. *Trends Biomater. Artif. Organs.* 1982, vol. 18, no. 2, p. 148-157.
- [4] WILLIAMS, F., D. Definitions in Biomaterials. Elsevier Scientific, Amsterdam, 1987, p.72.
- [5] PARK, J., B. Biomaterials Science and Engineering, New York: Plenum Press, 1981.
- [6] SÁENZ, A., MUNOZ, E., R., BROSTOW, W., CASTANO, V., M. Ceramic biomaterials: an introductory overview. *J.Mater. Educ.* 1999, vol.21 no. 5-6, p. 297 – 306.
- [7] BHAT, S., V. Biomaterials, Narosha Publishing House, New Delhi, 2002, p. 272.
- [8] PISKIN, E. Biodegradable polymers as biomaterials. *J. Biomater. Sci. Polym. Ed.* 1995, vol. 6, no. 9, p. 775-95.
- [9] NAIR, L., S., LAURENCIN, C., T. Biodegradable polymers as biomaterials. *Prog. Polym. Sci.* 2007, vol. 32, no. 8–9, p. 762–798.
- [10] NAIR, L., S., LAURENCIN, C., T. Polymers as Biomaterials for Tissue Engineering and Controlled Drug Delivery. *Adv. Biochem. Engin. Biotechnol.* 2006, vol. 102, p. 47-90.
- [11] LLOYD, A., W. Interfacial bioengineering to enhance surface biocompatibility. *Med. Device. Technol.* 2002, vol. 13, p. 18–21.
- [12] IKADA, Y., TSUJI, H. Biodegradable polyesters for medical and ecological applications. *Macromol. Rapid Commun.* 2000, vol. 21, p. 117–132.
- [13] VERT, M., LI, M., S., SPENLEHAUER, G., GUERIN, P. Bioresorbability and biocompatibility of aliphatic polyesters. *J. Mater. Sci.* 1992, vol. 3, p. 432–446.
- [14] VROMAN, I., TIGHZERT, L. Biodegradable Polymers. *Materials* 2009, vol. 2, p. 307-344.
- [15] JACOBY, M. Custom-made biomaterials: Applying engineering, materials, and chemistry principles, researchers produce safe, smart, and effective implantable devices. *Science & Technology* 2001, vol. 79, no. 6 p. 30-35.
- [16] CHANDRA, R., RUSTGI, R. Biodegradable polymers. *Prog. Polym. Sci.* 198, vol. 2, no. 7, p. 1273–1335.
- [17] KAPAN, D., L. Biopolymers from renewable resources. Springer Verlag, Berlin, 1998, p. 414.

- [18] QIAN, Z., LI, S., HE, Y., ZHANG, H., LIU, X. Preparation of biodegradable polyesteramide microspheres. *Colloid Polym. Sci.* 2004, vol. 282, p. 1083–1088.
- [19] PARK, J., H., YE, M., PARK, K. Biodegradable Polymers for Microencapsulation of Drugs. *Molecules* 2005, vol. 10, p. 146–161.
- [20] GRODZINSKI, J., J. Biomedical application of functional polymers. *React. Funct. Polym.* 1999, vol. 39, p. 99–138
- [21] SANTERREA, J. P., WOODHOUSEB, K., LAROCHE, G., LABOWF, R., S. Understanding the biodegradation of polyurethanes: From classical implants to tissue engineering materials. *Biomaterials* 2005, vol. 26, no. 35, p. 7457–7470.
- [22] KUMAR, N., LANGER, R., S., DOMB, A., J. Polyamides: an overview. *Adv. Drug Deliver. Rev.* 2002, vol. 54, no. 7, p. 889–910.
- [23] CHIAO, M., CHUAL, J. Biomaterials for MEMS. Pan Stanford Publishing Pte. Ltd, Singapore, 2011, p. 280.
- [24] KYLMA, J., TUOMINEN, J., HELMINEN, A., SEPPALA, J. Chain extending of lactic acid oligomers. Effect of 2,2'-bis(2-oxazoline) on 1,6-hexamethylene diisocyanate linking reaction. *Polymer* 2001, vol. 42, p. 3333 – 3343.
- [25] ALLOCK, H., R. Chemistry and applications of polyphosphazenes. Wiley, New York, 2003, p. 744.
- [26] WU, CH., WANG, J., CHANG, P., CHENG, H., YU, Y., WU, Z., DONG, D., ZHAO, F. Polyureas from diamines and carbon dioxide: synthesis, structures and properties. *Phys. Chem. Chem. Phys.* 2012, vol. 14, p. 464–468.
- [27] VAUTHIER, C., DUBERNET, C., FATTAL, E., ALPHANDARY, H., P., COUVREUR, P. Poly(alkylcyanoacrylates) as biodegradable materials for biomedical applications. *Adv. Drug. Deliver Rev.* 2003, vol. 55, no. 4, p. 519–548.
- [28] MORITA, M., WATANABE, Y. A Secondary Alcohol Oxidase: a Component of a Polyvinyl Alcohol Degrading Enzyme Preparation. *Agr. Bio. Chem. Tokyo* 1977, vol. 41, no. 8, p. 1535–1537.
- [29] FINK, J., K. Handbook of Engineering and Specialty Thermoplastics, Volume 2 - Water Soluble Polymers. John Wiley & Sons, Hoboken, 2011, p. 489.
- [30] SAAD, B., KUBOKI, Y., WELTI, M., UHLSCHMID, G., K., NEUENSCHWANDER, P., SUTER, U., W. DegraPol-foam: a degradable and highly porous polyesterurethane foam as a new substrate for bone formation. *Artif. Organs.* 2000, vol. 24, no. 12, p. 939–45.
- [31] ABRAHAM, G., A., MORCO-FERNANDEZ, A., ROMÁN, J., S. Bioresorbable poly(ester-ether urethane)s from L-lysine diisocyanate and triblock copolymers with different hydrophilic character. *J. Biomed. Mater. Res. A.* 2006, no. 76, vol. 4, p. 729–36.

- [32] GARLOTTA, D. A Literature Review of Poly(Lactic Acid). *J. Polym. Environ.* 2001, vol. 9, no. 2, p. 63-84.
- [33] GUPTA, A.,P., KUMAR, V. New emerging trends in synthetic biodegradable polymers - Polylactide: A critique. *Eur. Polym. J.* 2007, vol. 43, no. 10, p. 4053-4074.
- [34] RAHUL, M., R. Poly(lactic acid) modifications. *Prog. Polym. Sci.* 2010, vol. 35, no. 3, p. 338-356.
- [35] DOMB, A, J., KOST, J., WISEMAN, D., M. Handbook of Biodegradable Polymers. Harwood academic publisher, Amsterdam, 1997, p. 526.
- [36] MONTES DE OCA, H., WARD, I., M. Structure and mechanical properties of PGA crystals and fibres. *Polymer* 2006, vol. 47, no. 20, p. 7070-7077.
- [37] MIDDLETON, J., C., TIPTON, A., J. Synthetic biodegradable polymers as orthopedic devices. *Biomaterials* 2000, vol. 21, no. 23, p. 2335-2346.
- [38] WOODRUFF, M., A., HUTMACHER, D., W. The return of a forgotten polymer—Polycaprolactone in the 21st century. *Prog. Polym. Sci.* 2010, vol. 35, no. 10, p. 1217-1256.
- [39] ESHRAGHI, S., DAS, S. Mechanical and microstructural properties of polycaprolactone scaffolds with one-dimensional, two-dimensional, and three-dimensional orthogonally oriented porous architectures produced by selective laser sintering. *Acta. Biomater.* 2010, vol. 6, no. 7, p. 2467-2476.
- [40] BOLAND, E., D., COLEMAN, B., D., BARNES, C., P., SIMPSON, D., G., WNEK, G., E., BOWLIN, G., L. Electrospinning polydioxanone for biomedical applications. *Acta. Biomater.* 2005, vol. 1, p. 115-123.
- [41] SUGIH, A., K., PICCHIONI, F., HEERES, H., J. Experimental studies on the ring opening polymerization of p-dioxanone using an Al(OiPr)<sub>3</sub>-monosaccharide initiator system. *Eur. Polym. J.* 2009, vol. 4, p. 155-164.
- [42] JONES D. Pharmaceutical Applications of Polymers for Drug Delivery. iSmithers Rapra Publishing, Shropshire, 2004, p. 124.
- [43] STEINBUCHER, A., MERCHESSAULT, R., H. Biopolymers for medical and pharmaceutical applications. Vol. 1, Wiley-VCH, Weinheim, 2005, p. 1133.
- [44] LIM, L., T., AURAS, R., RUBINO, M. Processing technologies for poly(lactic acid). *Prog. Polym Sci.* 2008, vol. 33, no. 8, p. 820-852.
- [45] OKADA, M. Chemical syntheses of biodegradable polymers. *Prog. Polym. Sci.* 2002, vol. 27, no. 1, p. 87-133.
- [46] NARAYANAN, N., ROYCHOUDHURY, P., K., SRIVASTAVA, A. L (+) lactic acid fermentation and its product polymerization. *Electron. J. Biotechn.* 2004, vol. 7, no. 2, p. 167-179.
- [47] YANG, K., WANG, H., WANG Y. Poly( p-dioxanone) and its copolymers. *J. Macromol. Sci-Pol. R.* 2002, vol. C42, no. 3, p. 373-398.
- [48] CHANFREAU, S., MENA, M., PORRAS-DOMINGUEZ, J., R., RAMIREZ-GILLY M., GIMENO, M., ROQUERO, P., TECANTE, A.,

- BARZANA, E. Enzymatic synthesis of poly-lactide and poly-L-lactide-co-glycolide in an ionic liquid. *Bioprocess. Biosyst. Eng.* 2010, vol. 33, p. 629-638.
- [49] MAHARANAA, T., MOHANTY, B., NEGI, Y., S. Melt–solid polycondensation of lactic acid and its biodegradability. *Prog. Polym. Sci.* 2009, vol. 34, no. 1, p. 99-124.
- [50] KUCHARCZYK, P. The effect of impurities on the properties of the lactic acid polycondensates, 2010. 75 pages, [cit. 18.7.2012] Tomas Bata Univerzity in Zlin. Master thesis. Available at WWW: [http://www.pdfdownload.org/pdf2html/pdf2html.php?url=http%3A%2F%2Fdspace.k.utb.cz%2Fbitstream%2Fhandle%2F10563%2F13009%2Fkucharczyk\\_2010\\_dp.pdf%3Fsequence%3D1&images=yes](http://www.pdfdownload.org/pdf2html/pdf2html.php?url=http%3A%2F%2Fdspace.k.utb.cz%2Fbitstream%2Fhandle%2F10563%2F13009%2Fkucharczyk_2010_dp.pdf%3Fsequence%3D1&images=yes)
- [51] Singh, V., Tiwari, M. Structure-Processing-Property Relationship of Poly(Glycolic Acid) for Drug Delivery Systems 1:Synthesis and Catalysis. *Int. J. Polym. Sci.* 2010, no. 2010, p. 1-23.
- [52] DUTKIEWICZ, S., Grochowska-Łapienis, D., Tomaszewski, W. Synthesis of poly(L(+) lactic acid) by polycondensation method in solution. *Fibres. Text. East. Eur.* 2003, vol. 11, no. 4, p. 66-70.
- [53] BAMFORD, C., H., WAYNE, R., P. Polymerization in the solid phase: A polycondensation reaction. *Polymer* 1969, vol. 10, p. 661-681.
- [54] TAKAHASHI, K., TANIGUCHI, I., MIYAMOTO, M., KIMURA Y. Melt/solid polycondensation of glycolic acid to obtain high-molecular-weight poly(glycolic acid). *Polymer* 2000, vol. 41, p. 8725–8728.
- [55] MOON, S., I., LEEB, C., W., TANIGUCHIA, I., MIYAMOTOA, M., KIMURA, Y Melt/solid polycondensation of L-lactic acid: an alternative route to poly(L-lactic acid) with high molecular weight. *Polymer* 2001, vol. 42, no. 11, p. 5059-5062.
- [56] MOON, S., I., LEE, C., W., MIYAMOTO, M., KIMURA, Y. Melt polycondensation of L-lactic acid with Sn(II) catalysts activated by various proton acids: a direct manufacturing route to high molecular weight poly(L-lactic acid). *J. Polym. Sci. Part A: Polym. Chem.* 2000, vol. 38, p. 1673–1679.
- [57] AJIOKA, A., ENOMOTO, K., SUZUKI, K., YAMAGUCHI, A. The basic properties of poly(lactic acid) produced by the direct condensation polymerization of lactic acid. *J. Environ Polym. Degrad.* 1995, vol. 3, pp. 225–234.
- [58] RASAL, R., H., JANORKAR, A., V., HIRT, D., E. Poly(lactic acid) modifications. *Prog. Polym. Sci.* 2010, vol. 35, p.338–356.
- [59] WANG, S., CUI, W., BEI, J. Bulk and surface modifications of polylactide. *Anal. Bioana.l Chem.* 2005, vol. 381, p. 547–556.
- [60] AMASS, W., AMASS, A., TIGHE, B. A Review of Biodegradable Polymers: Uses, Current Developments in the Synthesis and

- Characterization of Biodegradable Polyesters, Blends of Biodegradable Polymers and Recent Advances in Biodegradation Studies. *Polym. Int.* 1998, vol. 47, p. 49-144.
- [61] YASIN, M., HOLLAND, S., J., JOLLY, A., M., TIGHE, B., J. Polymers for biodegradable medical devices. VI. Hydroxybutyrate-hydroxyvalerate copolymers: accelerated degradation of blends with polysaccharides. *Biomaterials* 1989, vol. 10, no. 6, p. 400-412.
- [62] WANG, H., SUN, X., SEIB, P. Properties of poly(lactic acid) blends with various starches as affected by physical aging. *J. Appl. Polym. Sci.* 2003, vol. 90, p. 3683–3689.
- [63] BROZ, M., E., VANDERHART, D., L., WASHBURN, N., R. Structure and mechanical properties of poly(d,l-lactic acid)/poly(e-caprolactone) blends. *Biomaterials* 2003, vol. 24, p. 4181–90.
- [64] CHUENJITKUNTAWORN, B., INRUNG, W., DAMRONGSRI, D., MEKAAPIRUK, K., SUPAPHOL, P., PAVASANT, P. Polycaprolactone/hydroxyapatite composite scaffolds: preparation, characterization, and in vitro and in vivo biological responses of human primary bone cells. *J. Biomed. Mater. Res. A.* 2010 vol. 94, no. 1, p. 241–251.
- [65] KASUGA, T., FUJIKAWA, H., ABE, Y. Preparation of polylactic acid composites containing -Ca(PO<sub>3</sub>)<sub>2</sub> fibers. *J. Mater. Res.* 1998, vol. 14, p. 418-424.
- [66] KASUGA, T., OTA, Y., NOGAMI, M., ABE, Y. Preparation and mechanical properties of polylactic acid composites containing hydroxyapatite fibers. *Biomaterials* 2001, vol. 22, p. 19-23.
- [67] MAKADIA, H., K., SIEGEL, S., J. Poly Lactic-co-Glycolic Acid (PLGA) as Biodegradable Controlled Drug Delivery Carrier. *Polymers* 2011, vol. 3, p. 1377-1397.
- [68] HUH, K., M.; CHO, Y., W.; PARK, K. PLGA-PEG Block Copolymers for Drug Formulations. *Drug Deliv. Technol.* 2003, vol. 3, p. 1-10.
- [69] HE, G., MA, L., L., PAN, J., VENKATRAMAN, S. ABA and BAB type triblock copolymers of PEG and PLA: A komparative study of drug release properties and “stealth” particle characteristics. *Int. J. Pharm.* 2007, vol. 334, p. 48–55.
- [70] XIAO, R., Y., ZENG, Y., W., ZHOU, G., L., WANG, J., J., LI, F., Y., WANG, A., M. Recent advances in PEG–PLA block kopolymer nanoparticles. *Int. J. Nanomed.* 2010, vol. 5, p. 1057–1065
- [71] HU, Y., LIU, Y., QI, X, LIU, P., FANA, Z, LI, S. Novel bioresorbable hydrogels prepared from chitosan-graft-poly lactide copolymers. *Polym. Int.* 2012, vol. 61, p. 74–81.
- [72] SUYATMA, N., E., COPINET, A., LEGIN-COPINET, E., FRICOTEAUX, F., COMA, V. Different Pla Grafting Techniques on Chitosan. *J. Polym. Environ.* 2011, vol. 19, p. 166–171.

- [73] WILLIAMS, C., K. Synthesis of functionalized biodegradable polyesters. *Chem. Soc. Rev.* 2007, vol. 36, p. 1573–1580.
- [74] THEATO, P., KLOK, H., A. Functional Polymers by Post-Polymerization Modification: First edition. Weinheim, Germany: John Wiley & Sons, 2013. ISBN 352765545X.
- [75] LOU, X., DETREMBLEUR, C., JEROME, R. Novel Aliphatic Polyesters Based on Functional Cyclic (Di)Esters. *Macromol. Rapid Commun.* 2003, vol. 24, p. 161–172.
- [76] TANIGUCHI, I., KUHLMAN, W., A., MAYES, A., M., GRIFFITH, L., G. Review Functional modification of biodegradable polyesters through a chemoselective approach: application to biomaterial surfaces. *Polym. Int.* 2006, vol. 55, p. 1385–1397.
- [77] PAN, J., WANG, Y., QIN, S., ZHANG, B., LUO, Y. Grafting Reaction of Poly(D,L)lactic acid with Maleic Anhydride and Hexanediamine to Introduce More Reactive Groups in Its Bulk. *J. Biomed. Mater. Res. Part B: Appl. Biomater.* 2005, vol. 74B, p. 476–480.
- [78] LEE, S., H., KIM, S., H., HAN, Y., K., KIM, Y., H. Synthesis and Degradation of End-Group-Functionalized Polylactide. *J. Polym. Sci. A: Polym. Chem.* 2001, vol. 39, p. 973–985.
- [79] ENGINEER, C., PARIKH, J., RAVAL, .Review on Hydrolytic Degradation Behavior of Biodegradable Polymers from Controlled Drug Delivery System. *Trends Biomater. Artif. Organs* 2011, vol. 25, no. 2, p. 79-85.
- [80] BURKERSRODA, F., SCHEDL, L., GÖPFERICH, A. Why degradable polymers undergo surface erosion or bulk erosion. *Biomaterials* 2002, vol. 23, no. 2, p.1 4221–4231.
- [81] TAMADA, J., A., LANGER, R. Erosion kinetics of hydrolytically degradable polymers. *Proc. Natl. Acad. Sci. USA* 1993, vol. 90, p. 552-556.
- [82] MILLER, R., A., BRADY, J., M., CUTRIGHT, D., E. Degradation rates of oral resorbable implants (polylactides and polyglycolates): rate modification with changes in PLA/PGA copolymer ratios. *J. Biomed. Mater. Res.* 1977, vol. 11, p. 711 – 719.
- [83] LENDLEIN, A. Polymere als Implantatwerkstoffe. *Chem. Unserer Zeit* 1999, vol. 33, no. 5, p. 279-295.
- [84] ULERY, B., D., NAIR, L., S., LAURENCIN, C., T. Biomedical applications of biodegradable polymers. *J. Polym. Sci., Part B: Polym. Phys.* 2011, vol. 49, no. 12, p. 832-864.
- [85] XU, H., H., K., QUIN, J., B., Calcium phosphate cement containing resorbable fibers for short-term reinforcement and macroporosity. *Biomaterials* 2002, vol. 23, no. 1, p. 193-202.

- [86] CICCONE, W., J., MOTZ, C., BENTLEY, C., TASTO, J., P. Bioabsorbable Implants in Orthopaedics: New Developments and Clinical Applications. *J. Am. Acad. Orthop. Surg.* 2001, vol. 9, p. 280-288.
- [87] FUKUZAKI, H., YOSHIDA, M., ASANO, M., KUMAKURA, M., MASHIMO, T., YUASA, H., IMAI, K., YAMANAKA, H. In vivo characteristics of low molecular weight copolymers composed of L-lactic acid and various DL-hydroxy acids as biodegradable carriers for drug delivery systems. *Biomaterials* 1990, vol. 11, p. 441-446.
- [88] STLOUKAL, P., KUCHARCZYK, P., SEDLARIK, V., BAZANT, P., KOUTNY, M. Low Molecular Weight Poly(lactic acid) Microparticles for Controlled Release of the Herbicide Metazachlor: Preparation, Morphology, and Release Kinetics. *J. Agr. Food. Chem.* 2012, vol. 60, no. 16, p. 4111-4119.
- [89] KUMAR, M., N., V., R. Nano and microparticles as Controlled Drug Delivery device. *J. Pharm. Pharmaceut. Sci.* 2000, vol. 3, no. 2, p. 234-258.
- [90] SIEPMANN, J., SIEPMANN, F. Microparticles Used as Drug Delivery Systems. *Progr. Colloid. Polym. Sci.* 2006, vol. 133, p. 15-21.
- [91] SMITH, I., O., LIU, X., H., SMITH, L., A., MA, P., X. Nanostructured polymer scaffolds for tissue engineering and regenerative medicine. *WIREs Nanomed. Nanobiotechnol.* 2009, Vol. 1, no. 2, p. 226-236.
- [92] DHANDAYUTHAPANI, B., YOSHIDA, Y., MAEKAWA, T., KUMAR, D., S. Polymeric Scaffolds in Tissue Engineering Application: A Review. *Int. J. Polym. Sci.* 2011, vol. 2011, p. 1-19.
- [93] SLAUGHTER, B., V., KHURSHID, S., S., FISHER, O., Z., KHADEMHOSEINI, A., PEPPAS, N., A. Hydrogels in Regenerative Medicine. *Adv. Mater.* 2009, vol. 21, p. 3307-3329.
- [94] LI, Y., RODRIGUES, J., TOMÁS, H. Injectable and biodegradable hydrogels: gelation, biodegradation and biomedical applications. *Chem. Soc. Rev.* 2012, vol. 41, p. 2193-2221.

# APPENDIX A –PAPER I

## Optimization of the Reaction Conditions and Characterization of L-Lactic Acid Direct Polycondensation Products Catalyzed by a Non-Metal-Based Compound

Vladimir Šedlarik,<sup>1,2</sup> Pavel Kucharczyk,<sup>1</sup> Vera Kasparkova,<sup>3</sup> Jan Drbohlav,<sup>4</sup> Alexandra Salakova,<sup>4</sup> Petr Saha<sup>1</sup>

<sup>1</sup>Polymer Centre, Faculty of Technology, Tomas Bata University at Zlin, Namestí T. G. Masaryka 275, 76272 Zlin, Czech Republic

<sup>2</sup>Innovation Centre, University Institute, Tomas Bata University at Zlin, Nad Ovcirnou 3685, 76001 Zlin, Czech Republic

<sup>3</sup>Department of Biochemistry and Food Analysis, Faculty of Technology, Tomas Bata University at Zlin, Namestí T. G. Masaryka 275, 76272 Zlin, Czech Republic

<sup>4</sup>Dairy Research Institute, Milcom A.S., Ke Dvooru 12a, 16000 Prague, Czech Republic

Received 8 July 2009; accepted 15 September 2009

DOI 10.1002/app.31445

Published online 5 January 2010 in Wiley InterScience (www.interscience.wiley.com).

**ABSTRACT:** In this article, we deal with the investigation into a poly(lactic acid) (PLA) preparation process catalyzed by a non-metal-based compound. Low-molecular-weight PLA was synthesized by the direct melt polycondensation of L-lactic acid catalyzed by methanesulfonic acid (MSA). This study was focused on the investigation into optimal MSA concentration determination and into the temperature (130, 145, 160, 175, and 190°C) and time (6, 12, 18, and 24 h) influence on the structure (Fourier transform infrared spectroscopy), molecular weight (viscometric measurements

and gel permeation chromatography), and thermal properties (differential scanning calorimetry) of the samples. The results show an optimal MSA content of 0.5 wt %. The highest molecular weight of PLA prepared by this method was reached after 18 h of reaction at 175°C (weight-average molar mass =  $17.2 \times 10^3$  g/mol). © 2010 Wiley Periodicals, Inc. *J Appl Polym Sci* 116: 1597–1602, 2010

**Key words:** calorimetry; catalysts; FT-IR; polyesters; synthesis

### INTRODUCTION

Biodegradable polymers have attracted increasing interest over the past 2 decades, both in fundamental research and also for practical use. Poly(lactic acid) (PLA) is a synthetic biodegradable polyester, and it represents potential applicability in a growing number of technologies, such as orthopedics, drug delivery, sutures, and scaffolds, because of its excellent biocompatibility and bioresorbability.<sup>1,2</sup> The synthesis of PLA can be carried out through either the ring-opening polymerization of lactones or the direct polycondensation of the L-lactic acid (LA) monomer. The former method can be characterized by high-purity requirements set on reactants and enables production of products with high and medium molecular weights. On the other hand, the latter does not provide high-molecular-weight products. Both of the mentioned

methods require the presence of a catalyst.<sup>3</sup> There are many publications dealing with PLA synthesis with metal-based compounds as catalysts, frequently those based on tin.<sup>4</sup> However, the residual metal catalyst can pose a problem with regard to both the thermal stability and biocompatibility of PLA.<sup>5</sup>

In this article, we deal with PLA preparation by direct melt polycondensation using a nonmetal catalyst based on methanesulfonic acid (MSA). This simple organic acid was already reported as a catalyst for the polycondensation of glycolic/LAs by Moon et al.<sup>6</sup> Their results show that MSA could be more effective than conventional metal salts. In addition, MSA is expected to be particularly versatile for biomedical application of the resulting PLA because it can readily be removed from the product by washing or evaporation to reduce the risky effects produced by the residual catalyst.<sup>6</sup> On the other hand, there is no literature reporting MSA catalyst use for the polycondensation of LA itself.

With these observations in mind, a detailed examination of the catalytic effect of MSA on PLA synthesis was the aim of this study. Special attention was paid to the optimization of the catalyst concentration and the characterization of the resulting polymer in terms of structure, molecular weight, and thermal properties.

Correspondence to: V. Šedlarik (sedlarik@ft.utb.cz)

Contract grant sponsor: Ministry of Education, Youth, and Sports of the Czech Republic; contract grant numbers: 2B08071, ME 09072, MSM 7088352101.

*Journal of Applied Polymer Science*, Vol. 116, 1597–1602 (2010)  
© 2010 Wiley Periodicals, Inc.

## EXPERIMENTAL

### Materials

An 80% water solution of pure LA with an optical rotation of  $10.6^\circ$  (measured by an Optech P1000 polarimeter at  $22^\circ\text{C}$ , concentration = 10%; Krüss, Hamburg, Germany) was purchased from Lachner Neratovice, Czech Republic. MSA ( $\text{CH}_4\text{O}_2\text{S}$ ; 99.5%) was supplied by Sigma Aldrich (Steinheim, Germany). The solvents chloroform ( $\text{CHCl}_3$ ), acetone ( $\text{C}_3\text{H}_6\text{O}$ ), and methanol ( $\text{CH}_4\text{O}$ ; analytical grade) were bought from IPL Lukes (Uhersky Brod, Czech Republic). All chemicals were used as obtained without further purification.

### Polycondensation

A typical procedure was as follows: LA (50 mL) was added to a double-necked flask (250 mL) equipped with a Teflon stirrer. The flask was then placed in an oil bath heated by a magnetic stirrer with heating and connected to a laboratory apparatus for distillation under reduced pressure. The dehydration step followed (in all cases;  $160^\circ\text{C}$ , 15 kPa, 4 h, continuous mixing at 250 rpm). After LA dehydration, the reactor was disconnected from the vacuum pump, and the relevant amount (see details later) of MSA was added dropwise under continuous stirring. The flask with dehydrated LA and the relevant amount of MSA was connected back to the source of the vacuum (15 kPa), and the reaction continued for a given period of time (6, 12, 18, or 24 h) at temperatures of 130, 145, 160, 175, and  $190^\circ\text{C}$ . The beginning of the reaction time (time = 0 h) was considered the time of catalyst addition in this study. The resulting product, in the form of colorless or light brown viscous melt, was allowed to cool to room temperature and dissolved in  $\text{C}_3\text{H}_6\text{O}$  then. The polymer solution was precipitated in a mixture of chilled  $\text{CH}_4\text{O}$ /distilled water 1 : 1. The obtained powder was filtered, washed with  $\text{CH}_4\text{O}$ , and dried at  $45^\circ\text{C}$  for 48 h.

### Methods

#### Viscometric measurements

Viscosity measurements were performed in  $\text{CHCl}_3$  at  $30^\circ\text{C}$  in an Ubbelohde viscometer with capillary 0a (Technosklo, Drzkov, Czech Republic). The intrinsic viscosity ( $[\eta]$ ) was calculated with eq. (1):

$$[\eta] = \lim_{c \rightarrow 0} \frac{\eta_{\text{rel}} - 1}{c} \quad (1)$$

where  $\eta_{\text{rel}}$  is the relative viscosity, which is equal to the ratio of the polymer solution and pure solvent viscosities, and  $c$  is the concentration of the polymer solution (0.4, 0.8, and 1.2 wt/vol %).

*Journal of Applied Polymer Science* DOI 10.1002/app

#### Determination of the molecular weight by gel permeation chromatography (GPC)

GPC analyses were performed with a Breeze chromatographic system (Waters, Milford, MA) equipped with a PLgel Mixed-D column ( $300 \times 7.8 \text{ mm}^2$ ,  $5 \mu\text{m}$ ; Polymer Laboratories, Ltd.). For detection, a Waters 2487 dual-absorbance detector at 239 nm was used. Analyses were carried out at room temperature with a flow rate of 1.0 mL/min in  $\text{CHCl}_3$ . The column was calibrated with narrow-molecular-weight polystyrene standards with molar masses ranging from 580 to 480,000 g/mol (Polymer Laboratories, Ltd.). A 100- $\mu\text{L}$  injection loop was used for all measurements. The sample concentration ranged from 1.6 to 2.2 mg/mL. Data processing was carried out with Waters Breeze GPC software (Waters). The weight-average molar mass ( $M_w$ ), number-average molar mass ( $M_n$ ), and polydispersity of the tested samples were determined.

#### Infrared spectroscopy

To identify the physicochemical structure of the LA polycondensation products, Fourier transform infrared (FTIR) analysis was carried out. The investigation was conducted on a NICOLET 320 FTIR spectrometer (Nicolet Instruments Co., Madison, WI) equipped with an attenuated total reflectance (ATR) accessory with a Zn-Se crystal and the software package OMNIC (Nicolet Instruments Co.) over the range  $4000\text{--}650 \text{ cm}^{-1}$  at room temperature. A uniform resolution of  $2 \text{ cm}^{-1}$  was maintained in all cases.

#### Differential scanning calorimetry (DSC)

For the determination of the glass-transition temperature ( $T_g$ ), melting point, and crystallinity ( $\chi_c$ ) of the polycondensates, DSC was used. Approximately 4 mg of sample was placed in an aluminum pan, sealed, and analyzed on a PerkinElmer (Waltham, MA) Pyris 1 differential scanning calorimeter calibrated with indium in terms of temperature and heat flow. The experiments were performed under a nitrogen atmosphere (20 mL/min) in two scans in the temperature range  $0\text{--}170^\circ\text{C}$  and at a heating rate of  $10^\circ\text{C}/\text{min}$ .  $\chi_c$  (%) was estimated by the following equation:

$$\chi_c = \frac{\Delta H_m}{\Delta H_m^0} \times 100 \quad (2)$$

where  $\Delta H_m^0$  is the enthalpy of mixing for 100% crystalline PLA (93.7 J/g) adopted from Fischer et al.<sup>7</sup> and  $\Delta H_m$  represents the measured melting enthalpy of the sample taken from the first heating scan.

## RESULTS AND DISCUSSION

### Optimal catalyst concentration determination

The syntheses of PLA were performed with the method of the direct polycondensation of LA in the

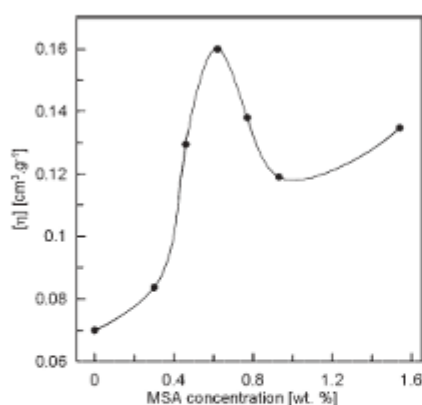


**Figure 1**  $[\eta]$  of the polycondensates (160°C, 24 h, and 15 kPa) versus the amount of the catalyst (MSA).

presence of MSA as non-metal-based catalyst. The use of this simple alkylsulfonic acid for the catalysis of LA and glycolic acid polycondensation was already reported by Moon et al.<sup>6</sup> The authors used a fixed amount of MSA (0.3 wt %). However, the catalyst content plays an important role in relation to the resulting product. The determination of the optimal MSA concentration for LA polycondensation was made through a series of experiments with different MSA contents (from 0 to 1.6 wt % related to the initial mass of LA) according to the method described previously. The temperature of reaction was 160°C, the pressure was 15 kPa, and the time was 24 h. The products were investigated by viscometric measurements. The dependence of  $[\eta]$  on the MSA catalyst content is shown in Figure 1. As shown,  $[\eta]$  of the polymer solutions representing the molecular weight of the products rose significantly with increasing content of MSA up to 0.5 wt %. Further additions of the catalyst led to  $[\eta]$  reduction. A color change, observed as a darkening of the product, was noticed also; it probably occurred because of the side and degradation reactions that may have taken place at higher MSA concentrations. Interestingly, a slight  $[\eta]$  enhancement was observed at the highest investigated MSA content, that is, 1.6 wt %. On the basis of these results, 0.5 wt % of MSA was selected as the optimal catalyst content for further experiments.

#### Viscometric characterization of the products

The results obtained from the viscosity measurements of the diluted polymer solutions ( $\text{CHCl}_3$ , 30°C) are summarized in Table I. The table shows values of  $[\eta]$  depending on the reaction time and

temperature. Generally, a higher reaction time produced a higher molecular weight (represented by  $[\eta]$ ) of the products. The only exceptions was found for the sample series prepared at 175°C, where the PLA obtained after 18 h of reaction showed a higher  $[\eta]$  than the product synthesized for 24 h. This unexpected result was verified several times with the same outcome. The data shown in Table I reveal the optimal polycondensation temperature and time of 175°C and 18 h, respectively. The lower reaction temperatures did not provide the product with comparable properties nor did the highest tested temperature of 190°C, which was more favorable for degradation reactions.

#### GPC analysis

The molecular weight of the polycondensation products prepared under various conditions was determined by the GPC method. The results of the analysis are presented in Table II. As shown, in accordance with viscosity, the highest molecular weight was detected in the sample with a polycondensation temperature of 175°C and a time of 18 h. The polydispersity of the sample was below 2 in all cases, which corresponded to the generally accepted polydispersity of polycondensation polymers.

The comparison of  $[\eta]$  (Table I) and  $M_w$  (Table II) showed a reasonably good correlation between these two parameters. Differential distribution curves recorded for the reactions conducted at the optimum temperature of 175°C for various reaction times are depicted in Figure 2. It was obvious that at a given temperature, the molecular weights of PLA increased with prolonged reaction time up to 18 h. This was evidenced by the gradual shift in the distribution curves to high-molecular-weight regions [Fig. 2(a,b,d)]. However, the reaction time of 24 h provided PLA with an  $M_w$  value that was lower than that observed in the sample synthesized for 18 h [Fig. 2(c)]. Here, a decrease in the molecular weight occurred because of decomposition.

**TABLE I**  
Temperature and Reaction Time Effects on the  $[\eta]$  Values of the Prepared PLA

Temperature (°C)	$[\eta]$ in $\text{CHCl}_3$ at 30°C ( $\text{cm}^3/\text{g}$ )			
	6 h	12 h	18 h	24 h
130	0.07	0.10	0.10	0.17
145	0.05	0.08	0.13	0.16
160	0.09	0.08	0.10	0.16
175	0.10	0.17	0.21	0.19
190	0.15	0.09	0.11	0.14

The catalyst was 0.5 wt % MSA, and the pressure was 15 kPa.

**TABLE II**  
**GPC Characterization of the LA Polycondensation**  
**Products Prepared Under Various Conditions**

Temperature (°C)	Reaction time (h)	$M_n$ ( $10^3$ g/mol)	$M_w$ ( $10^3$ g/mol)	$M_w/M_n$
130	6	3.0	4.1	1.3
	12	4.8	6.1	1.3
	18	3.3	4.9	1.5
	24	5.5	7.3	1.3
145	6	3.3	4.0	1.2
	12	4.0	4.7	1.2
	18	7.1	10.3	1.4
	24	9.4	14.3	1.5
160	6	3.9	4.7	1.2
	12	4.5	5.3	1.2
	18	6.0	8.6	1.4
	24	5.5	6.9	1.3
175	6	5.0	7.7	1.6
	12	8.2	14.1	1.7
	18	10.6	17.2	1.6
	24	7.9	11.6	1.5
190	6	7.6	11.6	1.5
	12	5.1	6.8	1.3
	18	8.6	12.8	1.5
	24	8.9	13.5	1.6

Reaction time 0 was considered to be the time of catalyst addition.

### Thermal properties

A series of PLA samples synthesized at 175°C was selected for detailed DSC analysis; DSC heating thermograms (first heating scan) of the dehydrated LA (4 h of dehydration without catalyst at 160°C and 15 kPa) and PLA obtained after 6, 12, 18, and 24 h of polycondensation are shown in Figure 3. Generally, the melting temperature is expected to increase with

increasing  $M_w$ .<sup>8</sup> As shown, the product of LA dehydration [Fig. 3(a)] showed two exothermic peaks located at 98 and 115°C. The addition of catalyst and the subsequent course of the reaction led to a shift in the transition peaks to higher temperatures, as was to be expected with rising molecular weight of the polycondensates [Fig. 3(b–d)]. The sample with the highest  $M_w$  [Fig. 3(d)] also showed the highest melting temperature. Its endothermic peaks occurred at 132 and 147°C. The occurrence of two melting peaks and their shift with increasing  $M_w$  revealed the presence of two types of crystalline structures. On the other hand, the PLA sample that was prepared for 24 h [Fig. 3(e)] had only one peak, found at 145°C. This fact could mean that the increase in the reaction temperature caused the formation of a more uniform crystalline structure. The occurrence of two crystalline structures might also have been caused by the precipitation procedure used for crude product purification, where a mixture of  $\text{CH}_2\text{O}$  and water was used. It would be interesting to follow the thermal transition of PLA purified by a different solvent or by the same solvent mixture with various  $\text{CH}_2\text{O}$ /water ratios. The second heating scans of the samples (not presented here) showed a clear presence of  $T_g$ , which increased with rising  $M_w$  of the samples. This typical trend is depicted in Figure 4 as a result of detected  $T_g$  on  $[\eta]$ . As shown, the measured  $T_g$  varied from 34°C (for the sample  $[\eta] = 0.07 \text{ cm}^3/\text{g}$ ) to 57°C (for the sample  $[\eta] = 0.21 \text{ cm}^3/\text{g}$ ). The literature data presented by Jamshidi et al.<sup>8</sup> demonstrated that a typical PLA  $T_g$  varies with its molecular weight (PLA with  $M_n = 430 \text{ g/}$

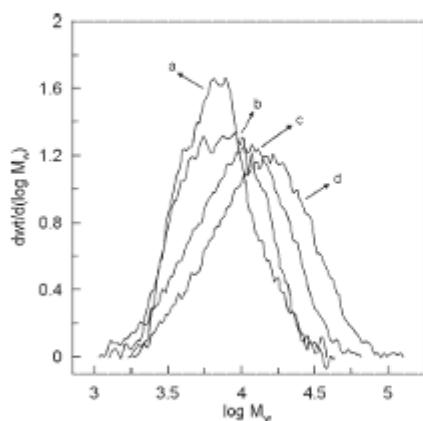


**Figure 2** Differential distribution curves of selected polycondensation products with various  $[\eta]$  values: (a) 0.1, (b) 0.17, (c) 0.19, and (d) 0.21  $\text{cm}^3/\text{g}$ .

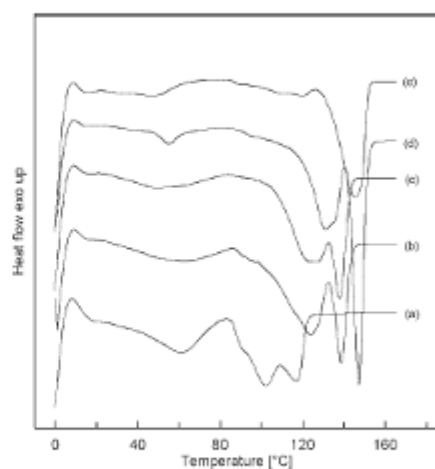


**Figure 3** DSC curves of (a) dehydrated LA (4 h, 160°C, and 15 kPa) and (b–e) PLA prepared at 175°C and 15 kPa for 6, 12, 18, and 24 h, respectively.

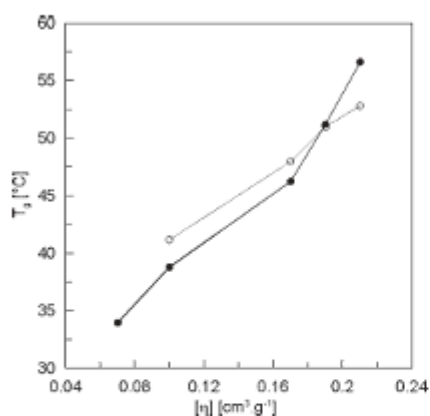


**Figure 4**  $T_g$  versus  $[\eta]$  for the prepared PLA [full symbols represent experimental results, and empty symbols represent values calculated according to eq. (3)].

mol shows  $T_g = -8^\circ\text{C}$  and PLA of  $M_n = 23 \times 10^3$  g/mol shows  $T_g = 55.5^\circ\text{C}$ .

The obtained results were in agreement with the  $T_g$  calculations (Fig. 4) performed according to the Fox-Flory equation:

$$T_g = T_g^\infty - \frac{K}{M_n} \quad (3)$$

where  $T_g^\infty$  is the glass-transition temperature at an infinite molecular weight of the polymer and  $K$  is a constant representing the excess free volume of the polymer chains end groups. The calculation of theoretical  $T_g$  was done with the  $M_n$  determined by GPC (Table II) and the values reported by Jamshidi et al.,<sup>9</sup> who reported  $T_g^\infty = 58^\circ\text{C}$  and  $K = 5.5 \times 10^4$  for low- $\chi_c$  PLLA.<sup>9</sup> However, eq. (3) failed in the low- $M_n$  product of LA dehydration ( $[\eta] = 0.07$  cm<sup>3</sup>/g). A negative deviation of the theoretical value from the measured  $T_g$  values was noticed because of a rising  $\chi_c$  (taken from the first heating scan), which occurred with the prolonged time of polycondensation (Fig. 5). However,  $T_g$  and  $\chi_c$  depended on the thermal history of the sample, as reported in many articles.<sup>3</sup>

### Infrared spectroscopy

The typical FTIR-ATR spectra of the polycondensation products synthesized at various temperatures over 24 h are shown in Figure 6. The qualitative analysis of the obtained FTIR-ATR records showed the typical spectra of PLA, which were in agreement with the results reported elsewhere.<sup>10,11</sup> All presented spectra were characterized by peaks located at 2997 and 2945 cm<sup>-1</sup>. These represented asymmet-

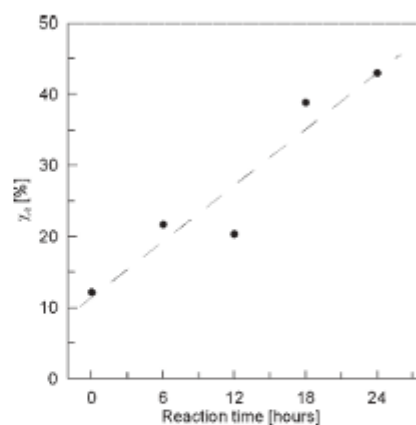


**Figure 5** Development of  $\chi_c$  with increasing polycondensation time (175°C, 0.5 wt % MSA, and 15 kPa).

ric and symmetric  $-\text{CH}-$  stretching, respectively. The C=O absorbance region was found at 1753 cm<sup>-1</sup>. The peak occurring at 1450 cm<sup>-1</sup> was typical for  $\text{CH}_2-$  banding.  $-\text{CH}-$  deformation and asymmetric banding appeared at 1381 and 1366 cm<sup>-1</sup>, respectively. The peak at 1265 cm<sup>-1</sup>, which was clear, especially in the case of the PLA prepared at 190°C, was assigned to the C—O stretching of the ester groups and carboxylic acid's oligomers.<sup>12</sup> The region between 1300 and 1050 cm<sup>-1</sup> showed four intensive absorption peaks at 1183, 1131, 1090

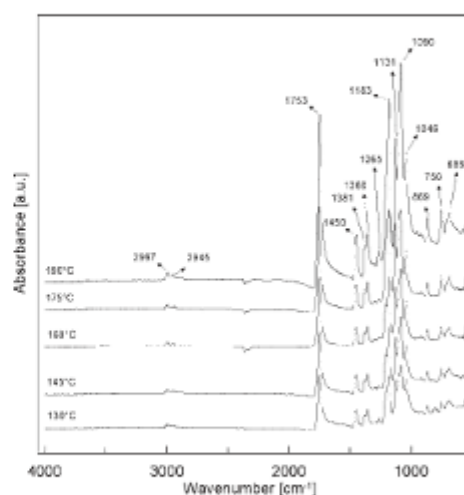


**Figure 6** FTIR-ATR spectra of PLA prepared at various temperatures (24-h reaction time, 0.5 wt % MSA, and 15 kPa).

(C—O—C stretching), and  $1046\text{ cm}^{-1}$  (—OH bending). According to Auras et al.,<sup>3</sup> the peaks located at  $869$  and  $750\text{ cm}^{-1}$  corresponded to —C—C— stretching. In addition, the peak at  $869\text{ cm}^{-1}$  was assigned to the amorphous phase, and the peak at  $750\text{ cm}^{-1}$  was assigned to the crystalline phase.<sup>3</sup>

Qualitative analysis of FTIR-ATR spectra, that is, the estimation of the molecular weight based on recorded FTIR-ATR spectra is generally possible. The peak at  $1450\text{ cm}^{-1}$  was reported to be a suitable internal standard for spectra normalization.<sup>11</sup> However,  $M_w$  differences among the samples prepared were not significant enough to reach reliable correlation between the normalized area of the selected peak and  $M_w$  in our case.

### CONCLUSIONS

PLA was prepared by method of the direct melt polycondensation of LA with the nonmetal catalyst MSA as a potential substitute for heavy-metal-based catalysts commonly used for PLA preparation. The influence of reaction time and temperature at a given catalyst content and pressure on the molecular weight was investigated through the characterization of the resulting product. The optimal catalyst concentration, molecular weight (viscometric measurements and GPC), thermal properties (DSC), and structure (FTIR spectroscopy) of the obtained PLA were investigated subsequently.

The results reveal that the optimal concentration of MSA was  $0.5\text{ wt } \%$  related to the mass of LA. This MSA concentration was kept for all LA polycondensates prepared at various temperatures and reaction times.

Generally, a temperature of  $175^\circ\text{C}$  was observed to be the most favorable for the direct melt polycondensation of LA. The highest  $[\eta]$  was obtained after

$18\text{ h}$  of reaction at  $175^\circ\text{C}$  and at a pressure of  $15\text{ kPa}$  ( $[\eta] = 0.21\text{ cm}^3/\text{g}$ ). This was in agreement with the molecular weight values measured by GPC analysis. The mentioned conditions provided PLA with  $M_w = 17.2 \times 10^3\text{ g/mol}$  and a polydispersity index below 2 in all cases. The thermal analysis of the prepared PLAs showed the possible occurrence of two crystalline phases. The melting temperature and  $T_g$  shifted toward higher values with rising  $M_w$ . The sample with the highest  $M_w$  showed melting peaks at  $132$  and  $147^\circ\text{C}$ ,  $T_g$  at  $57^\circ\text{C}$ , and  $\chi_c$  of  $40\%$ .

The qualitative analysis of the obtained infrared spectra confirmed the agreement with the data reported in already published literature sources dealing with structural characterization of PLA.

The use of non-metal-based catalysts for the synthesis of PLA through the direct melt polycondensation of LA provides an alternative to metal catalysts and is suitable for the production of low-molecular-weight biodegradable and biocompatible polymers designed for various biomedical applications.

### References

1. Jacobsen, S.; Degee, P. H.; Fritz, H. G.; Dubois, P. H.; Jerome, R. *Polym Eng Sci* 1999, 39, 1311.
2. Kricheldorf, H. R. *Chemosphere* 2001, 43, 49.
3. Auras, R.; Harte, B.; Selke, S. *Macromol Biosci* 2004, 4, 835.
4. Gupta, A. P.; Kumar, V. *Eur Polym J* 2007, 43, 4053.
5. Cam, D.; Marucci, M. *Polymer* 1997, 38, 1879.
6. Moon, S. I.; Deguchi, K.; Miyamoto, M.; Kimura, Y. *Polym Int* 2004, 53, 254.
7. Fischer, E. W.; Sterzel, H. J.; Wegner, G. *Colloid Polym Sci* 1973, 251, 980.
8. Ikada, Y.; Tsuji, H. *Macromol Rapid Commun* 2000, 21, 117.
9. Jamshidi, K.; Hyon, S. H.; Ikada, Y. *Polymer* 1988, 29, 2229.
10. Garlotta, D. *J Polym Environ* 2001, 9, 63.
11. Kister, G.; Cassanas, G.; Vert, M. *Polymer* 1998, 39, 267.
12. Socrates, G. *Infrared Characteristic Group Frequencies*, 2nd ed.; Wiley: Chichester, United Kingdom, 2004; p 15.

# APPENDIX B –PAPER II

## Functionalization of Polylactic Acid Through Direct Melt Polycondensation in the Presence of Tricarboxylic Acid

Pavel Kucharczyk,<sup>1</sup> Ida Poljansek,<sup>2,3</sup> Vladimír Sedlárik,<sup>1,4</sup> Verá Kasparková,<sup>5</sup>  
Alexandra Saláková,<sup>6</sup> Jan Drbohlav,<sup>6</sup> Uros Cvelbar,<sup>4</sup> Petr Saha<sup>1</sup>

<sup>1</sup>Centre of Polymer Systems, Polymer Centre, Tomas Bata University in Zlin, 760 01 Zlin, Czech Republic

<sup>2</sup>National Institute of Chemistry, Hajdrihova 19, 1000 Ljubljana, Slovenia

<sup>3</sup>Centre of Excellence Polymer Materials and Technologies, 1000 Ljubljana, Slovenia

<sup>4</sup>Jozef Stefan Institute, 1000 Ljubljana, Slovenia

<sup>5</sup>Department of Fat, Tensile and Cosmetics Technology, Faculty of Technology, Tomas Bata University in Zlin, 76272 Zlin, Czech Republic

<sup>6</sup>Milcom a.s. Ke Dvoru 12a, 16000 Prague, Czech Republic

Received 8 July 2010; accepted 30 January 2011

DOI 10.1002/app.34260

Published online 21 May 2011 in Wiley Online Library (wileyonlinelibrary.com).

**ABSTRACT:** The goal of the article was to describe the preparation of carboxyl-functionalized polylactic acid (PLA) through the method of direct melt copolycondensation of lactic and citric acid (CA). In addition, detailed study of copolycondensation process, its limitations and investigation of the reaction products properties are another issue this article deals with. The effect of tricarboxylic CA on the resulting properties of the functionalized lactic acid (LA) polycondensates was studied in a wide range of LA/CA molar ratios. The influence of CA on molecular weight, thermal and physicochemical properties, and chemical structure of the products was investigated, using viscometric measurements of the polymer solutions, gel permeation chromatography, <sup>1</sup>H nuclear magnetic resonance spectroscopy, differential scanning calorimetry,

acidity number determination, and Fourier-transform infrared and ultraviolet spectroscopy. The results show the significant effect of CA on the structure and physicochemical properties as well as high efficiency of functionalization. Furthermore, a branched structure was detected at low CA concentrations, while higher CA content leads to termination of the polycondensates chains by citryl units and a reduction in the molecular weight. Here, insights on the characterization methods of PLA-based materials are given by various experimental techniques. © 2011 Wiley Periodicals, Inc. *J Appl Polym Sci* 122: 1275–1285, 2011

**Keywords:** functionalization of polymers; biodegradable; polyesters; synthesis; gel permeation chromatography (GPC)

### INTRODUCTION

In recent years, biodegradable polymers have been investigated extensively for their potential applications in medical and pharmaceutical fields.<sup>1–4</sup> Polylactic acid (PLA) is one of the promising biodegradable polymers, which belongs to the group of aliphatic polyesters. The excellent properties of PLA

and its copolymers, such as biodegradability and biocompatibility, predetermine them to be used for medical devices (sutures, bone fixations, and implants) and also drug carriers (nano- and microparticles and polymer–drug conjugates) as reported in many publications.<sup>5–8</sup> In addition, there are other nonmedical areas of PLA use, which are objects of both scientific and practical use interest due the possibility of PLA production based on environmental friendly technologies availing renewable materials (biodegradable packaging, materials based on renewable resources).<sup>9,10</sup>

The demands made on the materials applied especially in medical area (biocompatibility, improved polymer–organism interaction, and functionality) lead to the subsequent necessity for further modifications of PLA.<sup>11</sup> The process of copolymerization has been already indicated above. It represents the most effective of PLA modifications in bulk. Many works dealing with preparation of lactic acid (LA)/glycolic acid copolymers have been reported.<sup>12,13</sup> The introduction of hydroxyl groups into PLA chains has been described by copolymerization of

Correspondence to: V. Sedlárik (sedlarik@ft.utb.cz)

Contract grant sponsor: Ministry of Education, Youth and Sports of the Czech Republic; contract grant number: 2B08071.

Contract grant sponsor: European Regional Development Fund; contract grant number: CZ.1.05/2.1.00/03.0111.

Contract grant sponsor: Ministry of Higher Education, Science and Technology of the Republic of Slovenia; contract grant numbers: P2-0145, P4-0015-0481.

Contract grant sponsor: Slovenian Research Agency (ARRS); Science and Education Foundation of the Republic of Slovenia.

*Journal of Applied Polymer Science*, Vol. 122, 1275–1285 (2011)  
© 2011 Wiley Periodicals, Inc.

LA with, e.g., polyethylene glycol.<sup>14</sup> The introduction of thiol groups into PLA chain ends can be mentioned as another example.<sup>15</sup> On the other hand, effective surface modifications can be achieved by plasmatic treatment of a polymer.<sup>16–18</sup> In case of PLA, noticeable improvement of surface biocompatibility has been obtained, for instance, by ammonia plasma treatment.<sup>19,20</sup>

This work is dedicated to the preparation of PLA-based copolymers with an increased amount of carboxyl functional groups. It is done by copolymerization of LA with, tricarboxylic, citric acid (CA) by direct polycondensation of LA and CA in the molten state. The resulting product, poly(*l*-lactic acid-co-citric acid) (PLACA) is expected to have improved interactions with living systems.<sup>21</sup> In addition, the introduction of carboxyl provides the eventuality for further functionalization of the material through immobilizing or entrapping of bioactive species.<sup>17</sup> The preparation of PLACA oligomer prepared by direct polycondensation has been already published by Yao et al.<sup>21</sup> However, his work concentrates only on two comonomer molar ratios (12 : 1 and 24 : 1). The reaction was catalyzed by stannous chloride in this work. The product of reaction has a molecular weight below 1500 and 2200 g mol<sup>-1</sup> for ratios 12 : 1 and 24 : 1, respectively (determined by GPC). It is clear that these materials are not suitable for load-bearing medical applications such as orthopedic implants because of their weak mechanical properties as a consequence of low-molecular weight. On the other hand, functionalized low-molecular weight polylactide and its copolymers can find their use in the areas where high-mechanical performance is not needed and where the main stress is put on chemical properties of the materials. Encapsulation<sup>22,23</sup> and coating<sup>24</sup> techniques or tissue adhesives<sup>25</sup> can be mentioned as an example. In addition, the presence of reactive groups in the polylactide structure offers a possibility for chain-linking reactions. For instance, Yao's group have further described the preparation of multiblock copolymer based on LA/CA copolycondensate and polyethylene glycol (10,000 g mol<sup>-1</sup>). The product of the reaction proved molecular weight over 75,000 g mol<sup>-1</sup>.<sup>26</sup>

Despite the polycondensation of the LA and CA has been already investigated<sup>21</sup> several, from the practical applicability point of view, questions remains to be answered. First, it is necessary to determine the maximal possible extend of PLA functionalization by carboxyl groups by the polycondensation method. Second, the effect of functionalization on the reaction product properties needs to be described. Last but not least, the structural parameters should be known for the purpose of the further intended application in the field of bioactive materials preparation. Keeping these facts in mind, the aim

of this study is to prepare and characterize the PLACA by direct melt polycondensation of LA and CA at high CA comonomer concentrations (0–20 wt %, i.e., LA:CA molar ratio from 9 : 1 up to 211 : 1). The crucial attention is paid to the determination of carboxyl functionalization on structural properties by using gel permeation chromatography (GPC), <sup>1</sup>H nuclear magnetic resonance (<sup>1</sup>H NMR), and Fourier-transform infrared (FTIR) spectroscopy. The observed results are correlated with thermal, viscometric, and acid-base properties of the copolycondensates by differential scanning calorimetry (DSC), viscometric measurements of polymer solutions, and titrimetric determination of carboxyl groups.

## EXPERIMENTAL

### Materials

*l*-LA C<sub>5</sub>H<sub>8</sub>O<sub>3</sub>, 80% water solution, optical rotation  $[\alpha] = 10.6^\circ$  (measured by the polarimeter Optech P1000 at 22°C, concentration of 10%) was purchased from Lachner Neratovice, Czech Republic. Stannous 2-ethylhexanoate (Sn(Oct)<sub>2</sub>) (~95%), dimethyl sulfide C<sub>2</sub>H<sub>6</sub>OS in deuterated form (DMSO-*d*<sub>6</sub>) (100 mol % purity) and tetramethylsilane C<sub>4</sub>H<sub>12</sub>Si (TMS) were supplied by Sigma Aldrich, Steinheim, Germany. The solvents acetone C<sub>3</sub>H<sub>6</sub>O, dichloromethane CH<sub>2</sub>Cl<sub>2</sub>, methanol CH<sub>4</sub>O, ethanol C<sub>2</sub>H<sub>6</sub>O, indicator bromothymol blue C<sub>27</sub>H<sub>28</sub>Br<sub>2</sub>O<sub>3</sub>S, potassium hydroxide KOH, and anhydrous CA C<sub>6</sub>H<sub>8</sub>O<sub>7</sub> (all analytical grade) were bought from IPL Lukes, Uhersky Brod, Czech Republic. Chloroform CHCl<sub>3</sub> (HPLC grade) was purchased Chromspec, Brno, Czech Republic. All chemicals were used as obtained without further purification.

### Polycondensation

A typical procedure was as follows: relevant portions of LA and CA (0, 1, 3, 5, 7, 10, 15, and 20 wt %-related to LA) were added into a double-necked flask (250 mL) equipped with a Teflon stirrer. Total mass of the mixture at the beginning of reaction was 50 g (water is not included). The flask was then placed in an oil bath heated by magnetic stirrer with heating and connected to a laboratory apparatus for distillation under reduced pressure. The dehydration step followed at 160°C, reduced pressure 15 kPa for 4 h. After that, the reactor was disconnected from the vacuum pump and the relevant amount (0.5 wt %, related to initial mass of the reactants) of the catalyst (Sn(Oct)<sub>2</sub>) was added dropwise under continuous stirring. The flask with dehydrated LA/CA/catalyst mixture was connected back to the source of vacuum (100 Pa) and the reaction continued for 24 h at the temperature 160°C. The resulting product was

allowed to cool down at room temperature and then dissolved in acetone. The polymer solution was precipitated in a mixture of chilled methanol/distilled water 1 : 1 (v/v). The obtained product was filtrated, washed with methanol, and dried at 45°C for 48 h. The dissolving-precipitation procedure was repeated three times. The pH value of the filtrate after polymer separation was checked to ensure that an unreacted CA is not present in the polymer.

### Characterization methods

#### Viscometric measurements

Viscosity measurements were performed in chloroform at 30°C in an Ubbelohde viscometer with capillary 0a. The intrinsic viscosity,  $[\eta]$ , was calculated using the eq. (1):

$$[\eta] = \lim_{c \rightarrow 0} \frac{\eta_{rel} - 1}{c} \quad (1)$$

where  $\eta_{rel}$  is the relative viscosity, which is equal to the ratio of polymer solution and pure solvent viscosities, and  $c$  is the concentration of the polymer solution (0.4, 0.8, and 1.2 w/v %).

#### Determination of molecular weight by GPC

GPC analyses were performed using a chromatographic system Breeze (Waters) equipped with a PLgel Mixed-D column (300 × 7.8 mm<sup>2</sup>, 5 μm) (Polymer Laboratories, Church Stretton, United Kingdom). For detection, a Waters 2487 Dual absorbance detector at 239 nm was employed. Analyses were carried out at room temperature with a flow rate of 1.0 mL min<sup>-1</sup> in chloroform. The column was calibrated using narrow molecular weight polystyrene standards with molar mass ranging from 580 to 480,000 g mol<sup>-1</sup> (Polymer Laboratories). A 100-μL injection loop was used for all measurements. The sample concentration ranged from 1.6 to 2.2 mg mL<sup>-1</sup>. Data processing was carried out using the Waters Breeze GPC Software (Waters). The weight average molar mass  $M_w$ , number average molar mass  $M_n$ , and polydispersity ( $M_w/M_n$ ) of the tested samples were determined.

#### Fourier-transform infrared spectroscopy

Functional groups in LA polycondensation products were identified using FTIR analysis. The investigation was conducted on NICOLET 320 FTIR, equipped with attenuated total reflectance (ATR) accessory utilizing Zn-Se crystal and the software package OMNIC over the range of 4000–650 cm<sup>-1</sup> at room temperature. The uniform resolution of 2 cm<sup>-1</sup> was maintained in all cases.

#### Differential scanning calorimetry

For the determination of glass transition temperature ( $T_g$ ), melting point ( $T_m$ ), and crystallinity ( $\chi_c$ ) of the polycondensates, the DSC was used. Approximately 8 mg of the sample was placed in an aluminum pan, sealed, and analyzed on NETZSCH DSC 200 F3, calibrated in terms of temperature and heat flow, using indium. The experiments were performed under nitrogen atmosphere (60 mL min<sup>-1</sup>) in two scans in the temperature range of 0–180°C and at the heating rate of 10°C min<sup>-1</sup>. Crystallinity (%),  $\chi_c$ , was estimated by the following equation:

$$\chi_c = \frac{\Delta H_m^0}{\Delta H_m} \times 100 \quad (2)$$

where,  $\Delta H_m^0$  is the enthalpy of melting for 100% crystalline PLA (93.7 J g<sup>-1</sup>) adopted from Fischer et al.<sup>27</sup> and  $\Delta H_m$  represents the measured melting enthalpy of the sample taken from the first heating scan.

#### <sup>1</sup>H Nuclear magnetic resonance

The composition of the selected polycondensation products (PLA, PLACA1%, PLACA 5%, and PLACA 20%), as well as the component structure, was determined with <sup>1</sup>H NMR spectroscopy using a Unity Inova 300 Varian NMR spectrometer operating at 300 MHz. The sample concentration was 1% (w/w) in the solvent DMSO-*d*<sub>6</sub> (Aldrich, 100.0 mol % purity). All the spectra were obtained at 25°C using 5-mm glass NMR tubes, and TMS as the internal standard. The conditions for the <sup>1</sup>H NMR were as follows: a 90° pulse angle, a 5-s delay between the pulses, an acquisition time of 5 s, and up to 32 repetitions. VNMRJ rev. 1.1D software was applied for the peak integration. The lactic-to-citric monomer ratio and the number molecular weight were calculated according to the procedure described by Yao et al.<sup>21</sup>

#### Acidity number determination

The concentration of terminal carboxyl groups was expressed as acidity number (AN), which represents the amount of KOH (in milligrams) for neutralization of 1 g of a substance. AN was determined by titration of the sample in methanol/dichloromethane (1 : 1 v/v) with 0.01M KOH ethanol solution. Bromothol blue was used as an indicator.<sup>21</sup>

#### Spectroscopy in ultraviolet light spectrum

The spectroscopic analysis of the samples in ultraviolet and part of the visible range of light was

TABLE I  
Characteristics of PLACA Polycondensates

Sample designation	$M_n^a$ (kg mol <sup>-1</sup> )	$M_w^a$ (kg mol <sup>-1</sup> )	$M_w/M_n^a$	$[\eta]^b$ (dL g <sup>-1</sup> )	Yield <sup>c</sup> (wt %)	AN/SD <sup>d</sup> (mg <sub>KOH</sub> g <sup>-1</sup> )	Appearance
PLA	22.6	46.9	2.1	0.47	62	23.6/1.9	White powder
PLACA 1%	10.8	27.0	2.5	0.25	46	30.0/1.5	Yellowish powder
PLACA 3%	1.9	7.7	4.1	0.20	25	35.7/1.7	Yellowish powder
PLACA 5%	1.1	4.7	4.3	0.14	22	50.5/1.2	Yellowish powder
PLACA 7%	0.9	4.0	4.4	0.15	53	54.0/1.3	Yellow powder
PLACA 10%	0.3	1.4	4.7	0.09	33	78.6/1.2	Waxy-light brown
PLACA 15%	0.2	1.2	6.0	0.08	43	98.4/1.7	Waxy-light brown
PLACA 20%	0.2	1.2	6.0	0.08	48	97.9/1.1	Waxy-light brown

<sup>a</sup> GPC analysis.

<sup>b</sup> Viscometry (30°C in CHCl<sub>3</sub>).

<sup>c</sup> Calculated on the basis of copolycondensation product mass after precipitation procedure.

<sup>d</sup> SD, standard deviation.

conducted on the prepared samples to reveal functionalization extend of the polycondensates with carboxyl groups. The samples were dissolved in chloroform to form a polymer solution (~0.1 mg/mL). The analysis was carried out by Helios Gamma UV-Visible spectrometer in a quartz cuvette (path length, 10 mm) over the wavelength range 200–400 nm with resolution 0.5 nm at room temperature.

## RESULTS AND DISCUSSION

The basic characteristics of the samples prepared by melt polycondensation of LA and CA are shown in Table I. It can be noticed that the increasing content of CA in the reaction mixture leads (beside the visual change of the product) to significant reduction of  $[\eta]$ . While the pure PLA has  $[\eta] = 0.47$  dL g<sup>-1</sup>, PLACA 5% in the mixture causes noticeable reduction of  $[\eta]$ , which poses >55% of the value obtained for pure PLA. However, noticeable reduction of  $[\eta]$  was observed already for PLACA 1% (>45%). The samples that were prepared in above 10 wt % CA presence are characteristic with low  $[\eta]$ , which corresponds to their waxy-like appearance unlike the powder form of the polycondensation products prepared at lower concentration of tricarboxylic acid.

The values of molecular weight determined by GPC (Table I) correspond to the intrinsic viscosity data. The highest  $M_w$  was achieved in case of PLA (46,900 g mol<sup>-1</sup>). The increasing content of CA in the reaction mixture decreases  $M_w$  steeply. Finally, the sample designated as PLACA 20% proves  $M_w$  of only 1200 g mol<sup>-1</sup>. In addition, polydispersity ( $M_w/M_n$ ) of the polycondensates increases from 2.1 (for PLA) to 6.0 (for PLACA 20%). These results reveal the possible integration of CA into the PLA chain during polycondensation process, which can be supported by the assumption that higher volume resistance corresponds to lower reactivity of CA. It

means that CA molecules rather do not react with each other. On the other hand, when LA or its oligomer reacts with one of the CA functional groups, it would be arduous for such molecule to undergo further condensation reaction because of the reasons mentioned above.<sup>21</sup> Moreover, CA contains three carboxylic and one hydroxyl group while LA possesses one from each. Thus the ratio COOH/OH is shifted toward values higher than 1 in the presence of CA in the reaction mixture. The reduction of molecular weight and the increasing polydispersity index is a logical consequence of that.

The incorporation of CA into the structure of a product through condensation reaction can be proved by the determination of carboxyl groups, which should be in excess in case the reaction took place during product formation. The titration method can provide such information in the form of AN as presented above. This method is considered to be a reliable tool for the determination of molecular weight of a polymer (end-groups determination). However, it cannot be used in case of PLACA polycondensates due to several reasons. First, PLA itself is not considered to be terminated by carboxyl groups. Second, the results indicate possible incorporation of citryl units into the structure of PLACA at lower CA concentration in the feed (see further). The values of AN, shown in Table I, are in accordance of the assumption of occurrence of the condensation reaction between LA and CA molecules. Despite the already mentioned assumption of carboxyl absence in the pure PLA, small AN was observed (26 mg KOH g<sup>-1</sup>). It can be ascribed to the presence of residual monomer. In addition, the indicator, bromothyl blue, has equivalence point above pH 7. The rising CA content causes an increase in AN up to 15 wt % CA in reaction mixture. The AN values for PLACA 15% and PLACA 20% are more or less identical, which reveals possible limits of CA incorporation into the structure of the product. This limit is

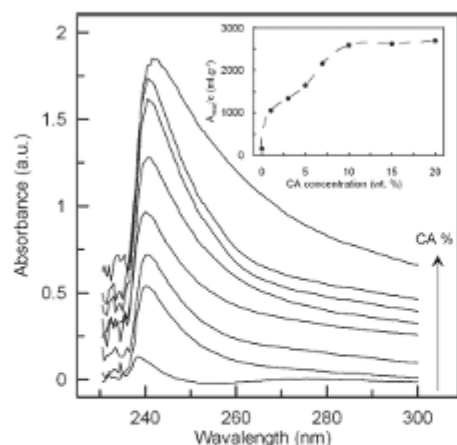


**Figure 1** UV spectra of PLA and PLACA polycondensates. Embedded figure shows dependence of  $A_{\max}$  normalized with respect to the sample concentration on CA content in the feed.

connected with the inhibition of condensation reaction that leads to reduction of molecular weight of the samples (Table I). It can be supposed that this method considers mostly the carboxyl groups appearing at the end of polymeric chains. The amount of such terminations increases with the increasing amount of short chains of the polymer or its branches. It should be mentioned that the yields shown in Table I represent pure yield of the polycondensation products after purification process described in the sample preparation section.

UV-Vis analysis of the samples can support the idea of COOH attachment on PLA chains. Generally, PLA shows maximal absorbance at wavelength ( $\lambda_{\max}$ ) 240 nm.<sup>6</sup> In our case, pure PLA proved  $\lambda_{\max} = 237$  nm. The increasing content of CA led to slight shift of  $\lambda_{\max}$  toward higher values. The sample with the highest investigated CA content in the feed (PLACA 20%) shows  $\lambda_{\max} = 242$  nm. Figure 1 shows spectra of the PLA and PLACA chloroform solutions within the range of 200–400 nm. It can be noticed that the absorption at  $\lambda_{\max}$  increases with rising content of CA. It can be considered that this phenomenon is a consequence of PLA functionalization. The embedded figure shows dependence of maximal absorption ( $A_{\max}$ ) normalized with the concentration of polymer in the solution,  $c$  ( $\text{g mL}^{-1}$ ) on CA concentration. It clearly shows that the most significant functionalization degree is proceeded up to 10 wt % of CA. Further additions of CA do not enhance  $A_{\max}/c$  value, which is proved by a plateau occurrence. These results are in full agreement with AN determination (see Table I).

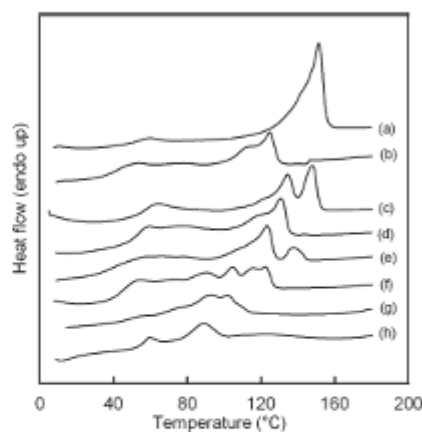


**Figure 2** DSC curve of polycondensates—first heating scan: (a) PLA, (b) PLACA 1%, (c) PLACA 3%, (d) PLACA 5%, (e) PLACA 7%, (f) PLACA 10%, (g) PLACA 15%, and (h) PLACA 20%.

The DSC spectra thermograms of the samples obtained from the first heating scan are shown in Figure 2 and the observed characteristics (melting point and melting enthalpy) are summarized in Table II. All samples containing CA proved double melting exothermic peaks while pure PLA is distinguished by a significant single melting peak situated at 151.2°C with melting enthalpy 48.9  $\text{J g}^{-1}$ . The phenomenon of cold crystallization was not observed. Similar results have been reported by Yao et al.<sup>21</sup> Generally, CA presence decreases  $T_m$  of the samples and this reduction corresponds to the CA concentration in the system [Fig. 2(b–h)]. The only exception is created by PLACA 1%, which shows a noticeably lower  $T_{m1}$  and  $T_{m2}$ . The experiment was conducted multiple times with similar results [Fig. 2(b)]. The reason of such behavior could be found in possible obstruction of the volume of CA molecules during development of organized polymer units. This may be possible under the condition that some of the CA

**TABLE II**  
DSC Characteristics of the PLA and PLACA Samples (First Heating Scan)

Sample designation	$T_{m1}$ (°C)	$\Delta H_{m1}$ ( $\text{J g}^{-1}$ )	$T_{m2}$ (°C)	$\Delta H_{m2}$ ( $\text{J g}^{-1}$ )
PLA	151.2	48.9	—	—
PLACA 1%	110.0	12.73	124.8	16.8
PLACA 3%	134.5	11.82	147.9	16.9
PLACA 5%	118.1	7.65	130.9	17.4
PLACA 7%	123.4	11.95	137.6	4.8
PLACA 10%	104.4	4.6	122.3	10.9
PLACA 15%	90.1	3.9	102.0	8.9
PLACA 20%	59.1	2.9	88.5	7.6

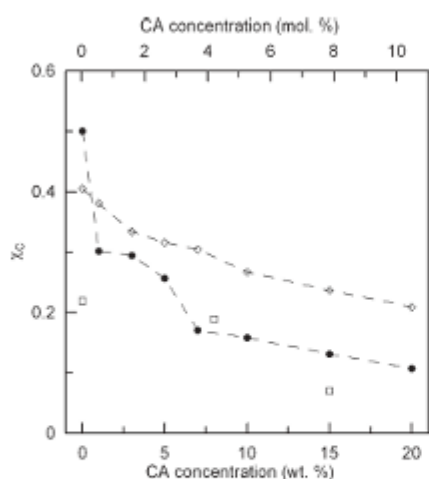


**Figure 3** Effect of CA concentration on crystallinity of the PLACA polycondensates determined by DSC (filled symbols) and FTIR (empty symbols) techniques. Square symbols represent data (DSC) published by Yao et al.<sup>21</sup>

molecules (present in low amount in case of PLACA 1%) is incorporated inside of the polymer chain; i.e., it does not terminate the chain. On the other hand, the polycondensation inhibition effect becomes predominant at higher concentrations of CA as a result of termination of polycondensate chains by sterically bulky citryl groups. Increasing content of CA in the feed obviously increasing the probability of that. This effect could be predominant here rather than excess of COOH groups. It is connected with the decreasing molecular mass (Table I),  $T_m$  and  $\Delta H_m$  (Table II). The effect of CA presence on crystallinity ( $\chi_c$ ) calculated according eq. (1) is shown in Figure 3. The dashed guiding line connecting individual experimental points clearly indicates that  $\chi_c$  decreases significantly at the lowest investigated addition of CA into reaction mixture (1 wt %). Further increase in CA concentration (up to 7 wt %) is characterized by a decrease of  $\chi_c$  values. However, it is not as steep as in the previous case and graphical depiction has a convex shape. The  $\chi_c$  reduction was observed to be gradual in case of the samples with higher CA contents (above 10 wt %), where the effect of CA presence becomes less significant.

Second DSC heating scans are shown in Figure 4. The positions of the midpoint stepwise increase of the specific heat provide the values of glass transition temperature ( $T_g$ ) of the samples (Fig. 4). On the other hand, the endothermic peaks revealing melting were diminished with incorporation of citryl units into the polycondensates structure, due to significant reduction of the PLACA chain ability to be organ-

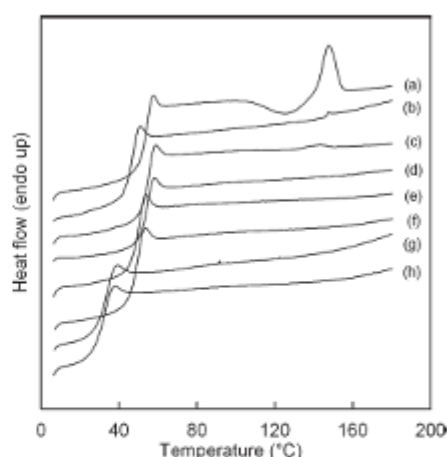


**Figure 4** DSC curve of polycondensates—second heating scan: (a) PLA, (b) PLACA 1%, (c) PLACA 3%, (d) PLACA 5%, (e) PLACA 7%, (f) PLACA 10%, (g) PLACA 15%, and (h) PLACA 20%.

ized into crystalline units. The dependence of  $T_g$  on CA concentration is depicted in Figure 5. As well as in the case of melting behavior, the  $T_g$  decreases with rising CA presence. The decrease is gradual and the difference between PLA and PLA with the highest investigated amount of CA (PLACA 20%) is almost 21.5°C. These experimental results fit well to

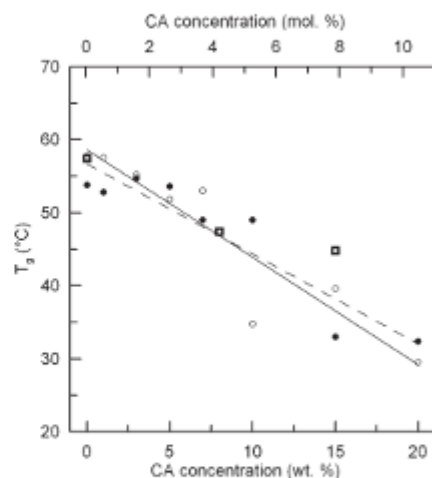


**Figure 5** Glass transition temperature ( $T_g$ ) versus CA concentration (experimental data—full symbols and solid line fit, theoretical data—empty symbols and dashed line fit). Square symbols represent data published by Yao et al.<sup>21</sup>

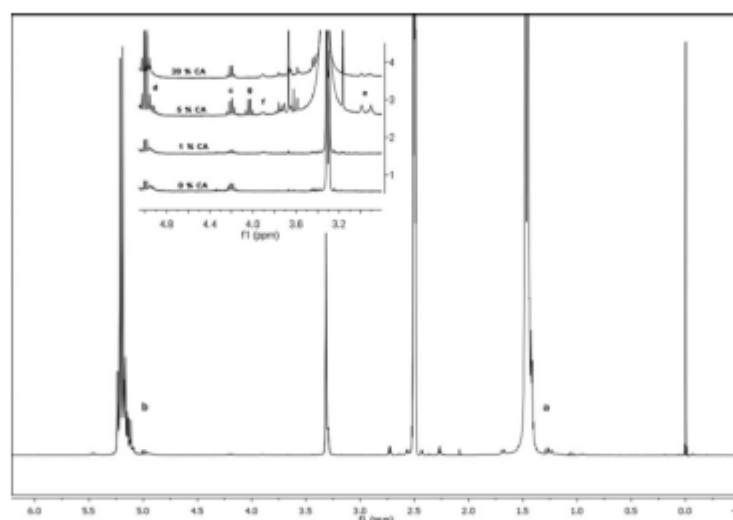


Figure 6  $^1\text{H}$  NMR spectra of the selected polycondensates. The master curve belongs to PLACA 1%.

theoretical predictions of  $T_g$ , which was performed according to Fox-Flory;

$$T_g = T_g^\infty - \frac{K}{M_n} \quad (3)$$

where  $T_g^\infty$  represents the glass transition temperature at an infinite molecular weight of polymer, and  $K$  is a constant representing the excess free volume of the polymer chains end groups.  $M_n$  was taken from GPC measurements (Table I). Jashimi et al. reported  $T_g^\infty = 58^\circ\text{C}$  and  $K = 5.5 \times 10^4$  (for low-crystalline PLA).<sup>28</sup> We have already informed that eq. (3) fails at low  $M_n$  of PLA.<sup>3</sup> Interestingly, the relation between  $T_g$  and  $M_n$  is relatively valid for PLACA samples even at low-molecular weights of the polycondensation products obtained at higher CA concentrations. The only significant deviation between experimental and theoretical  $T_g$  was observed for PLACA 10%. Nevertheless, these calculations are strongly dependent on  $M_n$  determination and their accuracy is in orders of hundreds of gram per mole in case of GPC. On the other hand, simplification by means of linear fitting of both experimental and theoretical data (solid and dashed lines in Fig. 5) may be considered acceptable for preliminary  $T_g$  estimation of the given material.

As already mentioned, polycondensation of LA and CA has been already reported by Yao et al.<sup>21</sup> Thermal properties of their polycondensation products were slightly different to the samples introduced in this work. First, Yao's copolycondensates did not prove double melting response. Second, the

values of  $\chi_c$  were found significantly higher for pure PLA and CA rich samples. Third,  $T_g$  of PLACA samples was lower at higher contents of CA in comparison with Yao's results after recalculation of CA concentrations (Figs. 3 and 5, square symbols). The reason of these variations can be found in the following factors: (a) optical activity of the monomer, LA; (b) slight differences in polycondensation procedure (catalyst, temperature, and pressure); (c) thermal history of the materials. On the other hand, the level of the functionalization [by means of AN (Table I)] was found noticeably higher in our case after recalculation of given parameters within the same units.

Figure 6 shows  $^1\text{H}$  NMR spectra and the ascription of the peaks in the spectra of pure PLA and PLACA polycondensates. On the basis of that, the scheme of the chemical structure of PLACA samples is proposed in Figure 7 together with the structures of monomers. The resonances at 5.16 ppm ( $-\text{CH}$  quartet, b), 1.46 ppm ( $-\text{CH}_3$  doublet, a), 4.2 ppm ( $-\text{CH}$  singlet, hydroxyl end units, c), and at 4.99 ppm ( $-\text{CH}$  singlet, carboxyl end units, d) originate from hydrogen of lactic unit.<sup>29</sup> The resonance of  $\text{CH}_2$  (e) of citric unit of PLACA located in terminal groups appear at 3.0 ppm, but the  $\text{CH}_2$  (f) of citric unit inside the molecular chain of PLACA move to 3.65 ppm. The quartet near 4.05 ppm is contributed by CH (g) of lactic unit connecting with citrate unit. From the  $^1\text{H}$  NMR spectra of PLACA, the mole ratio ( $r$ ) of LA/CA and the number molecular weight of PLACA were calculated according to eqs. (4) and (5), respectively.<sup>21</sup>

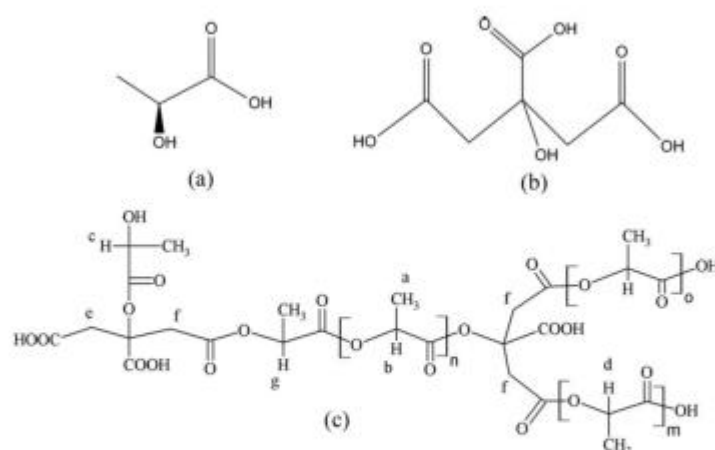


Figure 7 Schematic structure of (a) LA, (b) CA, and (c) PLACA copolymers.

$$r = \frac{4 \times I_b}{I_f + I_c} \quad (4)$$

$$\overline{M}_n = \frac{I_b}{I_d} \times 72 + \frac{I_b}{I_d} \times \frac{1}{r} \times 158 + 18 \quad (5)$$

where  $I$  represents the integral of the proton signals (peak areas). The calculated results are listed in Table III. The results show that mole ratio of LA/CA ( $r$ ) in PLACA decreases with the increasing concentration of CA in the reaction mixture at the beginning of the polycondensation (see Table IV). From this, it can be concluded that not all CA took part in polycondensation reaction, which was also observed by Yao et al.<sup>21</sup> However, in case of PLACA 1%, the comparison of the  $r$  (Table III) with LA:CA ratio calculated from the known masses of both components introduced into the reactor (LA:CA molar ratio, see Table IV) reveal the significant difference between known LA/CA ratio (211) and  $r$  determined by  $^1\text{H}$  NMR (7690). It could indicate the specific reactions between LA and CA, which occur only at low CA concentrations and do not involve termination of polymer chains mediated by CA units. The value of molecular weight determined by  $^1\text{H}$  NMR (Table III) decreases with increasing content of CA, which is in agreement with the results obtained from GPC anal-

TABLE III  
Characteristics of PLACA Polycondensates Determined by  $^1\text{H}$  NMR Spectroscopy

Sample designation	$r$	$M_n(\text{kg mol}^{-1})$	$m_c$	$P_{eg}$
PLA	–	14.4	0	–
PLACA 1%	7690	5.6	0.010	0.80
PLACA 5%	46	0.7	0.197	0.89
PLACA 20%	59	0.8	0.198	0.98

ysis (Table I). Nevertheless, significant discrepancies in the calculated molecular weight values were obtained. The reason can be found in the principles of the  $M_n$  determination and structural features of the polycondensates.

The combination of eqs. (4) and (5) allow the calculation of the molar fraction of the citryl units in 1 mol of PLACA product,  $m_c$  [eq. (6)].<sup>21</sup>

$$m_c = \frac{\overline{M}_n - 18}{158 + 72 r} \quad (6)$$

The values of  $m_c$  increase with the increasing amount of CA in the reaction mixture. On the other hand,  $m_c$  is almost identical for PLACA 5% and PLACA 20% (see Table III). It corresponds to the already proposed limitation of the CA incorporation into the structure of the PLACA polycondensates (inside or at the end of the chains), and it is partially in agreement with AN results presented in Table I.

TABLE IV  
Designation of the Samples and Characterization of the Reaction Mixture at the Beginning of the Polycondensation

Sample designation	LA		LA/CA (molar ratio)
	concentration (wt %)	CA concentration (wt/mol %)	
PLA	100	0/0	0
PLACA 1%	99	1/0.47	211
PLACA 3%	97	3/1.43	69
PLACA 5%	95	5/2.41	40
PLACA 7%	93	7/3.41	28
PLACA 10%	90	10/4.95	19
PLACA 15%	85	15/7.64	12
PLACA 20%	80	20/10.49	9

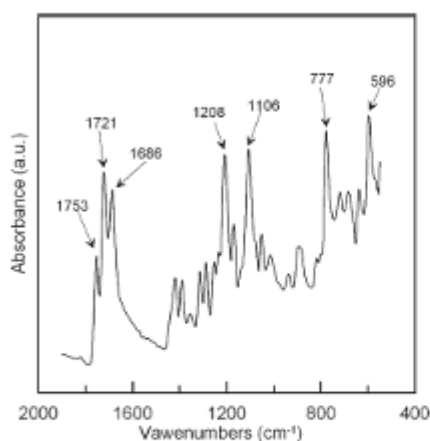


Figure 8 FTIR-ATR spectra of neat CA.

The evidence of CA incorporation inside the PLACA structure could be proved by determination of the percentage of the citryl units,  $P_{eg}$ , located at the end of the chains [eq. (7)].<sup>21</sup>

$$P_{eg} = \frac{2}{3 - \frac{I}{I_0}} \times 100 \quad (7)$$

Table III shows the values of  $P_{eg}$ . The results reveal that only 80% of the total present citryl units are located at the ends of the polycondensate's chains. Furthermore,  $P_{eg}$  rises with the increasing CA content in the reaction mixture. It can be considered as an evidence of hypothesis of the CA incorporation inside the structure of the PLACA polycondensates and possible occurrence of the structural inhomogenities which are connected with that (branching).

The FTIR-ATR spectra of neat CA are shown in Figure 8. CA as tricarboxylic acid has typical absorption peaks positioned at 1753, 1721, and 1686  $\text{cm}^{-1}$  ( $\text{C}=\text{O}$  stretching). It should be mentioned that databases report only two absorption peaks in the region 1800–1650  $\text{cm}^{-1}$ . As can be seen in Figure 7, the intensity of the signal is low, thus the peak at 1753  $\text{cm}^{-1}$  could be considered as random noise signal. Other significant peaks of CA were found at 1208, 1106  $\text{cm}^{-1}$  ( $\text{C}-\text{O}$  stretching) and 777  $\text{cm}^{-1}$  ( $\text{C}-\text{C}$  stretching). Typical FTIR-ATR spectra of the selected samples (PLA, PLACA 1, 5, 10, and 20%) are shown in Figure 9. All spectra prove typical absorptions at 2950  $\text{cm}^{-1}$ , which corresponds to  $\text{C}-\text{H}$  stretching (not presented in Fig. 8). Furthermore, typical PLA absorbance responses were detected at 1748  $\text{cm}^{-1}$  ( $\text{C}=\text{O}$  stretching), 1452  $\text{cm}^{-1}$

( $\text{CH}_2$  bending), 1381 and 1361  $\text{cm}^{-1}$  ( $\text{C}-\text{H}$  deformations and asymmetric bending), 1267  $\text{cm}^{-1}$  ( $\text{C}-\text{O}$  stretching—typical for PLA prepared by direct polycondensation), 1183, 1128, and 1084  $\text{cm}^{-1}$  ( $\text{C}-\text{O}-\text{C}$  stretching), 1043  $\text{cm}^{-1}$  ( $\text{C}-\text{OH}$  bending).<sup>3,8,20</sup> As reported by, e.g., Auras et al., the absorption peaks located at 868 and 753  $\text{cm}^{-1}$  correspond to amorphous and crystalline PLA phase, respectively.<sup>8</sup> The chemical similarities of LA and CA cause difficulties in qualitative analysis of the spectra. The only evidence for a difference can be noticed in the wavenumber region 1700–1600  $\text{cm}^{-1}$  where a slight increase in absorbance can be found. This is evident especially in case of PLACA 20% [Fig. 9(e)]. It could reveal the presence of carboxyl groups (originating from CA) in the structure of the polymer. On the other hand, the evidence of that is expected to be more distinguishable from quantitative analysis of carboxyl group. It was proceeded by comparison of peak areas corresponding to carboxyl groups present in the region 1800–1650  $\text{cm}^{-1}$  ( $A_c$ ), normalized by area of reference peak ( $A_R$ ). The peak at 1452  $\text{cm}^{-1}$  was chosen as internal standard for spectra normalization since it has been reported as suitable for this purpose.<sup>27</sup> The dependence of  $A_c/A_R$  on CA content is shown in Figure 10. It can be noticed that the amount of carboxyl groups grows with increasing concentration of CA in the reaction mixture, which gives evidence for CA units in the polymer structure.

It has been mentioned that FTIR spectra can provide information about the ratio of the crystalline to amorphous phase in the system through observation of the absorption peaks at 868 and 753  $\text{cm}^{-1}$ .<sup>8,10,31</sup> This assumption encouraged us to verify the

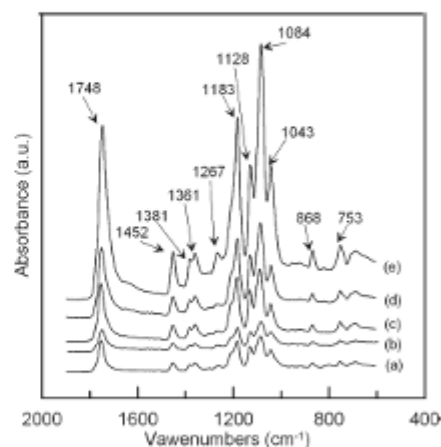
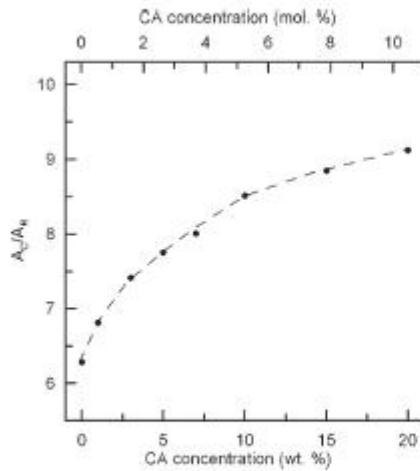
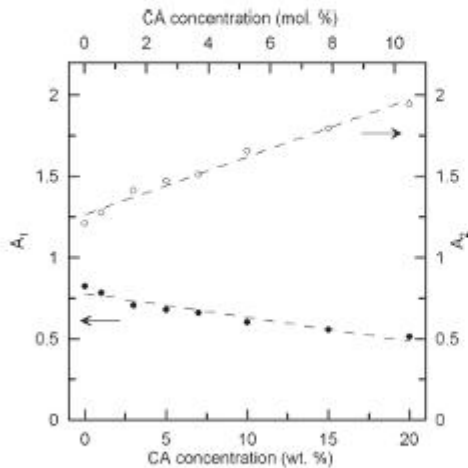


Figure 9 FTIR-ATR spectra of PLA (a), PLACA 1% (b), PLACA 5% (c), PLACA 10% (d), and PLACA 20% (e).



**Figure 10** Correlation of carboxyl groups semiquantitative FTIR determination and concentration of CA in reaction mixture.

authenticity of this theory and compare it with the experimental data obtained from FTIR-ATR and DSC. The normalization of the FTIR-ATR spectra was done in the same way like in case of carboxyl groups analysis; i.e., peak at  $1452\text{ cm}^{-1}$  was considered as the reference.<sup>27</sup> The areas of the discussed peaks  $A_{863}$  and  $A_{753}$  were measured by integration procedure mediated by Omnic Software. The normalized peak areas  $A_1$  ( $A_1 = A_{863}/A_R$ ) and  $A_2$  ( $A_2 = A_{753}/A_R$ ) are depicted against CA concentration in



**Figure 11** Dependence of normalized absorption peak areas on CA concentration ( $A_1 = A_{863}/A_{1452}$  and  $A_2 = A_{753}/A_{1452}$ ).

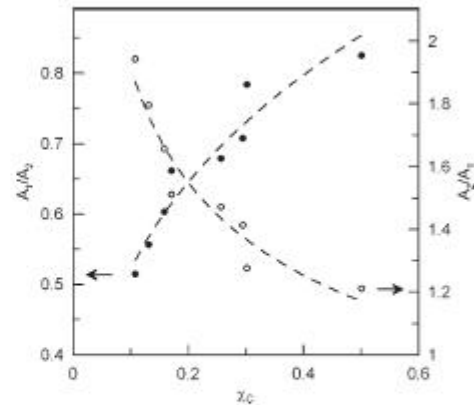


**Figure 12** Correlation between ratios FTIR and DSC results explaining correct assignment of the absorption peaks in PLA-based materials spectra.

Figure 10. The resulting dependences for both  $A_1$  (full symbols) and  $A_2$  (empty symbols) can be fitted by a linear model. The correlation coefficients are 0.96 and 0.99 for  $A_1$  and  $A_2$ , respectively. Figure 11 shows that  $A_1$  decreases with the increasing CA concentration. On the other hand,  $A_2$  proves an opposite trend. These changes are expectable since the peak areas  $A_1$  and  $A_2$  have been reported to express ratio of amorphous ( $A_1$ ) and crystalline ( $A_2$ ) phase of the material and DSC results show significant variation in crystallinity due to the presence of CA in the reaction mixture. However, crystallinity ( $\chi_c$ ) (determined by DSC), which should correspond to  $A_2$ , decreases with the increasing CA concentration. This is evident in Figure 12, where the ratios  $A_1/A_2$  and  $A_2/A_1$  are depicted against  $\chi_c$ . The dependencies were fitted (dashed lines) by a logarithmic model ( $A_1/A_2 = 0.20\ln(\chi_c) + 0.98$ ,  $r = 0.97$ ;  $A_2/A_1 = -0.46\ln(\chi_c) + 0.81$ ,  $r = 0.95$ ). These results indicate the serious discrepancies between previously published data<sup>8</sup> and our results. On the basis of that, it can be concluded that FTIR spectra could be used for PLA crystallinity investigation. However, absorption peak at  $863\text{ cm}^{-1}$  ( $A_1$ ) refers to crystalline and peak at  $753\text{ cm}^{-1}$  ( $A_2$ ) to amorphous phase. Comparison of crystallinity values obtained by FTIR and DSC analysis is shown in Figure 3. Generally, FTIR results provide higher  $\chi_c$  (except for pure PLA) with the significant variance. On the other hand, the trend of  $\chi_c$  reduction corresponds to DSC results.

## CONCLUSIONS

Functionalization of polylactide acid with carboxyl groups, description of the process, finding of limitations, and characterization of the products were

aims of this work. This technique can be used for further preparation of various products with improved bioactive response toward living organisms. This study follows the work, which has been already published by Yao et al.<sup>21</sup> The carboxyl-functionalized copolycondensates LA and CA were prepared by method of direct melt polycondensation.

Generally, the presence of CA in the reaction mixture leads to significant reduction of molecular weight of the polycondensation products. It is believed that CA terminates the growth of the polycondensates chain. We found that the formation of the structures involving citryl units into the polymer chain as well as subsequent branching is possible at low concentrations of CA in the reaction mixtures (up to 1 wt %). The termination processes are predominant at higher CA contents. This effect could be predominant here rather than excess of COOH groups.

The limitations of the CA involving into polycondensation processes have been observed. The AN determinations as well as <sup>1</sup>H NMR spectrometry results show the occurrence of a limit CA concentration (5 wt %). Above this concentration, the functionality degree of the polycondensates is not significantly dependent on CA content. However, the level of functionalization was observed to be noticeably higher in comparison with already published work.<sup>21</sup>

Beside that, the correlation of the data obtained from DSC and FTIR spectroscopy show the possibility of the semiquantitative analysis of the crystalline fraction of the polylactide-based materials.

## References

- Mehra, R.; Kumar, V.; Bhunia, H.; Upadhyay, S. N. *J Polym Sci: Polym R* 2005, 45, 325.
- Ajioka, M.; Suizu, H.; Higuchi, C.; Kashmina, T. *Polym Degrad Stab* 1998, 59, 137.
- Sedlarik, V.; Saha, N.; Sedlarikova, J.; Saha, P. *Macromol Symp* 2008, 272, 100.
- Gregorova, A.; Hrabalova, M.; Wimmer, R.; Saake, B.; Altaner, C. *J Appl Polym Sci* 2009, 114, 2616.
- Jacobsen, S.; Degee, P. H.; Friz, H. G.; Dubouis, P. H.; Jerome, R. *Polym Eng Sci* 1999, 39, 1311.
- Kricheldorf, H. R. *Chemosphere* 2001, 43, 49.
- Sedlarik, V.; Kucharczyk, P.; Kasparkova, V.; Drbohlav, J.; Salakova, A.; Saha, P. *J Appl Polym Sci* 2010, 116, 1597.
- Auras, R.; Harte, B.; Selke, S. *Macromol Biosci* 2004, 4, 835.
- Duda, A. *Przem Chem* 2003, 82, 905.
- Garlotta, D. *J Polym Environ* 2001, 9, 63.
- Sodergard, A.; Stolt, M. *Prog Polym Sci* 2002, 27, 1123.
- Moon, S. I.; Deguchi, K.; Miyamoto, M.; Kimura, Y. *Polym Int* 2004, 53, 254.
- Gupta, A. P.; Kumar, V. *Eur Polym Mater* 2007, 43, 4053.
- Wang, Z. Y.; Zhao, Y. M.; Wang, F. *J Appl Polym Sci* 2006, 102, 577.
- Popelka, S.; Rypacek, F. *Collect Czech Chem Commun* 2003, 69, 1131.
- Vesel, A.; Elersic, K.; Junkar, I.; Malic, B. *Mater Technol* 2009, 43, 323.
- Asadinezhad, A.; Novak, I.; Lehocky, M.; Sedlarik, V.; Vesel, A.; Saha, P.; Chodak, I. *Colloid Surface B* 2010, 77, 246.
- Asadinezhad, A.; Novak, I.; Lehocky, M.; Bilek, F.; Vesel, A.; Junkar, I.; Saha, P.; Popelka, A. *Molecules* 2010, 15, 2845.
- Wan, Y.; Tu, C.; Yang, J.; Bei, J.; Wang, S. *Biomaterials* 2006, 27, 2699.
- Safinia, L.; Datan, N.; Hohse, M.; Mantalaris, A.; Bismarck, A. *Biomaterials* 2005, 26, 7537.
- Yao, F.; Bai, Y.; Chen, W.; An, X.; Yao, K.; Sun, P.; Lin, H. *Eur Polym Mater* 2004, 40, 1895.
- Lecorre, P.; Estebe, J. P.; Chevanne, F.; Malledant, F.; Leverage, R. *J Pharm Sci-US* 1995, 84, 75.
- Norowski, P.A.; Bumgarder, J. D. *J Biomed Mater Res B* 2009, 88B, 530.
- Vasiliev, A. N.; Gulliver, E. A.; Krinast, J. G.; Riman, R. E. *Surf Coat Technol* 2009, 203, 2841.
- Cohn, D.; Lando, G. *Biomaterials* 2004, 25, 5875.
- Yao, F.; Bai, Y.; Zhou, Y.; Liu, C.; Wang, H.; Yao, K. *J Polym Sci: Polym Chem* 2003, 41, 2073.
- Fischer, E. W.; Sterzel, H. J.; Wegner, G. *Colloid Polym Sci* 1973, 251, 980.
- Jashimidi, K.; Hyon, S. H.; Ikada, Y. *Polymer* 1998, 29, 2229.
- Espartero, R. J.; Rashkov, I.; Li, S. M.; Manolova, N.; Vert, M. *Macromolecules* 1986, 29, 3535.
- Socrates, G. *Infrared Characteristic Group Frequencies*, 2nd ed.; Wiley: Chichester, United Kingdom, 2004, pp 10-17.
- Kister, G.; Cassanas, G.; Vert, M. *Polymer* 1998, 39, 267.

# APPENDIX C –PAPER III

This article was downloaded by: [Pavel Kucharczyk]

On: 13 September 2012, At: 02:10

Publisher: Taylor & Francis

Informa Ltd Registered in England and Wales Registered Number: 1072954 Registered office: Mortimer House, 37-41 Mortimer Street, London W1T 3JH, UK



## Journal of Macromolecular Science, Part A: Pure and Applied Chemistry

Publication details, including instructions for authors and subscription information:

<http://www.tandfonline.com/loi/lmsa20>

### The Effect of Various Catalytic Systems on Solid-State Polymerization of Poly-(L-lactic acid)

Pavel Kucharczyk <sup>a, b</sup>, Ida Poljansek <sup>c</sup> & Vladimir Sedlarik <sup>a, b</sup>

<sup>a</sup> Center of Polymer Systems, Polymer Center, Tomas Bata University in Zlin, Zlin, Czech Republic

<sup>b</sup> Polymer Center, Faculty of Technology, Tomas Bata University in Zlin, Zlin, Czech Republic

<sup>c</sup> University of Ljubljana, Biotechnical Faculty, Jamnikarjeva, Ljubljana

Version of record first published: 12 Sep 2012.

To cite this article: Pavel Kucharczyk, Ida Poljansek & Vladimir Sedlarik (2012): The Effect of Various Catalytic Systems on Solid-State Polymerization of Poly-(L-lactic acid), Journal of Macromolecular Science, Part A: Pure and Applied Chemistry, 49:10, 795-805

To link to this article: <http://dx.doi.org/10.1080/10601325.2012.714312>

PLEASE SCROLL DOWN FOR ARTICLE

Full terms and conditions of use: <http://www.tandfonline.com/page/terms-and-conditions>

This article may be used for research, teaching, and private study purposes. Any substantial or systematic reproduction, redistribution, reselling, loan, sub-licensing, systematic supply, or distribution in any form to anyone is expressly forbidden.

The publisher does not give any warranty express or implied or make any representation that the contents will be complete or accurate or up to date. The accuracy of any instructions, formulae, and drug doses should be independently verified with primary sources. The publisher shall not be liable for any loss, actions, claims, proceedings, demand, or costs or damages whatsoever or howsoever caused arising directly or indirectly in connection with or arising out of the use of this material.

# The Effect of Various Catalytic Systems on Solid-State Polymerization of Poly-(L-lactic acid)

PAVEL KUCHARCZYK<sup>1,2\*</sup>, IDA POLJANSEK<sup>3</sup>, and VLADIMIR SEDLARIK<sup>1,2</sup>

<sup>1</sup>Center of Polymer Systems, Polymer Center, Tomas Bata University in Zlin, Zlin, Czech Republic

<sup>2</sup>Polymer Center, Faculty of Technology, Tomas Bata University in Zlin, Zlin, Czech Republic

<sup>3</sup>University of Ljubljana, Biotechnical Faculty, Jamnikarjeva, Ljubljana

Received April 2012, Accepted May 2012

There are several methods for synthesizing polylactic acid. Solid-state polymerization is one of the most promising methods due to the great feasibility and beneficial properties of the final polymer. In terms of this study, the purpose was to evaluate the effect of various catalyst systems (based on tin dichloride, tin dioxide, tin octoate, citric acid, sulphuric acid, toluenesulfonic acid and methane sulfonic acid) and focus on the molecular weight, structure and thermal properties of the final products. The molecular weight was shown to be controlled by different catalytic systems and  $M_w > 100,000$  g/mol was achieved after 24 h of synthesis, which is more than in the conventional melt polycondensation process. Thermal stability was found to be negatively affected by the catalytic system, although relatively positive results can still be achieved.

**Keywords:** Poly(lactide), solid state synthesis, catalysts, thermal properties

## 1 Introduction

Poly(lactic acid) (PLA) is a biodegradable polymer with promising applicability within the production of environmentally friendly materials (e.g. packaging, disposable items) and medicine (medical devices, drug carriers) (1–7). Generally, PLA can be synthesized in three basic ways: (i) ring opening polymerization; (ii) azeotropic distillation in solution; (iii) polycondensation in a molten state. (8, 9) The first two methods are known to be experimentally difficult due to sensitivity to the presence of impurities, while the last of those mentioned facilitates relatively straightforward PLA preparation (10, 11). However, it is hampered by the low molecular weight of the polycondensation products, which is not acceptable for most engineering applications (12).

This disadvantage can be offset by introducing a subsequent technique – a post-polycondensation reaction, yielding a product with high molecular weight. Essentially, two

approaches are known. The first concerns coupling reactions between functional groups that are intentionally introduced at the ends of PLA chains (e.g. hydroxyl) and bifunctional compounds (e.g. diisocyanate) (13). The second method involves a reaction between ends of the PLA chains and/or residual monomer, which is usually carried out in solid state under specific conditions (8). This solid-state post-polycondensation (SSP) reaction is analogous to the method developed for increasing the molecular weight of poly(ethylene terephthalate) (14); incidentally, this has also been studied for potential utilization in medical applications (15–17). The advantages of SSP lie in the fact that polymer of a high molecular weight (>80,000 g/mol) can be facilitated under relatively moderate conditions, producing high yield but without adding external chemical agents (18).

An exhaustive review of solid-state polymerization has been published by Vouyiouka *et al.* (19). However, there is no information pertaining to polylactides. There are several works describing solid-state post-polycondensation of PLA. For instance, Zhang *et al.* (20) described a two-stage (melt/solid) preparation of PLA with high molecular weight. Nonetheless, in their work, only various binary catalysts and considerably higher reaction temperatures (150–180°C) were applied. In contrast, Moon *et al.* (21) investigated the melt/solid polycondensation of L-lactic acid within a temperature range of 140–150°C but, similar to the previous paper, only a binary catalyst (tin chloride

\*Address correspondence to: Pavel Kucharczyk, Center of Polymer Systems, Polymer Center, Tomas Bata University in Zlin, Nam. T.G. Masaryka 5555, 760 01 Zlin, Czech Republic and Polymer Center, Faculty of Technology, Tomas Bata University in Zlin, Nam. T.G. Masaryka 275, 762 72 Zlin, Czech Republic. Tel: +420576038013; Fax: +420 57 6031444; Email: p.kucharczyk@seznam.cz

dihydrate/*p*-toluenesulfonic acid) was employed. Another work, by Xu *et al.* (22), investigated the effect of crystallization on the SSP of PLA, but again only one catalyst ( $\text{SnCl}_2$ ) was used although the reaction temperature was relatively low ( $135^\circ\text{C}$ ). Different approaches for utilizing SSP were presented by Kazuya Shinno (23) and Kazuki Fukushima (24). While the first studied SSP as a method for reducing the remaining monomer, the later successfully applied SSP to synthesize stereo block poly(lactic acid). In all the above-mentioned papers, the molecular weight achieved was in the range of 20–150 kg/mol with molar-mass dispersity predominantly fixed below 2. Even though much research has been concerned with the SSP of poly(lactic acid), prior investigations in this field have largely been limited to merely several types of catalyst and, in contrast with other papers on this topic, no catalyst was added before SSP (during prepolymer synthesis); therefore, its effect could be evaluated separately. As a consequence, this particular work is dedicated to investigating solid-state post-polycondensation L-lactic acid polycondensates of low molecular weight, prepared via normal melt polycondensation. The concentration of the selected catalysts of 0, 0.5, 1 and 2 wt% were chosen according to their class, and the resultant products were characterized through gel permeation chromatography, differential scanning calorimetry and thermogravimetric analysis.

## 2 Experimental

### 2.1 Materials

L-LA  $\text{C}_3\text{H}_6\text{O}_3$ , 80% water solution with  $\rho = 1.21 \text{ g/cm}^3$ , Methane sulfonic acid (MSA)  $\text{CH}_3\text{SO}_3\text{H}$ ,  $\geq 99\%$ ,  $\rho = 1.48 \text{ g/cm}^3$  and Tin(II) 2-ethylhexanoate ( $\text{Sn}(\text{Oct})_2$ )  $\text{C}_{16}\text{H}_{30}\text{O}_4\text{Sn}$ ,  $\sim 95\%$ ,  $\rho = 1.25 \text{ g/cm}^3$  were purchased from Sigma Aldrich, Steinheim, Germany. Sulfuric acid  $\text{H}_2\text{SO}_4$ , 96%,  $\rho = 1.84 \text{ g/cm}^3$ ; Citric acid anhydrous (CA)  $\text{C}_6\text{H}_8\text{O}_7$ ,  $\geq 99.5\%$ ; Tin (II)chloride  $\text{SnCl}_2$ ,  $\geq 99\%$ ; *p*-Toluenesulfonic acid monohydrate (pTSA)  $\text{CH}_3\text{C}_6\text{H}_4\text{SO}_3\text{H}$ ,  $\geq 99\%$ ; Tin(IV) oxide  $\text{SnO}_2$ ,  $\geq 99\%$ . Solvents: chloroform  $\text{CHCl}_3$ , acetone  $\text{C}_3\text{H}_6\text{O}$ , methanol  $\text{CH}_3\text{OH}$ , and ethanol  $\text{C}_2\text{H}_5\text{OH}$  (all analytical-grade) came from IPL Lukes, Uhersky Brod, the Czech Republic. Chloroform (HPLC-grade) was sourced from Chromspec, Brno, the Czech Republic. All chemicals were used as received without further purification.

### 2.2 Sample Preparation

#### 2.2.1 Prepolymer Synthesis

The procedure of prepolymer synthesis is described in Figure 1. In brief, 200 ml L-LA solution was added to a 500 ml double necked flask equipped with a Teflon stirrer. The flask was then connected to a condenser and placed in an oil bath. Firstly, dehydration of L-LA solution at  $160^\circ\text{C}$

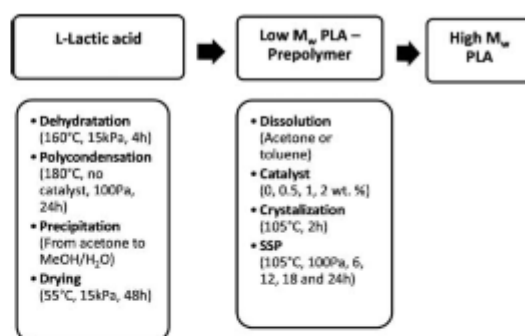


Fig. 1. Process of prepolymer preparation and solid state post-polycondensation.

took place, under a reduced pressure of 15 kPa for 4 h. Consequently, an oil vacuum pump was connected and the reaction continued at  $180^\circ\text{C}$  under a pressure of 100 Pa for another 24 h. When the reaction finished, the resultant product was cooled down to an ambient temperature and then dissolved in acetone. The polymer solution obtained was precipitated into a mixture of chilled methanol and distilled water at the ratio 1:1 (v/v) and filtered. In order to remove any unreacted monomer and other low molecular impurities, the prepolymer was further washed several times with hot distilled water ( $80^\circ\text{C}$ ) and ethanol. Finally, the product was dried in a vacuum oven at  $55^\circ\text{C}$  and 15 kPa for 48 h. The prepolymer was obtained in the form of white powder.

#### 2.2.2 Solid State Post-polycondensation (SSP)

Solid state post-polycondensation proceeded as follows: 6 g of the prepolymer was dissolved in 20 ml of acetone or toluene and the appropriate catalyst was added to the polymer solution (0, 0.5, 1 and 2 wt%). The toluene was used for  $\text{Sn}(\text{Oct})_2$  catalyst samples in order to prevent precipitation of the same. The solvent was then evaporated at an elevated temperature ( $80^\circ\text{C}$ ) and the residuals were dried for 6 h at  $30^\circ\text{C}$  under 3 kPa. Then, each sample containing the catalyst was placed in a test tube and crystallized at  $100^\circ\text{C}$  for 1 h. Finally, the test tubes were connected to the vacuum source (100 Pa) and approximately 1.5 g was taken from the tubes at each follow-up time (6, 12, 18 and 24 h). This crystallization step was adopted according to Moon *et al.* (21), because prepolymer became more resistive to fusion even when heated at a higher temperature and, therefore, partial melting of the samples was restricted.

### 2.3 Sample Characterization

#### 2.3.1 Molecular Weight Determination by GPC

GPC analysis was conducted using Waters chromatographic system. Samples were prepared by adding 1 ml of chloroform to approximately 1.5 mg of polymer taken from each follow-up time. Separation and detection took place on PL gel-mixed-D bed column (300 × 7.8 mm, 5 μm particles) with a UV response detector (Waters 2487) at 239 nm, respectively. Analyses were carried out at room temperature with a chloroform flow rate of 1.0 ml/min and a 100 μL injection loop. The GPC system was calibrated with narrow polystyrene standards ranging from 580 g/mol to 271,000 g/mol (Polymer Laboratories Ltd., United Kingdom). The weight average molar mass  $M_w$ , number average molar mass  $M_n$  and molar-mass dispersity ( $D_M = M_w/M_n$ ) of the tested samples were determined from their peaks corresponding to polymer fraction, and expressed as 'polystyrene equivalent' molecular weights. All data processing was carried out using Waters Breeze GPC software.

#### 2.3.2 Viscometric Measurements and Molecular Weight Determination via the Mark-Houwink (M-H) Equation

For determining intrinsic viscosity and the viscosity average molecular weight ( $M_\eta$ ) of the selected samples, the M-H equation was applied. Viscosity measurements were performed in  $\text{CHCl}_3$  at 30°C in an Ubbelohde viscometer with a 0a capillary. Intrinsic viscosity ( $[\eta]$ ) was calculated from Equation 1:

$$[\eta] = \lim_{c \rightarrow 0} \left( \frac{\eta_{rel} - 1}{c} \right) \quad (1)$$

Where  $\eta_{rel}$  is the relative viscosity, which is equal to the ratio of the polymer solution and pure solvent viscosities, whereas  $c$  is the concentration of the polymer solution (0.4, 0.8, and 1.2 wt/vol%).

According to the M-H equation, molecular weight is in direct relation with  $[\eta]$  through Equation 2:

$$[\eta] = K M_\eta^a \quad (2)$$

Where the values of the parameters,  $a$  and  $K$  depend on the particular polymer-solvent system. Here,  $K = 0.0131 \text{ ml/g}$ ,  $a = 0.777$  (25).

#### 2.3.3 <sup>1</sup>H-Nuclear Magnetic Resonance

The molecular mass of the synthesized polymer, as well as the component structure, was determined with <sup>1</sup>H-NMR spectrometry using a Unity Inova 300 Varian NMR spectrometer operating at 300 MHz. The sample concentration was 1% (w/w) in the solvent  $\text{CDCl}_3$  (Aldrich, 100.0 mol% purity). All the spectra were obtained at 25°C, and tetramethylsilane (TMS) was used as the internal standard. The conditions for the <sup>1</sup>H-NMR was as follows: a 90° pulse angle, a 5 s delay between the pulses, an acquisition time of

5 s, and up to 32 repetitions. VNMRJ rev. 1.1D software was applied for the peak integration. The number molecular weight and degree of polymerization of the synthesized polymers based on the integral of protons in a molecule per proton positioned in its end groups (Equations 4 and 5). The calculated results are listed in Table 1.

#### 2.3.4 Thermal Properties

The thermal properties of the samples retrieved were analyzed using a Mettler Toledo DSC1 STAR testing machine, over a temperature range of 5°C to 190°C at a heating/cooling rate of 10°C/min. and nitrogen flow of 20  $\text{cm}^3/\text{min}$ . The melting point temperature ( $T_m$ ) with enthalpy of fusion  $\Delta H_{\text{melt}}$  was obtained from the first heating cycle, whereas the value of glass-transition temperature ( $T_g$ ) was determined from the second heating scan, at the mid-point stepwise increase of the specific heat which is associated with glass transition. The heat of fusion of 100% crystalline PLA (26),  $\Delta H_{100} = 93.7 \text{ J/g}$  was then used to determine the polymers' percentage of crystallinities ( $X_c$ ) according to Equation 3:

$$X_c = \left( \frac{\Delta H_{\text{melt}}}{93.7} \right) \times 100 \text{ percent} \quad (3)$$

#### 2.3.5 Thermogravimetric Analyses (TGA)

The thermal stability of the PLA samples thus prepared was analyzed using a thermogravimeter (SETARAM TG-GA 12), in adherence to the samples possessing masses from 15 to 22 mg. The heating rate was set at 10°C/min over a temperature range from 25°C to 500°C; furthermore, a helium atmosphere (flow 30  $\text{cm}^3/\text{min}$ ) was employed. Both the corresponding decomposition temperature ( $T_{\text{dec}}$ ), in this paper estimated as 5% weight loss, and the temperature of total combustion ( $T_{\text{tc}}$ ), taken as nearly 100% weight loss, were evaluated.

## 3 Results and Discussion

### 3.1 Visual Examination

The appearance of all the PLA polycondensate obtained are summarized in Table 1. Initially, all the samples were solid materials as white in color as the prepolymer. When SSP started, some of them passed thorough visual changes from initially white to brown or even black, but all maintained their rigid solid form and no sticky or wax-like products were formed. It can be seen that  $\text{H}_2\text{SO}_4$  had a significant influence on the appearance of the resultant product. Even a 0.5% addition caused noticeable browning and 1 and 2% led to products of almost a black color. A similar trend was observed for the binary catalyst  $\text{SnCl}_2 + \text{pTSA}$ . Although in this case 0.5% of the catalyst changed the color of the sample to a subtle brown tinge, further increases of up to 2% did not bring about further darkening. All the other

Table 1. The molecular properties of obtained samples

Prepolymer	Catalyst Type	Catalyst (%)	$M_n$ [g/mol] <sup>b</sup> /PDI										$M_n^d$ [g/mol] 3,600	Appearance	$X_c^e$ [%] 44.3	
			0 [h]	6 [h]	12 [h]	18 [h]	24 [h]	$\eta$ [dL/g]	$M_n^{a,b}$ [g/mol] 3,100	$M_n^d$ [g/mol] 3,600	Appearance	$X_c^e$ [%] 44.3				
non-catalyzed SnCl <sub>4</sub> ·2H <sub>2</sub> O + pTSA (1:1)	0	2,750/2.8	2,750/2.8	2,700/2.4	4,300/2.37	5,400/2.1	5,400/2.2	5,400/2.2	5,400/2.1	5,400/2.1	5,400/2.1	0.19	14,600	4,700	White	63.8
	0.5	2,750/2.8	3,800/1.9	6,700/1.7	5,800/2.1	5,800/2.1	5,800/2.1	5,800/2.1	5,800/2.1	5,800/2.1	5,800/2.1	n.d.	n.d.	n.d.	Slight. Brown	
SnO <sub>2</sub>	1	2,750/2.8	7,400/2	17,500/1.5	13,700/1.8	19,600/1.5	19,600/1.5	19,600/1.5	19,600/1.5	19,600/1.5	19,600/1.5	0.29	25,900	740	Brown	66.2
	2	2,750/2.8	7,000/1.77	2,100/2.4	4,400/2.0	6,800/1.9	6,800/1.9	6,800/1.9	6,800/1.9	6,800/1.9	6,800/1.9	n.d.	n.d.	n.d.	Brown	
H <sub>2</sub> SO <sub>4</sub>	0.5	2,750/2.8	5,300/1.6	5,400/1.5	5,000/1.6	6,600/1.6	6,600/1.6	6,600/1.6	6,600/1.6	6,600/1.6	6,600/1.6	n.d.	n.d.	n.d.	White	52.2
	1	2,750/2.8	2,520/2.5	3,200/2.8	5,500/1.8	4,538/2.6	4,538/2.6	4,538/2.6	4,538/2.6	4,538/2.6	4,538/2.6	n.d.	n.d.	n.d.	White	
CA	2	2,750/2.8	6,700/1.5	2,100/1.9	4,800/1.7	4,600/2.2	4,600/2.2	4,600/2.2	4,600/2.2	4,600/2.2	4,600/2.2	n.d.	n.d.	n.d.	White	75.7
	0.5	2,750/2.8	22,000/2	29,200/1.8	39,300/1.9	45,300/1.9	45,300/1.9	45,300/1.9	45,300/1.9	45,300/1.9	45,300/1.9	0.59	65,100	1,200	Brown	69.2
MSA	1	2,750/2.8	20,600/1.9	26,800/1.7	32,000/2.0	35,800/1.8	35,800/1.8	35,800/1.8	35,800/1.8	35,800/1.8	35,800/1.8	0.50	56,700	580	Black	
	2	2,750/2.8	13,800/1.6	5,300/1.9	11,000/1.7	12,000/1.9	12,000/1.9	12,000/1.9	12,000/1.9	12,000/1.9	12,000/1.9	0.17	12,300	n.d.	Black	
Sn(Oct) <sub>2</sub> <sup>c</sup>	0.5	2,750/2.8	4,000/2	4,500/2.0	5,700/2.1	8,300/1.6	8,300/1.6	8,300/1.6	8,300/1.6	8,300/1.6	8,300/1.6	n.d.	n.d.	n.d.	White	51.2
	1	2,750/2.8	1,800/3.2	2,900/2.9	4,600/2.2	5,200/2.0	5,200/2.0	5,200/2.0	5,200/2.0	5,200/2.0	5,200/2.0	n.d.	n.d.	n.d.	White	
Sn(Oct) <sub>2</sub> <sup>c</sup>	2	2,750/2.8	5,800/1.6	1,800/2.3	2,900/2.3	2,900/2.6	4,100/1.9	4,100/1.9	4,100/1.9	4,100/1.9	4,100/1.9	n.d.	n.d.	n.d.	White	
	0.5	2,750/2.8	7,900/1.3	6,100/1.9	5,700/1.9	8,800/1.6	8,800/1.6	8,800/1.6	8,800/1.6	8,800/1.6	8,800/1.6	n.d.	n.d.	n.d.	White	71.2
Sn(Oct) <sub>2</sub> <sup>c</sup>	1	2,750/2.8	16,900/1.9	21,900/2.1	23,000/2.1	33,500/1.7	33,500/1.7	33,500/1.7	33,500/1.7	33,500/1.7	33,500/1.7	0.49	51,100	7,600	White	
	2	2,750/2.8	7,800/1.74	5,300/1.8	10,600/1.6	12,200/1.8	12,200/1.8	12,200/1.8	12,200/1.8	12,200/1.8	12,200/1.8	0.29	25,900	n.d.	White	
Sn(Oct) <sub>2</sub> <sup>c</sup>	0.5	2,750/2.8	2,300/2.6	3,100/1.7	4,700/2.0	3,900/2.3	3,900/2.3	3,900/2.3	3,900/2.3	3,900/2.3	3,900/2.3	n.d.	n.d.	n.d.	White	
	1	2,750/2.8	4,700/1.6	3,700/2.1	9,100/2.2	16,600/1.7	16,600/1.7	16,600/1.7	16,600/1.7	16,600/1.7	16,600/1.7	n.d.	n.d.	n.d.	White	
Sn(Oct) <sub>2</sub> <sup>c</sup>	2	2,750/2.8	15,000/2.6	10,500/2.4	21,000/2.9	57,200/1.6	57,200/1.6	57,200/1.6	57,200/1.6	57,200/1.6	57,200/1.6	0.85	105,300	22,300	White	71.9

a – determined by GPC, b – determined by M-H equation, c – polymer dissolved in toluene, d – <sup>1</sup>H-NMR, n.d. – not determined, e – crystallinity by D.

samples remained opaque and white in shade throughout the period of the study, with no evidence of darkening.

Indeed, reduced discoloration can be considered one of the advantages of SSP (27). However, this is strongly dependent on the catalyst used, reaction temperatures and times, side reactions and by-products (28). For example, Nam-pootheri(29) reported that sulphuric acid instigates accelerated and undesirable side reactions at temperatures above 120°C and Orozco (30), in his work, synthesized polylactide in a molten state with a SnCl<sub>2</sub>+pTSA (1:1) catalyst and a light brown product was also obtained. However, in this case, the reaction temperature was significantly higher and the reaction time lesser than in the research presented here.

### 3.2 Molecular Weight vs. Time

It is well known that esterification reactions during SSP especially take place in amorphous phase, as the mobility of the chain end groups is high and the catalyst and other unreacted compounds tend to concentrate. In the experiment described here, the values of PLA molecular weight-catalyzed and non-catalyzed – generally increased with time (Figures. 2–4). In fact, the prepolymer possessed M<sub>w</sub> 7,700 g/mol. After 24 h of non-catalyzed SSP, M<sub>w</sub> increased approximately by 155% to 11,900 g/mol. It is clear that in the case of non-catalyzed SSP only autocatalytic actions mediated by carboxyl end groups of prepolymer chains can occur; therefore, such a relatively small increment in M<sub>w</sub> was indicated. A similar trend was also observed for the catalyzed PLA samples. However, the increase in M<sub>w</sub> was strongly affected by the presence of the

catalyst and its concentration. In the case of 0.5% catalyst concentrations (Figure 2), the best result was achieved with H<sub>2</sub>SO<sub>4</sub>, when M<sub>w</sub> shot up to 44,000 g/mol within just 6 h and reached a maximum of 82,600 g/mol at the end of the experiment, which is equal with enhancement to 1,070%. Other catalysts at the concentration of 0.5% did not exhibit such a favorable effect for improving molecular weight during SSP, at best only reaching an M<sub>w</sub> of about 14,000 g/mol. Sulphuric acid is a very strong proton acid and its superb performance as a catalyst for esterification is generally acknowledged. For example, Hiltunen (31) studied the effect of various catalysts on the melt polycondensation of lactic acid, and sulfuric acid was found to provide the most beneficial effect on M<sub>w</sub> enhancement. However, M<sub>w</sub> ~ 33,000 g/mol was achieved in that study. The remarkable higher molecular weight obtained during SSP can be accounted for due to the significantly lower reaction temperature (130°C), when side reactions such as degradation are restricted.

When concentration of the catalysts was increased to 1%, more evident improvement in M<sub>w</sub> became noticeable (Figure. 3). As before, the catalyst H<sub>2</sub>SO<sub>4</sub> provided a notable rise in molecular weight in the same time (6 h), when M<sub>w</sub> reached 39,200 g/mol, finishing at the approximate value of 64,500 g/mol after 24 h, which is almost an increment of 837%. Similarly, the MSA had significant impact on PLA post-polycondensation, with the final product exhibiting 740% growth in M<sub>w</sub> in contrast with the initial value. A considerably lower but still interesting enhancement of M<sub>w</sub> was observed for the catalyzed reactions of SnCl<sub>2</sub>·2H<sub>2</sub>O+pTSA (1:1) and Sn(Oct)<sub>2</sub>. For both catalysts, the initial increase (after 6 h) was only in the magnitude of

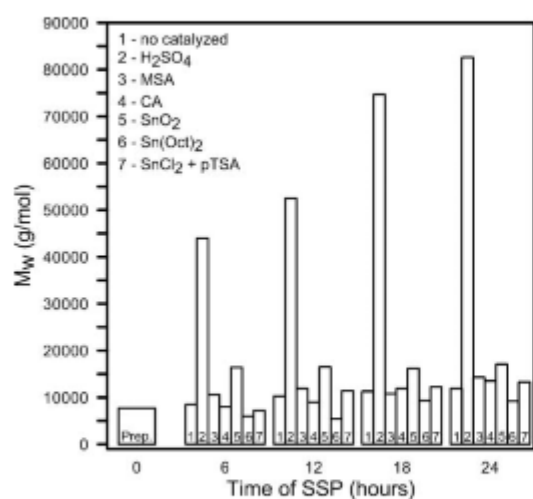


Fig. 2. Change in Mw during SSP with 0.5% catalyst content.

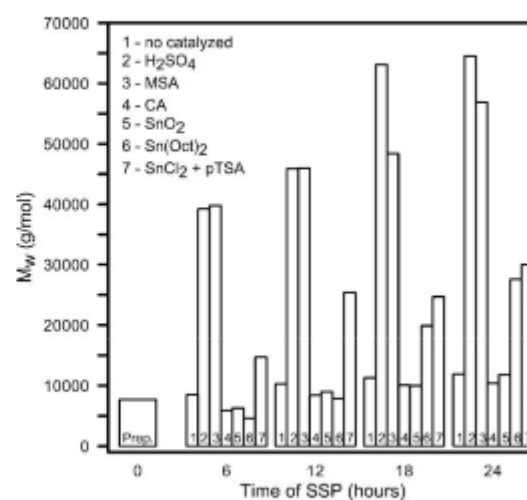


Fig. 3. Change in Mw during SSP with 1% catalyst content.

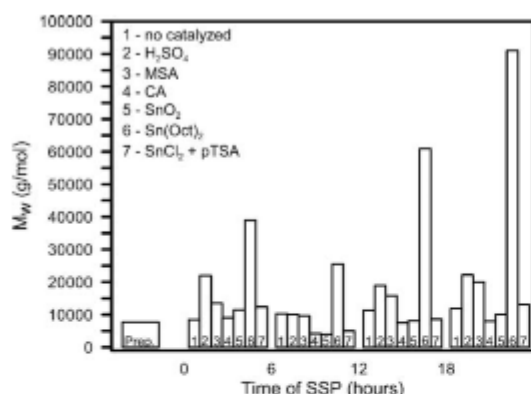


Fig. 4. Change in  $M_w$  during SSP with 2% catalyst content.

several thousand, but the final value of  $M_w$  reached approximately 28,500 g/mol, this being equal to 370% enhancement. The two remaining catalysts  $\text{SnO}_2$  and CA did not exhibit such a favorable effect on molecular weight increase as those mentioned previously, and final improvement was only about 134% for both.

In a previous work (12) by the authors, MSA was utilized for catalyzation of LA melt polycondensation, with a considerably lower  $M_w$  (17,000 g/mol) being achieved in the best instance. MSA was also used by Moon *et al.* (21) in the SSP of glycolic acid and a similar result (80,000 g/mol) was reported. The affectivity of MSA as a polyesterification catalyst is probably connected with its strong protonic acid and non-oxidizing qualities, which effectively restrict degradation and side reactions.

Finally, the effect of 2% concentration of the catalyst on  $M_w$  is depicted in Figure 4. In fact, this sample essentially set the trend; for longer reaction times, the higher  $M_w$  had not been as evident for all samples. Principally,  $\text{SnCl}_2 \cdot 2\text{H}_2\text{O} + \text{pTSA}$ ,  $\text{SnO}_2$ ,  $\text{H}_2\text{SO}_4$  and CA catalyzed samples reached the maximum value of  $M_w$  after 6 h, such increases lying between 60% and 286%. The longer reaction time led to a steady decline in  $M_w$  values, the cause probably being the high extent of reverse or decomposition reactions. However, when the catalyst  $\text{Sn}(\text{Oct})_2$  was used, significant enhancement - nearly 1,200% of  $M_w$  - was observed at the end of the reaction (from 7,700 to 91,500 g/mol). Indeed, this was also the best result achieved. The reason was probably due to the fact that  $\text{Sn}(\text{Oct})_2$  is a Lewis acid and a strong ester interchange catalyst, therefore, it produces polyesters of high molecular weight. It should be noted that this catalyst creates PLA with sufficiently high molecular weight (>100,000 g/mol), particularly during ring-opening polymerization of lactide, which is a different mechanism (32). In the previous work (12) by the authors, the  $M_w$  did not traverse 50,000 g/mol during traditional melt polymerization when  $\text{Sn}(\text{Oct})_2$  was used, with similar results also being

observed by Hiltunen (31) and Lee (33). The positive result obtained with this catalyst during SSP can be attributed to the especially low temperature, which prevents thermal decomposition, as  $\text{Sn}(\text{Oct})_2$  is known for its tendency to form lactide particularly at higher temperatures (31). However, the required amount (2%) is significantly higher than in case of the melt or ring-opening polymerization method (<1%) (32).

The beneficial effect of the binary catalyst system  $\text{SnCl}_2 + \text{pTSA}$  had previously been reported by Zhang and Moon (20, 21). A molecular weight from 73,000 to 320,000 g/mol was reached, which differs from that obtained in the experiment presented here ( $M_w = 30,000$  g/mol). Nevertheless, the reaction temperatures,  $M_w$  and PDI of the prepolymer were higher in their work. It is possible that this discrepancy can be explained by specific sample preparation (mixing catalysts in polymer solution), but it should be stated that both  $\text{SnCl}_2$  and pTSA proved highly soluble in acetone.

Finally, the low catalytic effect of citric acid and  $\text{SnO}_2$  in all the concentrations investigated can be due to their chemical qualities (both are weak Lewis acids). Furthermore,  $\text{SnO}_2$  was difficult to disperse in non-viscous polymer solution. As in the authors' previous work (12), PLA was synthesized in the presence of CA but a significant inhibitive effect on  $M_w$  was observed. However, the difference between this and the research presented here can be accounted for by fact that reaction temperatures were close to the decomposition temperature of CA, in addition to which another catalyst -  $\text{Sn}(\text{Oct})_2$  - was present in the reaction mixture.

The values of  $M_n$  of selected samples derived from the M-H equation are summarized in Table 1. They are in general accord with those obtained from GPC analysis. Considering the data presented in Table 1, no obvious pattern in the index of molar-mass dispersity within the entire range of reaction time could be observed. However, it can be seen that all the samples possessed a more or less reduced value of PDI than prepolymer, which is a logical consequence of chemical reactions among chain end groups in prepolymer.

### 3.3 <sup>1</sup>H-Nuclear Magnetic Resonance

Figure 5 shows <sup>1</sup>H-NMR spectra and the ascription of the peaks in the spectra of PLA. The resonances at 5.16 ppm (-CH quartet, a), 1.46 ppm (-CH<sub>3</sub> doublet), 4.2 ppm (-CH quartet, at hydroxyl end units, c), 4.99 ppm (-CH quartet, at carboxyl end units, d, e) and at 5.10 ppm ((-CH quartet, b) originate from hydrogen of lactic unit. The number molecular weight of PLA were calculated according to Equations 4 and 5, respectively.

$$\overline{DP}_n = \frac{Ia + Ib + Ic + Id + Ie}{Ic} \quad (4)$$

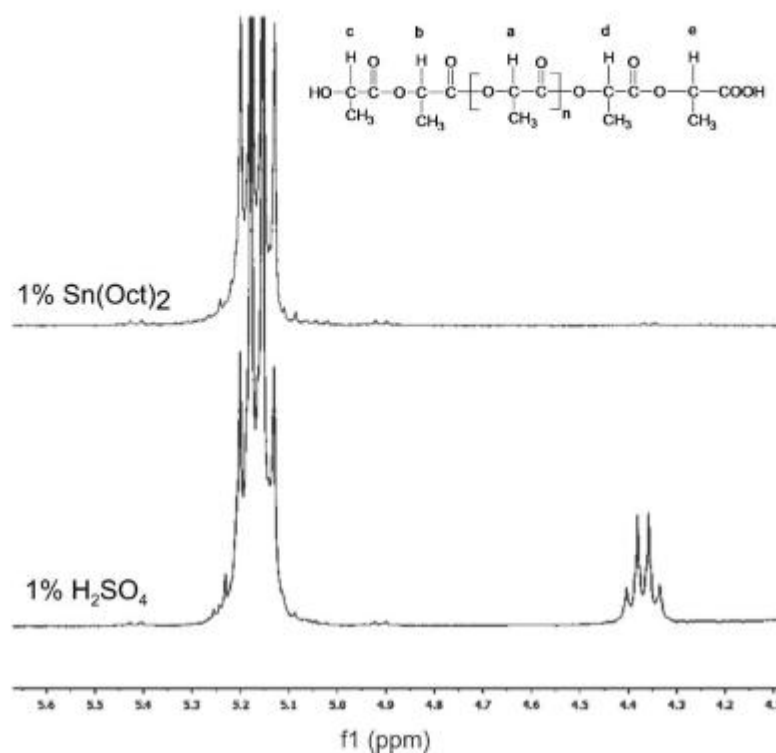


Fig. 5.  $^1\text{H-NMR}$  spectra of the selected polycondensates.

Where  $I$  represents the integral of the proton signals (peak areas, labelled in Figure 5).

$$\bar{M}_n = \overline{DP}_n \times 72 + 18 \quad (5)$$

The molecular weights measured by the NMR method were less than the molecular weight measured by GPC method. We assume that two agglomeration processes occur, chemical and physical. pTSA and  $\text{H}_2\text{SO}_4$  are not suitable catalysts for the synthesis of PLA polymer. The product is brown in color, in addition, resulting agglomerates, which are not soluble in DMSO solvent. NMR spectra recorded in DMSO are very poor. Calculation of molecular weight from NMR can be misleading because carboxylic groups of the synthesized polymer can react with the carboxylic group (Figure 6) of another polymer (chemical agglomeration). However, in the case of PLA catalyzed with pTSA and  $\text{H}_2\text{SO}_4$ , the comparison of the molecular weight reveals the significant difference between molecular weight determined by GPC method and molecular weights determined by  $^1\text{H-NMR}$ . It could indicate the specific reactions between PLA and pTSA and  $\text{H}_2\text{SO}_4$ , which occur only with this type of catalyst and effects to the structure of

the end groups and color of the polymer. We assume that another reason for such discrepancies is presumably due to the physical agglomeration process when pTSA and  $\text{H}_2\text{SO}_4$  were used as catalyst. These two acids are a strong oxidizer that removes most organic matter and it hydroxylates most surfaces making them extremely hydrophilic. Due to this hydrophilicity, physical agglomeration occurs. Nevertheless, significant discrepancies in the calculated molecular weight values were obtained. The reason can be found in the principles of the  $M_n$  determination and structural features of the polycondensates. The values of molecular weight determined by  $^1\text{H-NMR}$  (Table 1) for other polymers synthesized with another catalyst,  $\text{Sn}(\text{Oct})_2$ , are in agreement with the results obtained from GPC analysis.

### 3.4 DSC Analysis of the Products

The DSC thermograms of the first heating run for the PLA prepolymer and samples after SSP are shown in Figure 7 and the data summarized are in Table 1.

For all samples, the glass transition region was detected at around  $50^\circ\text{C}$ . As the temperature was further increased,

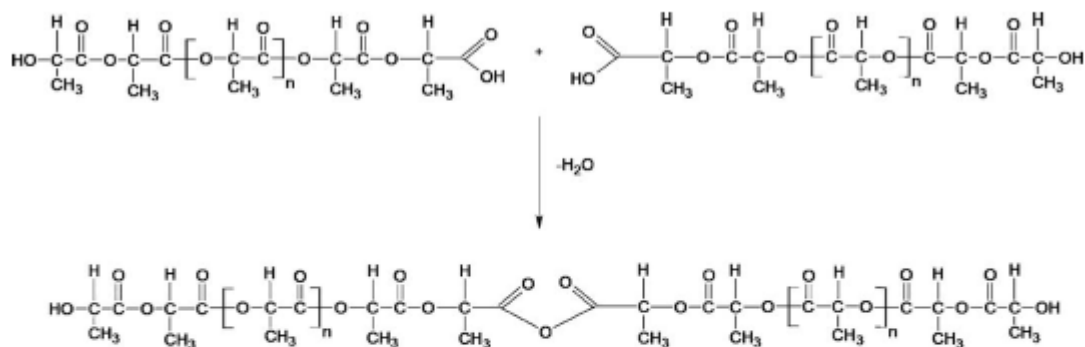


Fig. 6. Synthetic route of side reaction at polymerization of lactic acid.

the main melting peak was recorded. The value of  $T_m$  varied for different samples. The prepolymer exhibited  $T_m$  at  $149.6^\circ\text{C}$ , while other investigated samples displayed a higher  $T_m$ , ranging from  $157^\circ\text{C}$  to  $176^\circ\text{C}$ , which was attributed to the sample being catalyzed by 2%  $\text{Sn}(\text{Oct})_2$ . The enthalpy of melting, here expressed as the degree of crystallinity, generally followed the same trend. Its value increased from 44% for the initial prepolymer and reached values between 69.2% to 75.7% for the catalyzed samples of 1%  $\text{H}_2\text{SO}_4$ , 1% MSA, 2%  $\text{Sn}(\text{Oct})_2$  and 0.5%  $\text{H}_2\text{SO}_4$ . The results indicate that both  $T_m$  and  $X_c$  were directly related to the higher molecular weight of samples after SSP. Similar observations have been noted by many other authors (20, 21) Nevertheless, in several cases (samples catalyzed with CA,  $\text{SnO}_2$  and 1%  $\text{H}_2\text{SO}_4$ ) the values of  $T_m$  and/or  $X_c$  were lower in comparison with the non-catalyzed sample. It reveals that these catalysts also influence a quality and quantity of the crystalline phase of the resulting postpoly-

condensation products. It can be caused by either specific catalytic function or presence of degradation products, especially in the case of  $\text{H}_2\text{SO}_4$ .

It is generally accepted that  $T_g$  is related to molecular weight. An increase in  $M_n$  should lead to a drop in the number of end groups in a polymer chain, which lower free-volume, therefore,  $T_g$  ought to be higher than in low-molecular-weight polymer (free volume theory of  $T_g$ ). This behavior can be described via the Fox-Flory Equation 6.

$$T_g = T_g^\infty - \frac{K}{M_n} \quad (6)$$

Where  $T_g^\infty = T_g$  at infinite molecular weight and  $K$  = a constant representing the excess free volume of the end groups of the polymer chains. Here  $T_g^\infty = 58^\circ\text{C}$  and  $K = 55,000$  (34).

The prepolymer showed  $T_g$  at  $46.3^\circ\text{C}$ , while a significant increase was shown only in 1% MSA, 2%  $\text{Sn}(\text{Oct})_2$  and non-catalyzed samples, in which  $T_g$  increased to  $56.1^\circ\text{C}$ ,  $53.6^\circ\text{C}$  and  $51.8^\circ\text{C}$ , respectively. The remaining samples investigated did not exhibit any significant enhancement in  $T_g$ , whilst the CA catalyzed sample had an even slightly lower  $T_g$  than prepolymer, i.e.,  $44.4^\circ\text{C}$ . (Figures. 8 and 9).

As can be seen, a comparison of the measured data with the Fox-Flory model (Fig. 8) produces general accord merely for samples synthesized with 0% and 0.5%  $\text{SnO}_2$ , 1% MSA and 2%  $\text{Sn}(\text{Oct})_2$ . Conversely, prepolymer, 1%  $\text{SnCl}_2 \cdot 2\text{H}_2\text{O} + \text{pTSA}$  (1:1), 0.5% and 1%  $\text{H}_2\text{SO}_4$ , and 0.5% CA catalyzed samples did not adhere to this model and the measured values of  $T_g$  are lower than those predicted by Equation 6. This might be caused by fact that this model, based on free volume theory, is not totally suitable for low-molecular-weight polymer (35). For this reason, modifying Equation 6 was suggested by Ogawa (36). Instead of an inverse dependence on the values of average molecular weight, this author utilized the square root of the product

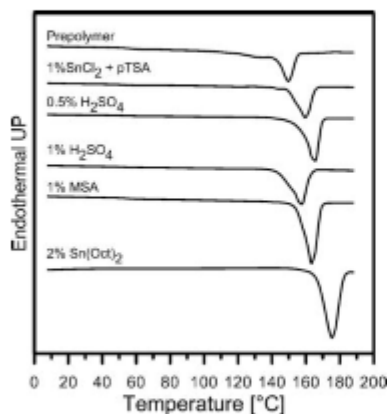


Fig. 7. DSC thermograms (1st scans) of selected samples obtained after 24 h of SSP.

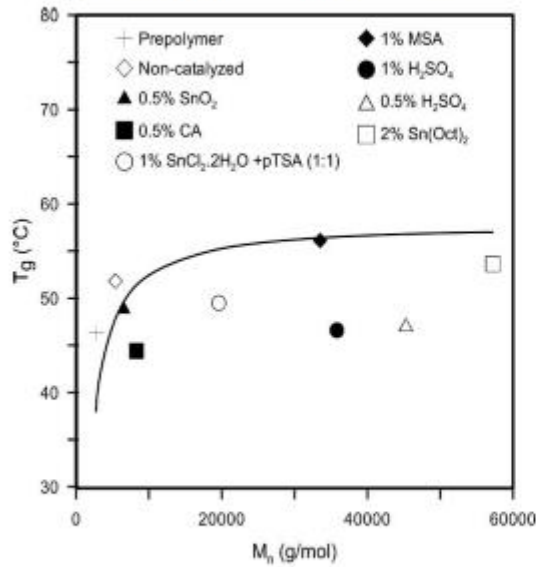


Fig. 8.  $T_g$  vs.  $M_n$  dependence. Solid line represents the Fox-Flory model (Eq. 6).

of mean weight and mean numerical values:

$$T_g = T_g^\infty - \frac{K}{(M_w M_n)^{0.5}} \quad (7)$$

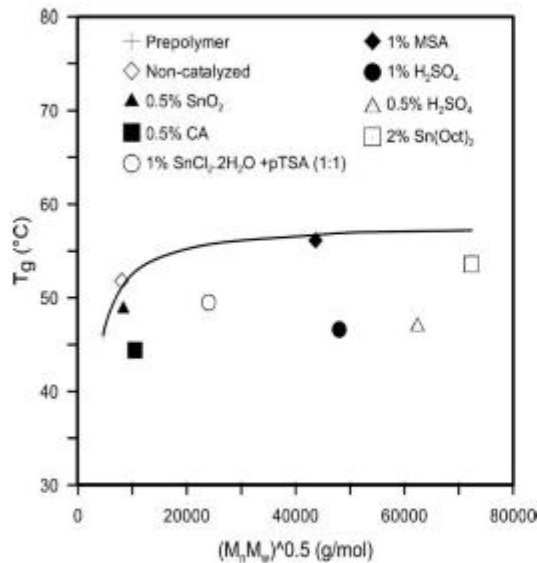


Fig. 9.  $T_g$  vs.  $(M_n M_w)^{0.5}$  dependence. Solid line represents Ogawa model (Eq. 7).

As is apparent, this model closely fits the experimental data for both low and high  $M_n$  samples (Figure 9). However, in the case of the catalyzed samples of citric acid, 1%  $\text{SnCl}_2 \cdot 2\text{H}_2\text{O} + \text{pTSA}$  (1:1) and  $\text{H}_2\text{SO}_4$ , the data measured does not correspond with either Equation 6 or 7. The cause of low  $T_g$  in a sample catalyzed by citric acid can be explained by the author's earlier work (12) dealing with lactic acid – a citric acid reaction. In all likelihood, the citric acid terminates some of the PLA chains and as a consequence free volume rises, resulting in a decrease in  $T_g$ . This can be supported by mild reaction conditions which occur below the CA decomposition temperature (150°C). In the case of 1%  $\text{SnCl}_2 \cdot 2\text{H}_2\text{O} + \text{pTSA}$  (1:1) and  $\text{H}_2\text{SO}_4$  catalyzed samples, the low values of  $T_g$  are mostly probably related to the presence of impurities and various degradation products, which presence was suggested by darkening of this products.

### 3.5 Thermogravimetry

The thermal stability of the selected PLA samples was investigated by TGA. The thermogravimetric (TG) curves and their derivative form (dTg) are shown in Figure 10. Additionally, the decomposition and total combustion temperatures for selected samples are summarized in Table 2. Usually, an increase in decomposition temperature results in a more thermally stable product. It can be noticed that the lowest  $T_{\text{dec}}$  was observed for the 2%  $\text{Sn}(\text{Oct})_2$  catalyzed sample ( $\sim 216^\circ\text{C}$ ), while the remaining products had considerably higher  $T_{\text{dec}}$ , ranging between  $263.6^\circ\text{C}$  and  $274^\circ\text{C}$ . The degradation of PLA at an elevated temperature can be principally attributed to thermal hydrolysis, zipper-like depolymerization, thermo-oxidative reactions, or intramolecular transesterification, resulting in formation of monomer and oligomers, but also other volatile products such as acetaldehyde, carbon dioxide, carbon monoxide and ketene (37).

Generally, the factors which can influence thermal stability are primarily: trace amounts of water, the presence of monomer/oligomers, residual catalysts and molecular weight (38). While dependence on the first three factors should be always directly proportional to their content in a polymer sample, the influence of  $M_w$  is usually inverse: the higher the  $M_w$ , the greater the thermal stability of the product. This is connected with the concentration of hydroxyl end groups, which prove to be the main accelerators of decomposition reactions if all other factors are excluded.

Interestingly, the greatest thermal stability ( $275^\circ\text{C}$ ) was observed for the non-catalyzed sample, possessing  $M_w$  several-fold lower than the other examined samples. Therefore, it was concluded that the presence of catalysts was fundamental for thermal stability of the final product. The very poor thermal stability of the catalyst 2%  $\text{Sn}(\text{Oct})_2$  was attributed to the intense activity of Sn to accelerate transesterification reactions leading to back-biting degradation, which was also observed by Cam (38). Nonetheless, both

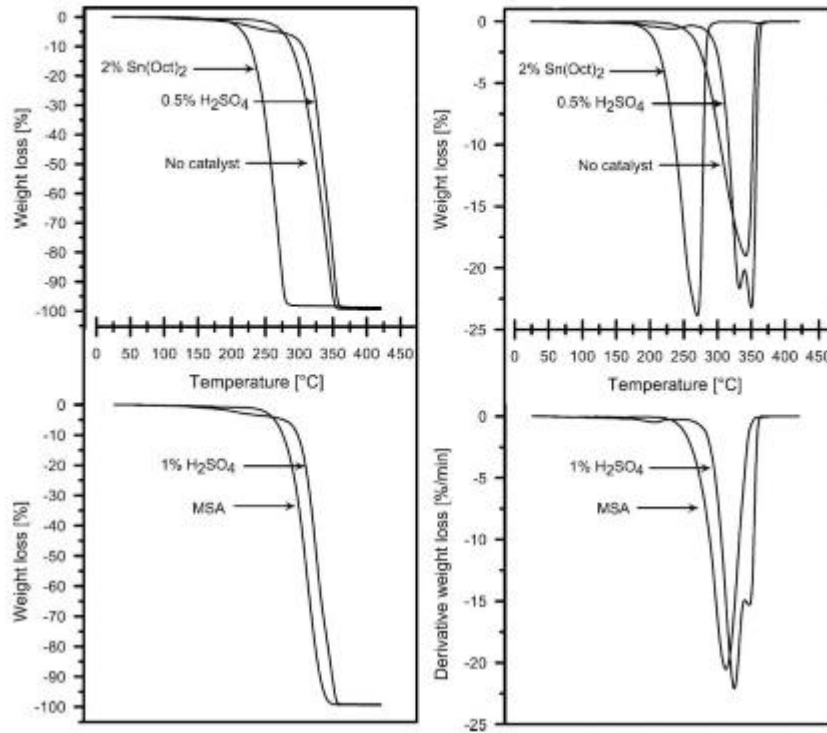


Fig. 10. TGA and dTGA curves of samples after 24 h of SSP.

0.5% and 1%  $\text{H}_2\text{SO}_4$  possessing products demonstrate relatively good performance during heating at a  $T_d$  of 274°C and 267°C, respectively. The presence of MSA in the sample led to a product with a  $T_d$  of 264°C, which is almost the same as in the case of 1%  $\text{H}_2\text{SO}_4$ , but considerably higher than 2%  $\text{Sn}(\text{Oct})_2$ .

Derivative curves revealed that while non-catalyzed, 1% MSA and 2%  $\text{Sn}(\text{Oct})_2$  catalyzed samples exhibited single-step decomposition, whereas those samples containing 0.5% and 1%  $\text{H}_2\text{SO}_4$  passed through three-stage decomposition. The dTG curve of 1% and 0.5%  $\text{H}_2\text{SO}_4$  catalyzed sam-

ples show the first peak corresponding to 3.3% and 2.4% weight loss at 230.5°C and 207.2°C, an 18.3% weight-loss peak at 325.7°C, and a 21.8% weight-loss peak at 322.5°C, followed by another 23% at 347.8°C and 15.3% at 341°C, respectively. The complicated decomposition pattern of these samples is probably attributable to the presence of strongly oxidizing acid –  $\text{H}_2\text{SO}_4$  – as well as impurities created during synthesis.

Based on these results, the thermal stability of the PLA samples prepared was ordered as follows: no catalyst < 0.5%  $\text{H}_2\text{SO}_4$  < 1%  $\text{H}_2\text{SO}_4$  < MSA << 2%  $\text{Sn}(\text{Oct})_2$

Table 2. TGA characterization of selected products

Sample	$T_{50}$ (°C)	$T_{10}$ (°C)	dTG 1 <sup>st</sup> peak (°C)	dTG 2 <sup>nd</sup> peak (°C)	dTG 3 <sup>rd</sup> peak (°C)
No catalyst	275.0	355	337.3	n.f	
0.5% $\text{H}_2\text{SO}_4$	274.0	365	230.5	322.5	341.0
1% $\text{H}_2\text{SO}_4$	267.1	360	207.2	325.7	347.8
1% MSA	263.6	345	308.7	n.f	
2% $\text{Sn}(\text{Oct})_2$	216.2	305	266.6	n.f	

n.f – not found.

#### 4 Conclusions

This paper is focused on the synthesis of poly(*L*-lactic acid) via solid-state post-polycondensation of low-molecular PLA in the presence of various catalyst systems. Primarily, attention was paid to determining the optimal catalyst type and concentration, the molecular weight and thermal properties of the final products (0.5 and 1% H<sub>2</sub>SO<sub>4</sub>, 1% MSA, 2% Sn(Oct)<sub>2</sub> and 0% catalyst).

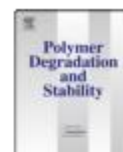
The results show that the role of the catalyst type and concentration is crucial to enhancing the molecular weight of the PLA during the solid-state post-polycondensation process. From the molecular weight enhancement point of view, H<sub>2</sub>SO<sub>4</sub>, MSA and Sn(Oct)<sub>2</sub> were found to be the most effective catalysts. The post-polycondensation process catalyzed with these compounds provided PLA with M<sub>w</sub> ~ 57,000–92,000 g/mol. However, H<sub>2</sub>SO<sub>4</sub> does not seem to be a suitable catalyst due to the occurrence of a competitive degradation reaction leading to darkening of the resulting products. On the other hand, their thermal stability was better in comparison with other investigated samples. The highest M<sub>w</sub> was observed for the systems catalyzed with 2 wt% Sn(Oct)<sub>2</sub> (91,500 g/mol). However, this reaction product exhibited the worst thermal stability, which can be limiting for its practical use. Finally, 1 wt% MSA can be considered as an optimal catalytic system for PLA post-polycondensation reaction due to providing of a reasonable balance between M<sub>w</sub> enhancement as well as thermal stability of the products.

#### Acknowledgments

This work was supported by the Ministry of Education, Youth and Sports of the Czech Republic (project ME09072) and Operational Program Research and development for Innovations co-funded by the European Regional Development Fund (project No. CZ.1.05/2.1.00/03.0111). P.K. and V.S. are also grateful to Internal Grant Agency of Tomas Bata University in Zlin (grant IGA/FT/2012/005) for co-funding.

#### References

- Gregorova, A., Hrabalova, M., Wimmer, R., Saake, B., and Altaner, C.J. (2010) *J. Appl. Polym. Sci.*, 114(5), 2616–2623.
- Sedlarik, V., Vesel, A., Kucharczyk, P., and Urbanek, P. (2011) *Mater. Technol.*, 45(3), 209–212.
- Poljansek, I., Gricar, M., Zagar, E. and Zigon, M. (2008) *Macromol. Symp.*, 272(1), 75–80.
- Sedlarik, V., Saha, N., Sedlarikova, J., and Saha, P. (2008) *Macromol. Symp.*, 272(1), 100–103.
- Hrabalova, M., Gregorova, A., Wimmer, R., Sedlarik, V., Machovsky, M., and Mundigler, N. (2010) *J. Appl. Polym. Sci.*, 118(3), 1534–1540.
- Jacobsen, S., Degee, P.H., Fritz, H.G., Dubois, P.H., and Jerome, R. (1999) *Polym. Eng. Sci.*, 39(7), 1311–1319.
- Kricheldorf, H.R. (2011) *Chemosphere*, 43(1), 49–54.
- Abraham, I.D. and Wiseman, D.M. (1997) *Handbook of Biodegradable*. Harwood Academic Publishers: Amsterdam 3–21.
- Auras, R., Harte, B., and Selke, S. (2004) *Macromol. Biosci.*, 4(9), 835–864.
- Poljansek, I., Kucharczyk, P., Sedlarik, V., Kasparkova, V., Salakova, A., and Drbohlav, J. (2011) *Mater. Technol.*, 45(3): 261–264.
- Sedlarik, V., Kucharczyk, P., Kasparkova, V., Drbohlav, J., Salakova, A., and Saha, P. (2010) *J. Appl. Polym. Sci.*, 116(2): 1597–1602.
- Kucharczyk, P., Poljansek, I., Sedlarik, V., Kasparkova, V., Salakova, A., Drbohlav, J., Cvelbar, U., and Saha, P. (2011) *J. Appl. Polym. Sci.*, 122(2), 1275–1285.
- Silvia, K.M.D., Tarverdi, T., Withnall, and R., Silver. (2011) *J. Plast. Rubber. Compos.*, 40(1), 17–24.
- Campanelli, J.R., Cooper, D.G., and Kamal, M.R. (1993) *J. Appl. Polym. Sci.*, 48(3), 443–451.
- Vesel, A., Mozetic, M., and Zalar, A. (2007) *Vacuum*, 82(2), 248–251.
- Krstulovic, N., Labazan, I., Milosevic, S., Cvelbar, U., Vesel, A., and Mozetic, M. (2006) *J. Phys. D: Appl. Phys.*, 17(39), 3799–3804.
- Vesel, A. (2011) *Mater. Technol.*, 45(2), 121–124.
- Maharana, T., Mohanty, B., and Negi, Y.S. (2009) *Prog. Polym. Sci.*, 34(1), 99–124.
- Vouyioukaet S.N., Karakatsani E.K., and Pappaspyrides C.D. (2005) *Prog. Polym. Sci.*, 30(1), 10–37.
- Zhang, W., and Wang, Y. (2008) *Chinese J. Polym. Sci.*, 26(4), 425–432.
- Moon, S.I., Lee, C.W., Taniguchi, I., Miyamoto, M., and Kimura, Y. (2001) *Polymer*, 42(11), 5059–5062.
- Xu, H., Luo, M., Yu, M., Teng, C., and Xie, S. J. (2006) *Macromol. Sci. B Phys.*, 45(4), 681–687.
- Shinno, K., Miyamoto, M., and Kimura, Y. (1997) *Macromolecules*, 30(21), 6438–6444.
- Fukushima, K., Furuhashi, Y., Sogo, K., Miura, S., and Kimura, Y. (2005) *Macromol. Biosci.*, 5(1), 21–29.
- Dorgan, J.R., Janzen, J., Knauss, D.M., Hait, S.B., and Limoges, B.R., Hutchinson, M.H. (2005) *J. Polym. Sci. Pol. Phys.*, 43(21), 3100–3111.
- Luia, W.C., and Liaua, W.B. (2003) *Polymer*, 44(26), 8103–8109.
- Gupta, A.P., and Kumar, V. (2007) *Eur. Polym. J.*, 43(10): 4053–4074.
- Moon, S.I., Lee, C.W., Miyamoto, M., and Kimura, Y. (2000) *J. Polym. Sci. Polym. Chem.*, 38(9): 1673–1679.
- Nampoothiri, K.M., Nair, N.R., and John, R.P. (2010) *Biore-source Technol.*, 101(22), 8493–8501.
- Orozco, V.H., Vargas, A.F., and Lopez, B.L. (2007) *Macromol. Symp.*, 258(1), 45–52.
- Hiltunen, K., Seppala, J.V., and Harkonen, M. (1997) *Macromolecules*, 30(3), 373–379.
- Steinbuechel, A., and Merchessault, R.H. *Biopolymers for Medical and Pharmaceutical Applications*. Wiley-VCH Verlag GmbH & Co. KGaA: Weinheim, 186–219, 2005.
- Lee, M.W., Tan, H.T., Chandrasekaran, M., and Ooi, C.P. (2005) *SIMTech. Techn. Rep.*, 6(3), 40–44.
- Gariotta, D. (2001) *J. Polym. Environ.*, 9(2), 63–84.
- Couchman, P.R. (1980) *J. Mater. Sci.*, 15(7), 1680–1683.
- Ogawa, T.J. (1992) *J. Appl. Polym. Sci.*, 44(10), 1869–1871.
- Murariu, M., Bonnaud, L., Yoann, P., Fontaine, G., Bourbigot, S., and Dubois, P. (2010) *Polym. Degrad. Stab.*, 95(3), 374–381.
- Cam, D., and Marucci, M. (1997) *Polymer*, 38(8), 1879–1884.



### Novel aspects of the degradation process of PLA based bulky samples under conditions of high partial pressure of water vapour

Pavel Kucharczyk<sup>a,b</sup>, Eva Hnatkova<sup>c</sup>, ZdenekDvorak<sup>a,c</sup>, Vladimir Sedlarik<sup>a,b,\*</sup>

<sup>a</sup> Centre of Polymer Systems, Tomas Bata University in Zlín, Nam. T.G. Masaryka 5555, 760 01 Zlín, Czech Republic

<sup>b</sup> Polymer Centre, Faculty of Technology, Tomas Bata University in Zlín, Nam. T.G. Masaryka 273, 76272 Zlín, Czech Republic

<sup>c</sup> Department of Production Engineering, Faculty of Technology, Tomas Bata University in Zlín, Nam. T.G. Masaryka 273, 76272 Zlín, Czech Republic

#### ARTICLE INFO

##### Article history:

Received 30 July 2012

Received in revised form

3 October 2012

Accepted 18 October 2012

Available online 29 October 2012

##### Keywords:

Hydrolytic degradation

Poly(L-lactic acid)

Morphology

Molecular weight

Thermal properties

#### ABSTRACT

This work describes differences between the degradation of poly(L-lactic acid) bulky samples in high partial pressure of a water vapour environment versus a buffered liquid medium. Analytical techniques (optical and electron microscopy, size exclusion chromatography, differential scanning calorimetry) were used to evaluate the material's morphology, molecular weight, crystallinity and thermal properties. In particular, the extent of degradation was studied separately in the core and surface of the testing specimens. The results reveal significant differences in the bulk degradation profiles and morphological changes for both environments. Degradation in the liquid medium leads to multiphase core cortex morphology formation, while the environment with high partial pressure of water vapour provides homogeneous-like bulk degradation of the samples due to significantly different diffusion conditions on the liquid-polymer and water vapour saturated air-polymer interface.

© 2012 Elsevier Ltd. All rights reserved.

#### 1. Introduction

Lactic acid based polymers have attracted increasing interest over the past few decades both in fundamental research and in practical application. Poly(lactic acid) (PLA) is a synthetic biodegradable and bioresorbable polyester which occurs either in crystalline or amorphous form [1,2]. Under normal conditions PLA is a brittle and hard polymer. Its homopolymer as well as various copolymers are highly suitable for potential utilization in a growing number of applications, such as orthopaedics, drug delivery and sutures [1–3].

For application of bioresorbable polymers, an understanding is essential of the mechanism and rate of degradation. This depends on many factors such as temperature, pH, crystallinity, size, the presence of specific enzymes and molecular weight [4–7]. The degradation process of polylactide homopolymers and copolymers under various conditions has been described by many authors. One of the most comprehensive studies was conducted by Tsuji H. et al. They focused on various conditions of the degradation experiment,

especially enzymatic hydrolysis [4,8–10,12], alkaline or acid [4–14] and phosphate buffer solution (pH = 7.4) [15–19]. Furthermore, they also investigated various other factors, e.g. temperature [14,17,20] and crystallinity [9,15,18,21–24]. Works by other authors on polylactide degradation especially in liquid buffer solutions (pH close to neutral) or in vivo are listed in the paper under references [25–33].

On the contrary, the degradation of PLA in a humid environment has been paid noticeably less attention. Ho et al. [34] investigated the effect of temperature and high partial pressure of water vapour (relative humidity) on PLA hydrolysis by observing loss in mechanical properties and molecular weight. Similar experiments were conducted by Copinet [35] and Cairncross [36]. However, in all cases no information about inner morphology can be found. In addition, the samples were made from commercially available polymers of high molecular weight and degradation was performed on samples possessing minimal thickness (films <2 mm), where hydrolysis behaviour could prove significantly different in contrast with that of dimensions >2 mm.

On the basis of works investigating PLA hydrolysis in phosphate buffer solution (pH ~ 7) and a high relative humid environment, the generally accepted findings may be summarized below:

- 1) the hydrolysis of PLA films proceeds homogeneously along the film cross section via a bulk-erosion mechanism;

\* Corresponding author. Centre of Polymer Systems, Polymer Centre, Tomas Bata University in Zlín, nam. T.G. Masaryka 5555, 760 01 Zlín, Czech Republic. Tel.: +420 57 603 8013.

E-mail address: [sedlarik@ft.utb.cz](mailto:sedlarik@ft.utb.cz) (V. Sedlarik).

- 2) the hydrolytic scission of PLA chains occurs predominantly in the amorphous region between the crystalline regions inside and outside the spherulites. This results in bimodal molecular weight distribution curves;
- 3) an increase in temperature does not alter the hydrolysis mechanism of the PLA films;
- 4) in specimens (>2 mm), there is more rapid degradation inside rather than on its surface layers (core–cortex phenomenon);
- 5) higher relative humidity tends to enhance degradation and decrease the mechanical properties of PLA foils.

When considering PLA as a potential implant in a human body, the liquid medium is usually applied as the hydrolysis environment in research studies. However, some specific areas, an example being the respiratory tract or middle ear area, exhibit different conditions. In such places a relative humidity of about 100% and temperature of 37 °C are typical [37]. For instance, developing tympanostomy tubes (also called ventilation tubes) can be viewed as an example of practically utilizing PLA in the middle ear area [38,39]. In terms of the respiratory tract, PLA and its copolymers have been studied for tracheal tissue engineering [40]. Thus, a thorough investigation of the degradation process under these conditions is necessary. On the basis of this, the aim of the work presented here was to investigate the degradation of PLA samples in an environment of 100% relative humidity and its comparison with hydrolysis in phosphate buffer solution (pH = 7.4). The reason for using the buffered solution for such a comparison instead of pure water is that this particular study should compare degradation behaviour in two different conditions in the human body; therefore, the use of a standard environment simulating interstitial fluids instead of water is logical in this context. The degradation process was investigated by optical and electron microscopy, gel permeation chromatography and differential scanning calorimetry.

## 2. Experimental

### 2.1. Materials

*l*-lactic acid (LA), 80% water solution and tin(II) 2-ethylhexanoate (Sn(Oct)<sub>2</sub>), ~95%, were purchased from Sigma Aldrich, Steinheim, Germany. Disodium phosphate dihydrate and sodium phosphate monobasic dodecahydrate were supplied by Penta, Prague, the Czech Republic, (both in analytical grade with purity ≥99%). Solvents chloroform, acetone, methanol (all analytical grade) came from IPL PetruLukes, UherskyBrod, the Czech Republic. Chloroform (HPLC-grade) was sourced from Chromspec, Brno, the Czech Republic.

### 2.2. Polymer synthesis

The procedure of polymer synthesis was described previously [1]. In brief, 50 g LA was added to a 250 ml double necked flask equipped with a Teflon stirrer. The flask was then connected to an oil vacuum pump through a condenser and placed in an oil bath. Firstly, dehydration of *l*-LA solution at 160 °C took place, under a reduced pressure of 15 kPa for 4 h. Consequently, pressure was lowered to 100 Pa and the reaction was continued at 180 °C for another 24 h. The resultant product was cooled down to an ambient temperature and then dissolved in acetone. The polymer solution obtained was precipitated into a mixture of chilled methanol and distilled water 1:1 (v/v) and filtered. In order to remove any unreacted monomer and other low molecular impurities, the prepolymer was further washed several times with hot distilled water

(80 °C) and ethanol. Finally, the product was dried in a vacuum oven at 55 °C and 15 kPa for 48 h. The prepolymer was obtained in the form of white powder.

### 2.3. Specimen preparation

The specimens for hydrolysis were processed as follows: Firstly, the polymer powder was melted in a 25 ml glass bottle at 190 °C under a high vacuum of 100 Pa for 5 min. Then, the vacuum was released suddenly and hot melt was poured into approximately one half of a 1 ml glass vial (with the dimensions 40 × 6 mm in length and inner diameter, respectively). The role of the vacuum was to avoid the thermal degradation of heat sensitive polymer and also to de-gas the polymer melt. Once the melt had been poured into the vial, a silicon tube (of inner diameter 4 mm) was inserted into the vial with the still molten polymer. The melt was left to cool down in an ambient temperature and then the silicone tube was withdrawn. Finally, the silicone tube was removed and the resulting sample, resembling a cylinder in form, was cut into specimens of about 8 mm in length.

### 2.4. Density measurement

The density of the cylindrical sample was measured by the differential weighing method, when firstly the weight of the sample in air and then its weight in water of temperature 24 °C was determined. The densities were calculated from Eq. (1):

$$\rho(\text{g/cm}^3) = \frac{0.997295 \times w_{\text{air}}}{(w_{\text{air}} - w_{\text{water}})} \quad (1)$$

where,  $w_{\text{air}}$  and  $w_{\text{water}}$  are weights of the sample in air and water, respectively. The value of 0.997295 is the density of water at 24 °C (g/cm<sup>3</sup>).

### 2.5. Degradation test

At the beginning, the initial weight ( $w_0$ ) of each dried specimen was recorded. For the degradation test in liquid solution the procedure went as follows: The specimens were each placed in 25 ml glass bottles, then fully immersed in phosphate buffer solution (PBS, 37 °C, pH = 7.4, 0.1 M) and closed. To investigate degradation in an environment of high partial pressure of water vapour (hereinafter referred to as 100% RH) environment, the following procedure was applied: the test specimens were each placed on a glass cover slip and then put into a desiccator, which contained a low level of distilled water in the bottom, and this was closed. The desiccator was moved into an oven at a temperature of up to 37 °C, and the relative humidity was monitored by a digital hygrometer throughout the experiment. In both cases, six samples were removed at each follow-up time, wiped with a paper towel carefully, dried in a vacuum oven at 35 °C, 3 kPa for 30 h and weighed to obtain their weight at the time. Their remaining mass was then calculated from Eq. (2):

$$\text{remaining mass (\%)} = 100 - \frac{w_0 - w_t}{w_0} \times 100 \quad (2)$$

where,  $w_0$  is the initial weight and  $w_t$  is weight at the appropriate interval of time.

### 2.6. Morphological investigation

The surfaces of samples were investigated under the magnification range of 1 ×–4.5 × with a stereoscopic microscope (STM 722

3223, Intraco Micro, Tachlovice, the Czech Republic), and a digital camera (DCM 310 USB Microscope Camera, Scopetek, Hangzhou, China) was used to take photographic images. Both the surfaces and cross sections of the specimens were observed. The inner morphology of the samples was investigated via a (SEM) Vega II LMU scanning electron microscope (Tescan, the Czech Republic). The dried samples were cut and sputter coated with a layer of gold prior to examination.

### 2.7. Molecular weight determination by GPC

GPC analysis was conducted using a Breeze (Waters, the United Kingdom) chromatographic system. Samples were prepared by adding 1 ml of chloroform to approximately 1.5 mg of polymer taken from each follow-up time and appropriate section of the sample. Separation and detection took place on a PL gel-mixed-D bed column (300 × 7.8 mm, 5 μm particles) with a UV response detector (Waters 2487, the United Kingdom) at 239 nm, respectively. Analyses were carried out at room temperature with a chloroform flow rate of 1.0 ml/min and a 100 μl injection loop. The GPC system was calibrated with narrow polystyrene standards ranging from 580 g/mol to 271,000 g/mol (Polymer Laboratories Ltd., the United Kingdom). The average molecular weight  $M_n$  and molecular-weight dispersity ( $D_M = M_w/M_n$ ) of the tested samples were determined from their peaks corresponding to polymer fraction, and expressed as 'polystyrene equivalent' molecular weights. All data processing was carried out using Waters Breeze GPC software.

### 2.8. Water uptake

The procedure for determining water uptake was carried out as follows. The specimens were pre-dried (at 30 °C up to constant weight) before further investigation. Then they were immersed in distilled water and incubated at 37 °C under static conditions. The specimens were removed, blotted and immediately weighed after predetermined time intervals. Water uptake, WU (%), was calculated by using Eq. (3):

$$\text{water uptake (\%)} = 100 - \frac{w_1 - w_0}{w_0} \times 100 \quad (3)$$

where,  $w_0$  is the initial weight of the specimen after pre-drying and  $w_1$  is the wet mass of the specimen at the given time. Three specimens were tested in parallel.

### 2.9. Thermal properties

The thermal properties of the samples retrieved were analysed using a Mettler Toledo DSC1 STAR testing machine (Mettler Toledo, the Czech Republic), over a temperature range of 5–190 °C at a heating/cooling rate of 10 °C/min and under nitrogen flow of 20 cm<sup>3</sup>/min. The samples for DSC measurements were taken from whole cross sections of the specimens (approximately 8 mg). Melting point temperature ( $T_m$ ) with enthalpy of fusion  $\Delta H_{\text{melt}}$  was obtained from the first heating cycle, whereas the value of glass-transition temperature ( $T_g$ ) was determined from the second heating scan, at the mid-point stepwise increase of the specific heat which is associated with glass transition. The heat of fusion of 100% crystalline PLA [2],  $\Delta H_{100} = 93.7$  J/g was then used to determine the polymers' percentage of crystallinity ( $X_c$ ) according to Eq. (4):

$$X_c [\%] = \left( \frac{\Delta H_{\text{melt}}}{93.7} \right) \times 100 \quad (4)$$

## 3. Results and discussion

### 3.1. Morphology

The appearance of all the specimens under optical and electron microscopy can be seen in Figs. 1 and 2, respectively. Initially, each sample was stiff and brittle with a smooth cross section (Fig. 1a). The clearly visible porous structure along each sample was a consequence of the preparation process, as the inner surface of the silicone tube was not entirely smooth. After two weeks of degradation, considerable changes occurred between the samples placed in PBS and 100% RH. Specimens exposed to liquid PBS medium turned white, and a porous cortex (~0.5 mm in thickness) that had formed along cross section was observed (Fig. 1b). Conversely, samples exposed to 100% RH retained their original colour with slight surface cracks. The interior possessed a fine and homogenous structure (Fig. 2a).

Over a continuous time of degradation, the samples in PBS became rougher, exhibiting cracks, holes on the surface and slight changes in shape regularity. The cortex structure remained porous, but the core's texture turned from smooth to remarkable rough (Fig. 1b vs c). At the end of the experiment, the interface between the cortex and inner core was noticeably separated and corrupted and the whole structure was highly porous (Fig. 1c and d). The observed whitening, cracking and the porous structure of samples degraded in PBS result from degradation, heightened water content and crystallization, and are in general accord with results presented elsewhere [8,18].

Nevertheless, the samples placed in the 100% RH environment exhibited completely different behaviour. Even after 12 weeks of degradation, no significant disintegration or non-homogeneous core structure was observed by optical microscopy and the samples remained highly compact. Only a change in colour to a whitish shade and the eventual surface scarring (Fig. 2b and c) were visible. However, further investigation by SEM revealed changes in the cross section over the course of the degradation time. In contrast with the PBS soaked samples, it can be clearly seen that the structure did not turn porous, but the roughness of the same gradually became more acute over the degradation period.

The principle of PLA degradation in buffer solutions with a neutral pH and approximate temperature of 37 °C is driven by a bulk-erosion mechanism. It has also been described that in some cases the rate of degradation inside a specimen can be faster than on its surface. This is due to the autocatalytic effect of newly formed acid groups inside the matter, which cannot diffuse out to the surrounding environment. However, the degradation products from outer layers can be subsequently released and neutralized in the surrounding buffer medium. This phenomenon is especially affected by the dimensions and shape of a sample [15].

On the basis of above-described theory and the images resulting from optical and electron microscopy, it can be stated that a different degradation behaviour exists between the core and cortex in the PBS solution. However, in the case of 100% RH exposed samples, the lack of visual core-cortex separation along the cross section indicates the occurrence of either another degradation mechanism other than bulk erosion (surface-erosion based), or the same bulk degradation pattern exists in both the interior and surface layers.

### 3.2. Mass and molecular weight changes

The time varying  $M_n$  and mass loss of residual polymer in PBS and 100% RH degradation experiments are shown in Figs. 3 and 4, respectively. In order to reveal the degradation process in detail, the

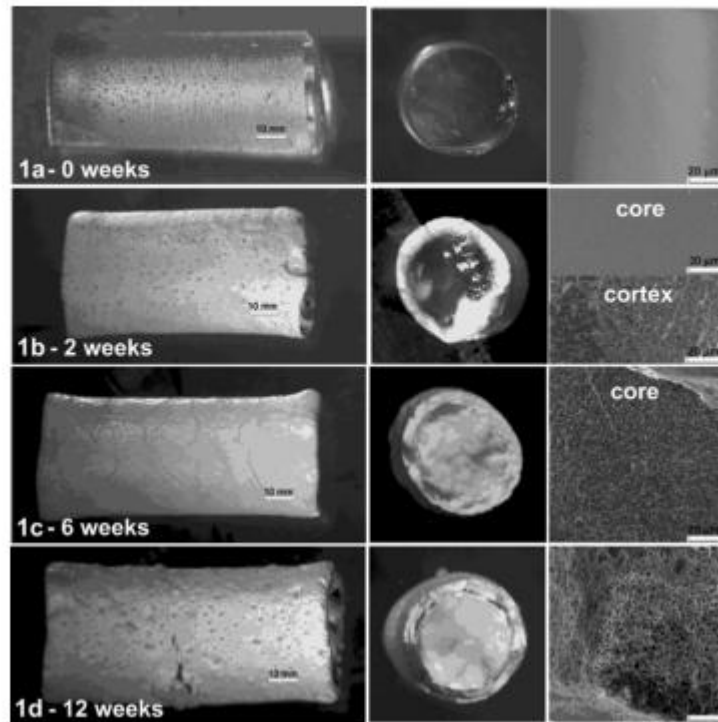


**Fig. 1.** Optical and electron microscopic view of the surfaces and cross sections of specimens exposed to PBS environment at 37 °C. (a) original specimen, not degraded; (b) specimen degraded 2 weeks; (c) specimen degraded 6 weeks; (d) specimen degraded 12 weeks.

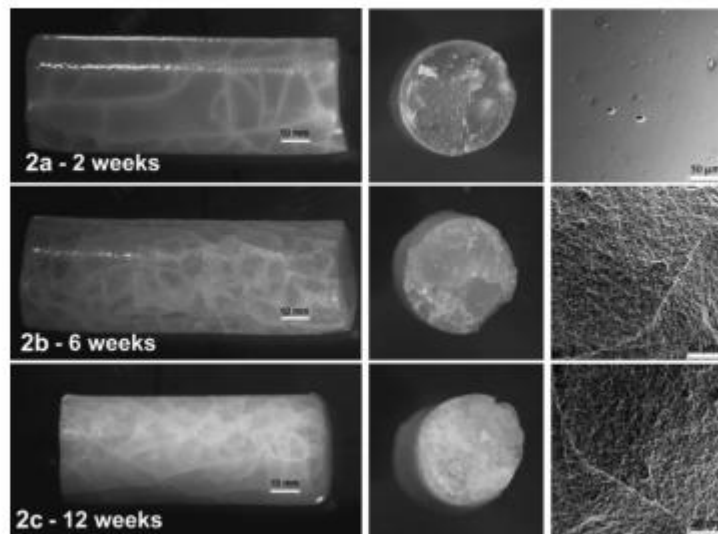


**Fig. 2.** Optical and electron microscopic view of the surfaces and cross sections of specimens exposed to 100% RH environment at 37 °C. 2a, specimen degraded 2 weeks; 2b, specimen degraded 6 weeks; 2c, specimen degraded 12 weeks.

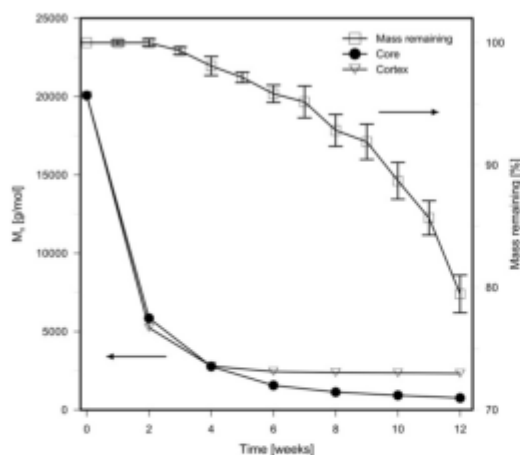


Fig. 3. The  $M_n$  (g/mol) and mass changes (%) of the samples exposed to PBS environment at 37 °C.

samples for GPC analysis were taken from the inner core as well as the cortex layers of the specimens.

The trend is the same for both hydrolysis environments. In combination with the lengthening duration of degradation, weight loss is also increased. With a focus on the first remarkable change in weight, it is obvious that a sample immersed in PBS starts to lose mass (3 weeks, Fig. 3) earlier than a 100% RH exposed sample (5 weeks, Fig. 4). Moreover, the final weight of samples also differs. In PBS, 20.5% loss in mass was detected in contrast with 15.7% in the 100% RH environment.

The changes in the weight of polymer samples exposed to hydrolytic degradation could logically be achieved only through the movement of their mass (fragments of degraded chains or monomers) to the surrounding medium. In the case of PBS, the water

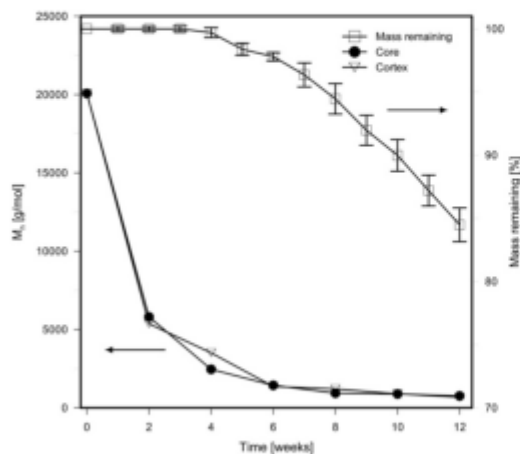


Fig. 4. The  $M_n$  (g/mol) and mass changes (%) of the samples exposed to 100% RH environment at 37 °C.

soluble fragments can easily diffuse to liquid PBS, especially from layers close to the surface (cortex); while for the 100% RH environment, mass transfer is merely restricted to the degradation product swelling out to the surface.

A significant decrease in  $M_n$  for both PBS (Fig. 3) and 100% RH (Fig. 4) was recorded in just 2 weeks, which is earlier than had occurred for the first loss in mass. This indicated that although hydrolysis of the ester bonds began almost immediately after the test had started, the fragments formed were not able to diffuse out to the surrounding environment. Based on the relation between the time when the first instance of remarkable weight loss and molecular weight occurred, it can be stated that it is necessary to achieve, for samples degraded in PBS, the  $M_n$  of fragments <3000 g/mol in order for effective removal to take place; while for 100% RH it is less than 1500 g/mol. The former value is comparable with those found by Farahani et al., although they worked with a copolymer of polylactide and polyglycolide [41].

Other interesting findings can be observed in differences between the core and cortex layer molecular weights. While in 100% RH there are no changes in  $M_n$  along the cross section, excluding a small deviation at the beginning of the experiment, in PBS the decrease in  $M_n$  was similarly extensive in the interior as well as the cortex layer till the 5th week (~2500 g/mol). Afterwards the  $M_n$  of the cortex remained unchanged, and the  $M_n$  of the core further decreased to the value of 800 g/mol. This underlines the theory of autocatalysis phenomenon connected with fast core degradation for samples in PBS. In the case of 100% RH, the homogenous degradation process was observed.

Molecular weight distribution curves are depicted in Figs. 5 and 6, respectively. The bimodal-like distribution in the core and cortex structures of the PBS degraded sample can clearly be seen (the peak shoulder) at the end of the experiment. This observation became visible after the 8th week of degradation (not shown). The bimodal distribution profile is typical when the selective degradation of the amorphous region takes place [29]. The reason for very poor resolution of the cortex structure is probably due to the lesser difference

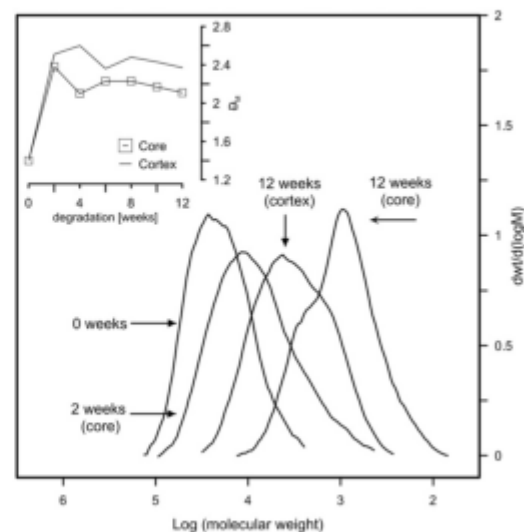


Fig. 5. Molecular weight distribution curves and polydispersity of the samples exposed to PBS environment at 37 °C.

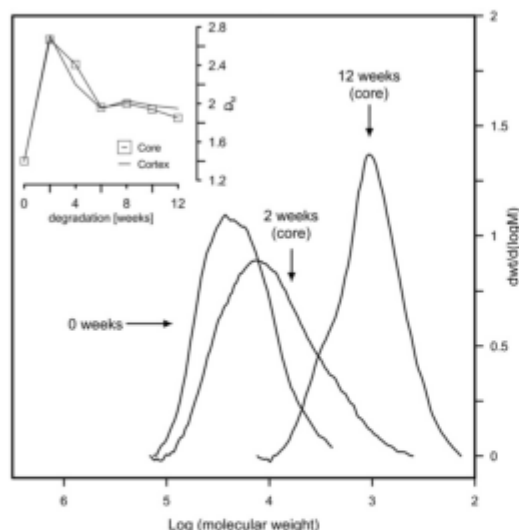


Fig. 6. Molecular weight distribution curves and polydispersity of the samples exposed to 100% RH environment at 37 °C.

between the  $M_n$  of the crystalline and amorphous phase than expected, as the lowest  $M_n$  components could diffuse out.

Through evaluating  $D_M$ , it became apparent that (Fig. 5, the upper part) polydispersity increased noticeably from the initial 1.4 to a value of approximately 2.3 after two weeks of degradation in both the core and cortex parts, which was caused by random scission of the polymeric chain. With the lengthening of the duration of degradation, the value of  $D_M$  slightly decreased to the value of 2 for the core part; however, the cortex remained more or less constant at  $\sim 2.4$ . The greater and more or less constant  $D_M$  in the cortex layer, in comparison with that of the core, may be attributable to a lesser extent of hydrolysis inside the cortex than in the core. As the diffusion of low molecular weight product was restricted in the core, and hydrolysis was faster, the difference between the chain lengths (represented as  $D_M$ ) underwent decrease. However, slow hydrolysis and relatively long chains in the cortex layer (originating especially from crystalline phase) contributed to a higher  $D_M$ .

The situation for the 100% RH exposed samples is similar (Fig. 6). The curves were very similar for both the inner and surface structures (only the core is shown). As in the previous case, bimodal distribution lends support to the idea of slower hydrolysis of the crystalline phase than the amorphous. Although, based on the position of the peaks and shoulders associated with the crystalline phase, it can be discerned that their  $M_n$  values are ordered as follows:

$$M_n^{\text{crist}}(\text{PBS - cortex}) > M_n^{\text{crist}}(\text{PBS - core}) \sim M_n^{\text{crist}}(100\% \text{ RH - core and cortex})$$

This leads to the conclusion that crystallites in PBS are hydrolyzed more in the core than in the cortex layer, while for 100% RH it is the same in the entire cross section. In other words, the degradation of crystalline domains in 100% RH environment is very similar to degradation in the PBS-core part.

Changes in the  $D_M$  of samples exposed to humidity (Fig. 6, the upper part) show a considerably different trend than in the previous case. Despite a comparable initial increase being observed after two weeks, further degradation caused a drop in the  $D_M$  of both the core and cortex parts to the value  $\sim 2$  (after 6 weeks). This behaviour was analogous to those observed in the PBS-core and underlines the above-mentioned theory of a similar degradation process between PBS-core and 100% RH.

### 3.3. Water uptake

The results of the water uptake experiment are summarized in Fig. 7. It can be observed that both profiles differ significantly. In PBS the amount of water in the sample increased immediately after several days and then further increased to the value of 33% after eight weeks. Conversely, water uptake in 100% RH varied noticeably. The increase was observed only during the first 3 weeks and it then dropped to the value of approximately 2% after eight weeks. In the case of PBS, the high initial increment can be explained by the considerably greater ability of  $H_2O$  molecules to diffuse from water to polymer than from moisture saturated air. The subsequent increase in weight is attributed to further absorption of water by the polymer structure. The drop in water uptake after approximately 3 weeks in the 100% RH environment can be connected with mass loss of the sample, which was probably higher than the diffusion of water molecules from air.

So as to comprehend this further, the authors studied water uptake over the brief interval of merely the first few days of degradation (when no change in mass occurred, Fig. 7, the upper part). It can be noticed that the water uptake in both PBS and 100% RH equals the same during the first approximate 24 h. This is probably attributed to the diffusion of water molecules into layers very close to the surface. Afterwards the water content rose steeply in the PBS solution, in contrast with 100% RH. This definitely indicates a higher diffusion in the case of PLA/PBS than in that of the PLA/water vapour saturated environment.

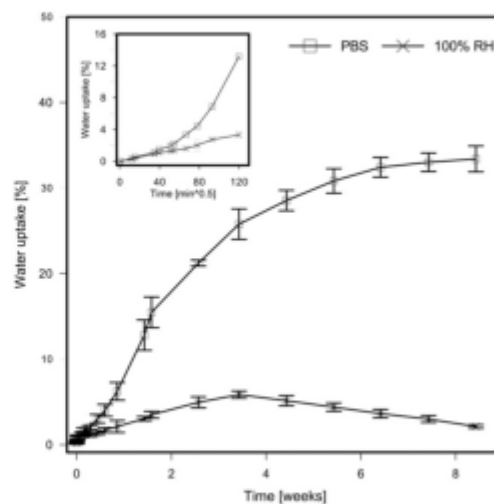


Fig. 7. Water uptake of the samples degraded in PBS and in 100% RH environment at 37 °C.

### 3.4. Thermal properties

The thermal properties investigated by DSC are depicted in Figs. 8–10. As can be seen from the first heating scan (Fig. 8), the samples were initially highly amorphous since only a small endothermic peak, situated at around 134 °C, was discerned. This also clearly corresponds with the relatively low density [30]. The degree of crystallinity of less than 1% was worked out via the heat of fusion associated with an area of melting peak. After two weeks of degradation, the cold crystallization peak appeared in both environments. This indicated that some newly formed degradation products possessed sufficient mobility to produce a crystalline lattice, but a higher temperature (above 70 °C, peak onset) was necessary to achieve this. Moreover, the second melting peak appeared at a lower temperature (around 120 °C) than that demonstrated by the original one in the presence of an imperfect population of crystals [29].

Such continuous degradation led to a difference in behaviour between samples from the two separate environments. Regarding the samples degraded in phosphate buffer solution, both melting temperatures tailed off very slowly ( $T_{m1}$  from 134 °C to 131 °C by the end of the experiment), while the change in the value of the second melting peak did not exhibit any specific trend and oscillated between 121 °C and 116 °C. The negligible depression of  $T_{m1}$  can be attributed to the selective degradation of the amorphous phase rather than crystallinity, in addition to the higher molecular weight of the cortex material.

In contrast, the thermal properties of PLA degraded in the 100% RH environment (Fig. 9) show significantly different trends from the second week of degradation onwards. Both ( $T_{m1}$  and  $T_{m2}$ ) melting points declined noticeably alongside the lengthening degradation time, and reached the value of approximately 119 °C and 106 °C at the end of experiment, respectively. It is believed that the steady drop in both  $T_{m1}$  and  $T_{m2}$  was connected to the presence of low molecular weight products with decreased lattice disordering, leading to a lower  $T_m$ .

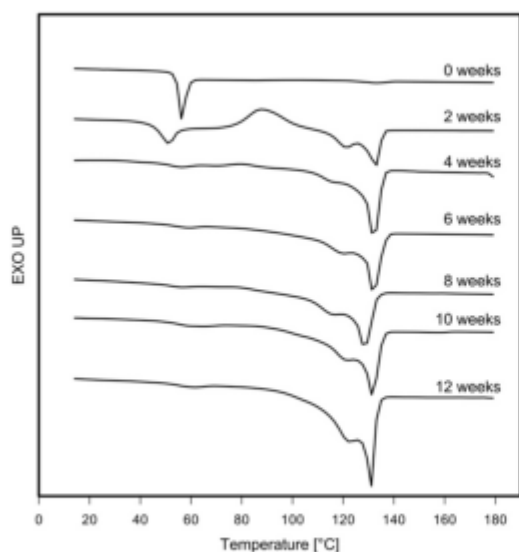


Fig. 8. The first heating scan of specimens degraded in PBS environment at 37 °C.

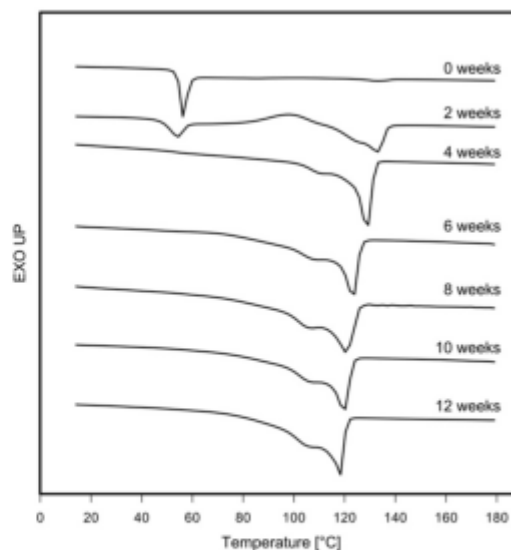


Fig. 9. The first heating scan of samples degraded in 100% RH environment at 37 °C.

The value of glass transition temperature (Fig. 10) principally underscores the above-described behaviour. From an initial  $T_g$  of 46 °C, a decrease to 37 °C was only observed in samples degraded in PBS during the first 4 weeks. Conversely, the  $T_g$  values of the samples degraded in 100% RH fell gradually to the value of 21 °C (after 5 weeks) and then remained more or less constant. The likely cause of this is generally a lower  $M_n$  of the 100% RH exposed samples in comparison with PBS hydrolyzed ones (more end groups leading to a lower  $T_g$  – free volume theory), especially in the

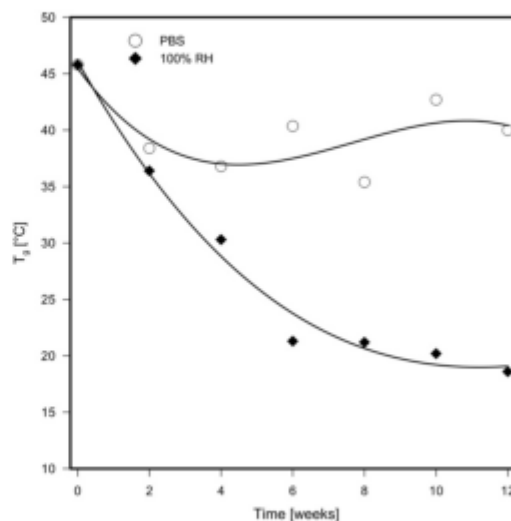


Fig. 10. The values of  $T_g$  [°C] as a function of degradation time and environment.

amorphous phase. This low molecular weight fragments act as a plasticizer, lowering the  $T_g$ .

#### 4. Conclusions

The comparison of degradation of relatively low molecular weight poly(L-lactide) in buffer solution and an environment possessing high partial pressure of water vapour has been investigated in this paper. Samples taken at a predetermined time interval were especially characterized by GPC, SEM and DSC. From analyses of inner and surface parts of the samples, it was found that degradation in liquid PBS is different from that of an environment of 100% relative humidity. It was proven, that the general mechanism of bulk erosion was essentially the same in both environments; however, no core cortex structure was found in the 100% RH degraded samples in contrast with PBS. This was probably caused by significantly different diffusion relationships between liquid-polymer and saturated air-polymer conditions. The measuring of thermal properties showed a noticeable decrease in the  $T_g$  and  $T_m$  of 100% RH exposed samples in comparison with PBS, most likely caused by the presence of low molecular weight degradation products. Moreover, according to GPC distribution curves, the degradation process of the crystalline phase of 100% RH exposed samples appears similar to that of the core part of PBS soaked samples. These results could prove crucial for predicting the degradation of polylactide implants in high humidity environments; for example, the respiratory tract or middle ear area.

#### Acknowledgements

This work was supported by the Ministry of Education, Youth and Sports of the Czech Republic (project ME09072) and Operational Programme Research and Development for Innovations co-funded by the European Regional Development Fund (project CZ.1.05/2.1.00/03.0/11). The authors are also grateful to the Internal Grant Agency of Tomas Bata University in Zlín (grant IGA/FT/2012/005) for co-funding.

#### References

- Ulery BD, Nair LS, Laurencin CT. Biomedical applications of biodegradable polymers. *J Polym Sci B Polym Phys* 2011;49(12):832–64.
- Ratner BD, Hoffman AS, Schoen FJ, Lemons JE. *Biomaterials science: an introduction to materials in medicine*. 2nd ed. San Diego: Elsevier Academic Press; 2004.
- Middleton JC, Tipton AJ. Synthetic biodegradable polymers as orthopedic devices. *Biomaterials* 2000;21(23):2335–48.
- Kricheldorf HR. Syntheses and application of polylactides. *Chemosphere* 2001;43(1):49–54.
- Sedlárik V, Saha N, Sedláriková J, Saha P. Biodegradation of blown films based on poly(lactic acid) under natural conditions. *Macromol Symp* 2008;272(1):100–3.
- Tsuji H, Ishida T. Poly(L-lactide): X. Enhanced surface hydrophilicity and chain-scission mechanisms of poly(L-lactide) film in enzymatic, alkaline, and phosphate-buffered solutions. *J Appl Polym Sci* 2003;87(10):1628–33.
- Kale G, Auras R, Singh SP, Narazan R. Biodegradability of polylactide bottles in real and simulated composting conditions. *Polym Test* 2007;26(8):1049–61.
- Zhou ZH, Liu XP, Liu QJ, Liu LH. Morphology, molecular mass changes, and degradation mechanism of poly(L-lactide) in phosphate-buffered solution. *Polym-Plast Technol Eng* 2009;47(2):115–20.
- Cam D, Hyon SH, Ikada Y. Degradation of high molecular weight poly(L-lactide) in alkaline medium. *Biomaterials* 1995;16(11):833–43.
- Tsuji H, Muramatsu H. Blends of aliphatic polyesters. 5. Nonenzymatic and enzymatic hydrolysis of blends from hydrophobic poly(L-lactide) and hydrophilic poly(vinyl alcohol). *Polym Degrad Stab* 2001;71(3):403–13.
- Tsuji H, Miyauchi S. Poly(L-lactide): 6. Effects of crystallinity on enzymatic hydrolysis of poly(L-lactide) without free amorphous region. *Polym Degrad Stab* 2001;71(3):415–24.
- Tsuji H, Echizen Y, Nishimura Y. Enzymatic degradation of poly(L-lactic acid): effects of UV irradiation. *J Polym Environ* 2006;14(3):239–48.
- Tsuji H, Kidokoro Y, Mochizuki M. Enzymatic degradation of poly(L-lactic acid) fibers: effects of small drawing. *J Appl Polym Sci* 2007;103(5):2064–207.
- Tsuji H, Ikada Y. Properties and morphology of poly(L-lactide). II. Hydrolysis in alkaline solution. *J Polym Sci: Part A: Polym Chem* 1998;36(1):59–66.
- Tsuji H, Kazumasa N. Poly(L-lactide). IX. Hydrolysis in acid media. *J Appl Polym Sci* 2002;80(1):186–94.
- Tsuji H, Tsuruno T. Accelerated hydrolytic degradation of poly(L-lactide)/poly(D-lactide) stereocomplex up to late stage. *Polym Degrad Stab* 2010;95(4):477–84.
- Tsuji H, Mizuno A, Ikada Y. Properties and morphology of poly(L-lactide). III. Effects of initial crystallinity on long-term in vitro hydrolysis of high molecular weight poly(L-lactide) film in phosphate-buffered solution. *J Appl Polym Sci* 2000;77(7):1452–64.
- Tsuji H, Ikada Y. Properties and morphology of poly(L-lactide). 4. Effects of structural parameters on long-term hydrolysis of poly(L-lactide) in phosphate-buffered solution. *Polym Degrad Stab* 2000;87(1):179–89.
- Tsuji H, Nakahara K, Ikarashi K. Poly(L-lactide): 8. High temperature hydrolysis of poly(L-lactide) films with different crystallinities and crystalline thicknesses in phosphate-buffered solution. *Macromol Mater Eng* 2001;286(7):398–406.
- Tsuji H, Ikarashi K, Fukuda N. Poly(L-lactide): XII. Formation, growth, and morphology of crystalline residues as extended-chain crystallites through hydrolysis of poly(L-lactide) films in phosphate-buffered solution. *Polym Degrad Stab* 2004;84(3):512–23.
- Tsuji H. Hydrolysis of biodegradable aliphatic polyesters. In: Pandlaj SG, editor. *Recent research developments in polymer science*, vol. 4. Trivandrum: Transworld Research Network; 2000. p. 13–37.
- Faisal M, Saeki T, Tsuji H, Daimon H, Fujie K. Recycling of poly lactic acid into lactic acid with high temperature and high pressure water. *WIT Trans Ecol Environ* 2008;92(1):225–33.
- Tsuji H. Autocatalytic hydrolysis of amorphous-made polylactides: effects of L-lactide content, tacticity, and enantiomeric polymer blending. *Polymer* 2002;43(6):1789–96.
- Tsuji H, Del Carpio CA. In vitro hydrolysis of blends from enantiomeric poly(lactide)s: 3. Well-homo-crystallized and amorphous blend films. *Biomacromolecules* 2003;4(1):7–11.
- Tsuji H. In vitro hydrolysis of blends from enantiomeric poly(lactide)s: 4. Well-homo-crystallized blend and nonblended films. *Biomaterials* 2003;24(4):537–47.
- Tsuji H, Miyauchi S. Poly(L-lactide): 7. Enzymatic hydrolysis of free and restricted amorphous regions in poly(L-lactide) films with different crystallinities and a fixed crystalline thickness. *Polymer* 2001;42(9):4463–7.
- Pistner H, Stallforth H, Gutwald R, Mühling J, Reuther J, Michel C. Poly(L-lactide): a long-term degradation study in vivo. Part II: physico-mechanical behaviour of implants. *Biomaterials* 1994;15(6):439–50.
- Gopferich A. Polymer bulk erosion. *Macromolecules* 1997;30(9):2388–904.
- Nakamura T, Hitomi S, Watanabe S, Shimizu Y, Jamshidi K, Hyon S-H, et al. Bioabsorption of polylactides with different molecular properties. *J Biomed Mater Res* 1989;23(10):1115–30.
- Fukuzaki H, Yoshida M, Asano M, Kumakura M. Synthesis of copoly(L, D-lactic acid) with relatively low molecular weight and in vitro degradation. *Eur Polym J* 1989;25(10):1019–26.
- Li S, Garreau H, Vert M. Structure property relationship in the case of the degradation of massive poly(L-lactide) in aqueous media. Part 3. Influence of the morphology of poly(L-lactide). *J Mater Sci Mater Med* 1990;1(4):198–206.
- Migliarese C, Fambri L, Cohn D. A study on the in vitro degradation of poly(L-lactide). *J Biomater Sci Polym Ed* 1994;6(6):591–600.
- Pegunetti A, Fambri L, Migliarese C. In vitro degradation of poly(L-lactide) fibers produced by melt spinning. *J Appl Polym Sci* 1997;64(2):213–23.
- Ho KLG, Pometto AL, Hint PN. Effects of temperature and relative humidity on polylactide acid plastics degradation. *J Environ Polym Degrad* 1999;7(2):83–92.
- Copinat A, Bertrand C, Coma SGV, Couturier Y. Effects of ultraviolet light (315 nm), temperature and relative humidity on the degradation of polylactide acid plastic films. *Chemosphere* 2004;55(5):763–73.
- Cairncross RA, Becker JG, Ramaswamy S, O'Connor R. Moisture sorption, transport, and hydrolytic degradation in polylactide. *Appl Biochem Biotechnol* 2006;131(1–3):774–83.
- Majoral C, Coates AL, Diot P, Vecellio L. Development of an in vitro model for aerosol sizing at 37 °C and 100% relative humidity. *Rev Mal Respir* 2000;23(5):520.
- Massey BL, Wen XJ, Rohr LR, Tresco PA, Dahlstrom L, Park AH. Resorption rate and biocompatibility characteristics of two polyester ventilation tubes in a guinea pig model. *Otolaryngol Head Neck Surg* 2004;131(6):921–5.
- Gray S, Lusk RP. Tympanic membrane tympanostomy tubes. In: Cummings CW, Frederickson JM, Harker LA, Krause CJ, Schuller DE, editors. *Otolaryngology head and neck surgery*. 2nd ed. St. Louis, MO: Mosby Year Book; 1993.
- Ott LM, Weatherly RA, Detamore MS. Overview of tracheal tissue engineering: clinical need drives the laboratory approach. *Ann Biomed Eng* 2011;39(8):2091–113.
- Farahani TD, Entezami AA, Mobei H, Abtahi M. Degradation of poly(L, D-lactide-co-glycolide) 50:50 implant in aqueous medium. *Iran Polym J* 2005;8(14):753–63.